

INFORMATION TO USERS

This manuscript has been reproduced from the microfilm master. UMI films the text directly from the original or copy submitted. Thus, some thesis and dissertation copies are in typewriter face, while others may be from any type of computer printer.

The quality of this reproduction is dependent upon the quality of the copy submitted. Broken or indistinct print, colored or poor quality illustrations and photographs, print bleedthrough, substandard margins, and improper alignment can adversely affect reproduction.

In the unlikely event that the author did not send UMI a complete manuscript and there are missing pages, these will be noted. Also, if unauthorized copyright material had to be removed, a note will indicate the deletion.

Oversize materials (e.g., maps, drawings, charts) are reproduced by sectioning the original, beginning at the upper left-hand corner and continuing from left to right in equal sections with small overlaps.

Photographs included in the original manuscript have been reproduced xerographically in this copy. Higher quality 6" x 9" black and white photographic prints are available for any photographs or illustrations appearing in this copy for an additional charge. Contact UMI directly to order.

**ProQuest Information and Learning
300 North Zeeb Road, Ann Arbor, MI 48106-1346 USA
800-521-0600**

UMI[®]

University of Alberta

**Effects of Imperfect Bonding on Inclusion-
Matrix Crack Interaction in Fiber Composites**

by

Yu Liu ©

A thesis submitted to the Faculty of Graduate Studies and Research in partial
fulfillment of the requirements for the degree of Master of Science

Department of Mechanical Engineering

Edmonton, Alberta

Fall 2001



**National Library
of Canada**

**Acquisitions and
Bibliographic Services**

**395 Wellington Street
Ottawa ON K1A 0N4
Canada**

**Bibliothèque nationale
du Canada**

**Acquisitions et
services bibliographiques**

**395, rue Wellington
Ottawa ON K1A 0N4
Canada**

Your file Votre référence

Our file Notre référence

The author has granted a non-exclusive licence allowing the National Library of Canada to reproduce, loan, distribute or sell copies of this thesis in microform, paper or electronic formats.

L'auteur a accordé une licence non exclusive permettant à la Bibliothèque nationale du Canada de reproduire, prêter, distribuer ou vendre des copies de cette thèse sous la forme de microfiche/film, de reproduction sur papier ou sur format électronique.

The author retains ownership of the copyright in this thesis. Neither the thesis nor substantial extracts from it may be printed or otherwise reproduced without the author's permission.

L'auteur conserve la propriété du droit d'auteur qui protège cette thèse. Ni la thèse ni des extraits substantiels de celle-ci ne doivent être imprimés ou autrement reproduits sans son autorisation.

0-612-69809-2

University of Alberta
Faculty of Graduate Studies and Research

Name of Author: Yu Liu

Title of Thesis: Effects of Imperfect Bonding on Inclusion-Matrix Crack
Interaction in Fiber Composites

Degree: Master of Science

Year this Degree Granted: 2001

Permission is hereby granted to the University of Alberta Library to reproduce single copies of this thesis and to lend or sell such copies for private, scholarly or scientific research purposes only.

The author reserves all other publication and other rights in association with the copyright in the thesis, and except as herein before provided, neither the thesis nor any substantial portion thereof may be printed or otherwise reproduced in any material form whatever without the author's prior written permission.



Yu Liu
Department of Mechanical Engineering
University of Alberta
Edmonton, Alberta T6G 2G8
CANADA

Date: April 27, 2001

University of Alberta

Faculty of Graduate Studies and Research

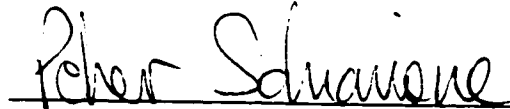
The undersigned certify that they have read, and recommend to the Faculty of Graduate Studies and Research for acceptance, a thesis entitled **Effects of Imperfect Bonding on Inclusion-Matrix Crack Interaction in Fiber Composites** submitted by **Yu Liu** in partial fulfillment of the requirements for the degree of Master of Science.



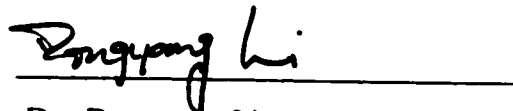
Dr. Chongqing Ru (Supervisor)



Dr. Andrew Mioduchowski (Co-Supervisor)



Dr. Peter Schiavone (Co-Supervisor)



Dr. Dongyang Li

Date: April 17, 2001 17/04/01

ABSTRACT

This dissertation presents a systematical study of the effects of an imperfect inclusion/matrix interface on stress intensity factors (SIF) at a radial matrix crack in a fiber composite under different mechanical loadings. Since the existing dislocation-density method cannot be applied to an imperfect interface, a novel power-series method is developed to obtain the deformation and stress fields in the matrix and inclusion in the presence of the radial matrix crack. The interaction between the radial matrix crack and the inclusion is demonstrated numerically for different material geometrical parameters and the imperfect interface parameters.

The results indicate that the inclusion can either promote or retard crack propagation in the matrix, depending not only on the ratio of the moduli, but also on the interface imperfection. Some qualitatively new phenomena are predicted for radial matrix cracking, specifically the influence of imperfect bonding at the inclusion-matrix interface on the direction of crack growth. For example, in the case of an circular inclusion perfectly bonded to the surrounding matrix, the SIF at the nearby crack tip is greater than that at the distant crack tip only when the inclusion is more compliant than the matrix. In contrast, the effects of imperfect bonding at the inclusion-matrix interface allow for the SIF at the nearby crack tip to be greater than that at the distant crack tip *even when the inclusion is stiffer than the matrix*. In fact, for any given case when the circular inclusion is stiffer than the matrix, we show that there is a corresponding critical value of the imperfect interface parameter below which a radial matrix crack grows *toward* the interface

leading eventually to complete debonding. In particular, this critical value of the imperfect interface parameter tends to a non-zero finite value when the stiffness of the inclusion approaches infinity.

To our knowledge, these results provide, for the first time, a clear quantitative description of the relationship between interface imperfections and the direction of propagation of radial matrix cracks, as well as useful information for the design of fiber-matrix interface of fiber composites against matrix cracking.

ACKNOWLEDGMENT

The author sincerely wishes to express his deepest gratitude to his supervisor, Dr. Chongqing Ru, and co-supervisors, Dr. Andrew Mioduchowski and Dr. Peter Schiavone, for their invaluable guidance, support and advice in coaching the author through this research, which made this thesis possible.

In addition, the author would like also to express his sincere appreciation to all his friends for their help during the course of his studies.

This report is dedicated to my parents and all my family members, whom I dearly love. Thanks for your support and encouragement.

TABLE OF CONTENTS

CHAPTER 1: INTRODUCTION

1.1 Fiber Composites	1
1.2 Matrix Cracking in Fiber composites	4
1.3 Imperfect Interface Model	8
1.4 The Limitations of the Dislocation-Density Method for Crack-Inclusion Interaction	12
1.5 Objective of the Present Work	14

CHAPTER 2: FORMULATION OF A SERIES METHOD

2.1 Introduction	16
2.2 Complex Variable Method	
2.2.1 Problem Formulation	16
2.2.2 Analytic Continuation Theory	20

2.3 Stress Intensity Factor	25
2.4 Conclusions	26

CHAPTER 3: EFFECT OF IMPERFECT BONDING ON RADIAL MATRIX CRACKING --UNIAXIAL LOADING NORMAL TO THE CRACK

3.1 Description of the Problem	28
3.2 Problem Solutions	
3.2.1 Problem Formulation	29
3.2.2 The Spring-Layer Interface ($m=n$)	39
3.2.3 The Elastic Interphase Layer ($m=3n$)	39
3.2.4 The Sliding Interface ($m = \infty$, $n=0$)	39
3.3 Numerical Results and Discussions	39
3.4 Conclusions	46

CHAPTER 4: EFFECT OF IMPERFECT BONDING ON RADIAL MATRIX CRACKING --UNIAXIAL LOADING PARALLEL TO THE CRACK

4.1 Description of the Problem	48
4.2 Problem Solutions	

4.2.1 The Elastic Interphase Layer ($m=3n$)	48
4.3 Numerical Results and Discussions	52
4.4 Conclusions	55

CHAPTER 5: EFFECT OF IMPERFECT BONDING ON RADIAL MATRIX CRACKING -- PURE SHEAR LOADING

5.1 Description of the Problem	56
5.2 Problem Solutions	
5.2.1 The Sliding Interface ($m = \infty$, $n=0$)	56
5.2.2 The Elastic Interphase Layer ($m=3n$)	60
5.3 Numerical Results and Discussions	64
5.4 Conclusions	67

CHAPTER 6: CONCLUSIONS AND FUTURE WORK

6.1 Conclusions	68
6.2 The Future Work	71
REFERENCE	72
APPENDIX 1	90
APPENDIX 2	109

LIST OF TABLES

<u>Table 3.1:</u> Comparison between the calculated nearby SIF with very large interface parameter and the SIF corresponding to perfect bonding -----	44
<u>Table 3.2:</u> Comparison between the calculated distant SIF with very large interface parameter and the SIF corresponding to perfect bonding -----	44
<u>Table 3.3:</u> Comparison between the calculated nearby and distant SIF and SIF corresponding to traction-free hole -----	45

LIST OF FIGURES

Figure 2.1: A circular inclusion with a radial matrix crack -----	78
Figure 3.1: The SIFs of crack tips via interface parameter N' (uniaxial load perpendicular to crack, $m=n$, $\mu_1 / \mu_2 = 0.5$, $l/R=1$) -----	78
Figure 3.2: The SIFs of crack tips via interface parameter N' (uniaxial load perpendicular to crack, $m=n$, $\mu_1 / \mu_2 = 2$, $l/R=1$) -----	79
Figure 3.3: The shear modulus ratio of inclusion to matrix determined by the condition $K_I(a)=K_I(b)$ for different interface parameters ($m=n$, $l/R=1$) -----	79
Figure 3.4: The shear modulus ratio of inclusion to matrix determined by the condition $K_I(a)=K_I(b)$ for different interface parameters ($m=n$, $l/R=0.1$) -----	80
Figure 3.5: Near-by crack tip stress intensity factor versus interface parameter (uniaxial load perpendicular to crack, $m=3n$, $\mu_1 / \mu_2 = 2$, $l/R=1$) -----	80
Figure 3.6: Near-by crack tip stress intensity factor versus interface parameter (uniaxial load perpendicular to crack, $m=3n$, $\mu_1 / \mu_2 = 0.5$, $l/R=1$) -----	81
Figure 3.7: Distant crack tip stress intensity factor versus interface parameter (uniaxial load perpendicular to crack, $m=3n$, $\mu_1 / \mu_2 = 2$, $l/R=1$) -----	81
Figure 3.8: Distant crack tip stress intensity factor versus interface	

parameter (uniaxial load perpendicular to crack, $m=3n$,
 $\mu_1 / \mu_2 = 0.5, l/R=1$) ----- 82

Figure 3.9: The mode-I SIFs via the distance d/R for different
modulus ratio (sliding interface, uniaxial load perpendicular to
the crack, $l/R=1$) ----- 82

Figure 4.1: Nearby crack tip stress intensity factor versus interface
parameter (uniaxial load parallel to crack, $m=3n$,
 $\mu_1 / \mu_2 = 0.5, l/R=1$) ----- 83

Figure 4.2: Near-by crack tip stress intensity factor versus interface
parameter (uniaxial load parallel to crack, $m=3n$,
 $\mu_1 / \mu_2 = 2, l/R=1$) ----- 83

Figure 4.3: Near-by crack tip stress intensity factor versus interface
parameter (uniaxial load parallel to crack, $m=3n$,
 $\mu_1 / \mu_2 = 0.1, l/R=1$) ----- 84

Figure 4.4: Nearby crack tip stress intensity factor versus interface
parameter (uniaxial load parallel to crack, $m=3n$,
 $\mu_1 / \mu_2 = 10, l/R=1$) ----- 84

Figure 4.5: Distant crack tip stress intensity factor versus interface
parameter (uniaxial load parallel to crack, $m=3n$,
 $\mu_1 / \mu_2 = 0.5, l/R=1$) ----- 85

Figure 4.6: Distant crack tip stress intensity factor versus interface
parameter (uniaxial load parallel to crack, $m=3n$,
 $\mu_1 / \mu_2 = 2, l/R=1$) ----- 85

Figure 4.7: Distant crack tip stress intensity factor versus interface
parameter (uniaxial load parallel to crack, $m=3n$,
 $\mu_1 / \mu_2=0.1$, $l/R=1$) ----- 86

Figure 4.8: Distant crack tip stress intensity factor versus interface
parameter (uniaxial load parallel to crack, $m=3n$,
 $\mu_1 / \mu_2=10$, $l/R=1$) ----- 86

Figure 5.1: The mode-II nearby SIFs via the distance d/R for different
modulus ratio (sliding interface, pure shear load, $l/R=1$) ----- 87

Figure 5.2: Mode-II nearby crack tip SIF versus interface parameter
(pure shear loading, $m=3n$, $\mu_1 / \mu_2=2$, $l/R=1$) ----- 87

Figure 5.3: Mode-II nearby crack tip SIF versus interface
parameter (pure shear loading, $m=3n$, $\mu_1 / \mu_2=0.5$, $l/R=1$) ----- 88

Figure 5.4: Mode-I nearby crack tip SIF versus interface parameter
(pure shear loading, $m=3n$, $\mu_1 / \mu_2=2$, $l/R=1$) ----- 88

Figure 5.5: Mode-I nearby crack tip SIF versus interface parameter
(pure shear loading, $m=3n$, $\mu_1 / \mu_2=0.5$, $l/R=1$) ----- 89

LIST OF SYMBOLS

Symbol	Description & dimension
a	nearby crack tip point
b	distant crack tip point
d	distance between the inclusion-matrix interface and the nearby crack tip, M
D	the domain outside the circle Γ minus the matrix crack L
l	half crack length of the radial matrix crack, M
L	the finite radial matrix crack
m	imperfect interface parameter along normal direction in plane elasticity, PA/M
n	imperfect interface parameter along tangential direction in plane elasticity, PA/M
M	defined by $\frac{m-n}{2}$, PA/M
N	defined by $\frac{m+n}{2}$, PA/M
N'	$\frac{R}{\mu_2} N$ (dimensionless)
N^*	the minimum critical value of N'
R	radius of the circular inclusion
SIF	stress intensity factor, $N/M^{3/2}$

S_1	domain occupied by the matrix
S_2	domain occupied by the circular inclusion
u, v	displacement components in plane-strain, M
u^o	the additional displacement induced by the uniform eigenstrains, M
Γ	the circular interface separating S_2 and S_1
ε_{ij}	strain tensor
ε_{ij}^0	uniform eigenstrain prescribed within the inclusion
μ_1	shear modulus of the matrix, GPA
μ_2	shear modulus of the inclusion, GPA
ν_1	Poisson's ratio in the matrix
ν_2	Poisson's ratio in the inclusion
σ_{ij}	stress tensor, N/M^2
$\varphi(z), \psi(z)$	analytic functions in plane elasticity
$\Phi(z), \Psi(z)$	two analytic functions in domain D
$ * _\Gamma$	denotes the jump across Γ

CHAPTER 1

INTRODUCTION

1.1 FIBER COMPOSITES

The word “*composite*” means “consisting of two or more distinct parts.” Thus, a material having two or more distinct constituent materials or phases may be considered a composite material. Composites consist of one or more discontinuous phases embedded in a continuous phase. The discontinuous phase is usually harder and stronger than the continuous phase and is called the reinforcement or reinforcing material, whereas the continuous phase is termed the matrix. When the shape of the reinforcement is characterized by its length being much greater compared to its cross-sectional dimensions, it is called a fiber. Composite materials are ideal for structural applications where high strength-to weight and stiffness-to-weight ratios are required. In total, there are three commonly accepted types of composite materials: *fibrous composites* which consist of fibers in a matrix, *laminated composites* which consist of layers of various materials, and *particulate composites* which are composed of particles in a matrix.

Fibers, because of their small cross-sectional dimension, are not, in themselves, suitable for engineering applications. They are, therefore, embedded in

matrix materials to form fibrous composites. The matrix serves to bind the fibers together, transfers loads to the fibers and protects them against environmental attack and damage due to handling. The high strength and modulus of fibers makes them useful as a reinforcement for polymers, metals, carbons, and ceramics, even though they are brittle.

Fibrous composites can be broadly classified as single-layer and multilayer (angle-ply) composites on the basis of studying both their theoretical and experimental properties. Single-layer composites may actually be made from several distinct layers with each layer having the same orientation and properties, and thus the entire laminate may be considered a “single-layer” composite. Most composites used in structural applications are multilayered; that is, they consist of several layers of fibrous composites. Each layer or lamina is a single-layer composite, and orientation of the layers is varied according to design. Each layer of the composite is usually very thin, typically of a thickness of 0.1mm, and hence cannot be used directly. Several identical or different layers are bonded together to form a multilayered composite suitable for engineering applications.

Reinforcing fibers in a single-layer composite may be short or long compared to the overall dimensions of the composite. Composites with long fibers are called continuous-fiber-reinforced composites, and those with short fibers are called discontinuous-fiber reinforced composites or short-fiber composites. A further distinction is that a discontinuous-fiber reinforced composite can be considered to be one in which the fiber length affects the properties of the composite. In continuous-fiber reinforced composites, it may be assumed that the load is directly

applied to the fibers and that the fibers in the direction of the load are the principal load-carrying constituent. The latter assumption is particularly valid when high-modulus fibers are used in large concentrations. The orientation of short or discontinuous fibers cannot be easily controlled in a composite material. For example, in injection molding of a fiber-reinforced polymer, considerable orientation can occur in the flow direction. However, in most cases, the fibers are assumed to be randomly oriented in the composite. Therefore, properties of a short-fiber composite can be isotropic; that is, they do not change with direction within the plane of the sheet.

The two outstanding features of oriented fiber composites are their high strength-to-weight ratio and controlled anisotropy. Fiber composites are generally superior to metals with respect to specific strength and modulus (glass-fiber composites, however, are superior to neither steel nor aluminum in specific stiffness). Furthermore, whether a comparison is made on the basis of actual properties or “specific” properties depends on whether the weight of the structure is a factor in the design. “Controlled anisotropy” means that the desired ratio of property values in different directions can be easily varied. For example, in a unidirectional composite, the ratio of longitudinal strength to transverse strength can be easily changed by changing the volume fraction of fibers. Similarly, other directional properties can also be altered by changing the material and manufacturing variables. These two features make fiber composites extremely attractive as structural materials. Other advantages of fiber composites include ease of processing and their use in structural forms that are otherwise inconvenient or

impossible to manufacture. Their utilization, therefore, in aerospace and transportation industries is continuously increasing.

Effective reinforcement requires good bonding between the fibers and the matrix, especially for short fibers. For a unidirectional composite (i.e., one containing continuous fibers all in the same direction), the longitudinal tensile strength is quite independent of the fiber-matrix bonding, but the transverse tensile strength and the flexural strength (for bending in longitudinal or transverse directions) increase with increasing fiber-matrix bonding. On the other hand, excessive fiber-matrix bonding can cause a composite with a brittle matrix (e.g., carbon or ceramic) to become more brittle, as the strong fiber-matrix bonding causes cracks to propagate in a straight line, in the direction perpendicular to the fiber-matrix interface without being deflected to propagate along this interface. In the case of a composite with a ductile matrix (e.g., metal or polymer matrix), a crack initiating in the brittle fiber tends to be blunted when it reaches the ductile matrix, even when the fiber-matrix bonding is strong. Therefore, an optimum degree of fiber-matrix bonding is needed for brittle- matrix composites, whereas a high degree of fiber-matrix bonding is preferred for ductile-matrix composites.

1.2 MATRIX CRACKING IN FIBER COMPOSITES

The anisotropic characteristics of composite materials cause a complex failure mechanism under static and fatigue loading and this is accompanied by extensive

damage to the composite. Unidirectional continuous fiber composites, on the other hand, have excellent fatigue resistance and are essentially linear to failure. If, however, the composite contains off-axes plies, various damage mechanisms can occur under load, causing the composite to be redistributed and the stress-strain response to become non-linear. In the four basic failure mechanisms, which are matrix cracking, delamination, fiber breakage and interface debonding, matrix cracking is usually the first damage mechanism in the off-axis plies. The density of the cracks increases as the load increases until this process appears to stabilize at a unique value for a given laminate. This state has been called a “characteristic damage state” (see, for example, Reifsnider and Talug, 1980).

In fracture studies of ceramics and other composite materials, it is generally conjectured that the fracture of the solid will initiate at and will propagate from a “dominant flaw.” This may be a manufacturing flaw, it may be caused by residual stresses or some other type of loading before the part is put into use, or it may result from the growth of a “micro flaw” due to cyclic nature of the operating stresses. In some cases, it may be possible to detect such flaws by using nondestructive testing techniques. More often, in studies relating to structural integrity and reliability, one simply assumes their existence. Generally, the flaw is assumed to be an internal crack the size of which is of the same order of magnitude as that of the inclusion.

For example, thermal mismatch between the fibers (inclusions) and surrounding matrix may lead to high residual stresses in the vicinity of the inclusion-matrix interface. These stresses can be tensile in nature and lead to matrix

cracking or interface separation. Consequently, the study of matrix cracking in fiber-reinforced composites has been an area of intense investigation in the literature concerning mechanical failure of fiber-reinforced composite materials (see, for example, Budiansky, et al., 1986; Achenbach and Zhu, 1989, 1990; Hashin, 1990; Goto and Kagawa, 1994; Budiansky, et al., 1995; Ghosh, et al., 2000; Lenci and Menditto, 2000; Liu, et al., 2000; Xiao and Chen, 2000; Liu, et al., 2001).

As mentioned above, the strength of metals and toughness of ceramics, as well as other mechanical properties of ductile or brittle materials, can be greatly improved by fibrous reinforcements. It is known that the mechanical behavior of fiber-reinforced composites is significantly affected by the nature of the bond between fibers and the surrounding matrix material. In addition, the study of the interaction between cracks in the surrounding matrix and any nearby fibers (inclusions) is also extremely significant in attempting to understand and predict the strengthening and hardening mechanisms of fiber-reinforced composites.

In the literature, one of the main results concerning an inclusion/crack interaction, in the case of a *perfect* interface, is that the stress intensity factor at the nearby tip of a radial matrix crack is greater (smaller) than the SIF at the distant crack tip, if and only if the inclusion is more compliant (stiffer) than the matrix (see, for example, Tamate, 1968; Atkinson, 1972 and Guo et al., 1998). This result is of major importance since it determines whether the radial crack grows towards or away from the inclusion. In this thesis, we show that this conclusion is qualitatively invalid when imperfect bonding is present at the inclusion/matrix

interface. In fact, we show that the imperfect bonding allows for the SIF at the nearby crack tip to be greater than the SIF at the distant crack tip even when the inclusion is much stiffer than the matrix. Further, for any given case when the inclusion is stiffer than the matrix, we show that there is a corresponding critical value of the imperfect interface parameter below which the radial matrix crack will grow toward the interface leading eventually to interface debonding.

There are also many problems concerning “matrix cracking” in the study of bone-mechanics. In recent years, there has been an increasing amount of research focused on bone tissue quality and fragility as a result of the need to understand age-related bone fractures. Structural features, such as osteons and cement lines, may dominate fracture mechanisms. In addition, the occurrence and mechanisms associated with microdamage also have attracted great interest, due to its possible relationship to bone fracture and remodeling. For example, microcracks have been observed, both in human cadaveric materials, and following *in vivo* or *in vitro* cyclic loading (Guo, et al., 1998). The microcrack density in human femoral diaphyses has been shown to increase dramatically with aging. The significance of these microcracks is unknown and the mechanical parameters that govern microcrack propagation have not been quantified. From a microstructural and mechanical behavior perspective, osteonal cortical bone shares several similarities with fiber-ceramic matrix composites; osteons are analogous to fibers, interstitial bone tissue is analogous to matrix material, and the cement line acts as a weak interface.

1.3 IMPERFECT INTERFACE MODEL

Traditionally, the fiber (inclusion)-matrix interface is considered as a surface across which both the displacements and tractions are continuous. This assumption is commonly referred to as 'the perfect bonding assumption' or the 'perfect interface' (Dundurs and Zienkiewicz, 1964; Benveniste et al., 1989; Dundurs, 1989; Honein and Herrmann, 1990; Jasiuk et al., 1992; Jayaraman et al., 1992; Ru and Schiavone, 1996). In many practical problems however, various kinds of interfacial damage arising from, for example, microcracks or regions of partial debonding, make the perfect bonding assumption inadequate when modeling the inclusion-matrix interface. In these cases it becomes necessary to model the interface as an *imperfectly bonded interface* incorporating the influence of interface imperfections on the mechanical behavior of the composite. The same is true when an interphase layer (i.e. a non-uniform, thin interfacial zone between the inclusion and the matrix) is created either intentionally, by coating the individual fibers (for example, to improve adhesion) or inadvertently, during the manufacturing process, as a result of chemical reactions between the contacting fiber and surrounding matrix materials. Although small in thickness, interphase layers can significantly affect local stress fields and the subsequent analysis of the mechanical failure of the composite, (see, for example, Benveniste 1984; Aboudi, 1987; Achenbach and Zhu, 1989, 1990; Hashin, 1990, 1991; Gao, 1995; Tandon and Pagano, 1996; Ru and Schiavone, 1997 and Ru, 1998b). Consequently, it becomes important to try to

understand and predict the influence of an imperfectly bonded interphase on the mechanical failure of fiber-reinforced composites.

Many research efforts have been made to investigate the complex behavior of the interphase. The following general observations were discussed in Jayaraman et al., 1992: a) the interphase is responsible for transmitting any interaction between the fiber and the matrix; b) interphasial degradation has a definite effect on the global properties and response of the composite material; and c) interphasial failure may often lead to global failure of composite materials. Given the nature of the interphase and its effect on interfacial bonding, it is important to consider the interfacial bonding stiffness together with the corresponding elastic fields. Thus, incorporating the interphase properties into the analysis not only requires complete knowledge about the interphase, but also demands a more complicated model. A significant amount of research has been devoted to investigating the impact of the interphase, or coating properties (Agarwal and Bansal, 1979; Benveniste et al., 1989; Pagano and Tandon, 1990; Jayaraman et al., 1992) on the mechanical properties of the composites. Recognizing the existence of an interphase implies that the composite has to be regarded, at least, as a three-phase material. Such a consideration requires complete knowledge of the physical properties of the interphase, which is very difficult to measure.

On the other hand, in contrast to the interphase approach outlined above, the concept of *interface* becomes a natural candidate to solve the complex problems associated with an interphase. In three-dimensional problems, an *interface* is defined as a two-dimensional imaginary entity, or border, that physically separates

distinct material phases such as fiber and matrix. Physically, it can be viewed as a limiting case of an interphase layer with very thin (vanishing) thickness. This imaginary boundary separates the bulk materials and, consequently, allows the material properties to be changed abruptly across the interface. Therefore, unless the actual bonding mechanism of the composite or the physical/chemical properties of the interphase is of concern, this model provides a much-simplified way of modeling the complex behavior of the interphase.

One of the widely used mechanical models in describing an imperfect bonding condition is based on the premise that the interphase layer has mechanical properties different from those of either the inclusion or the matrix. The interphase effect can then be described by continuous tractions but discontinuous displacement across the interphase layer. One of the more useful assumptions is that the displacement jumps are proportional, in terms of spring-factor type parameters, to their respective traction components. This type of condition corresponds to modeling the imperfectly bonded interphase layer by a linear spring-layer of vanishing thickness (i.e. an imperfect interface, see, for example, Hashin, 1991; Gao, 1995). The usefulness of this particular model lies in the fact that it allows the representation of intermediate states of bonding between the inclusion and the matrix: from perfect bonding to complete debonding. Hashin (1991) used the aforementioned interface model to examine the stress field inside a spherical inclusion imperfectly bonded to a surrounding matrix. In contrast to the uniform interior stress field associated with a perfectly bonded interface, he found that the

stress field inside the inclusion was no longer uniform. The analogous problem in plane elasticity has been examined by Gao (1995) and Bigoni, et al.(1998).

Most of the existing analytical models are based on the assumption that the fiber-matrix interface has uniform properties, e.g., that the interphase layer has uniform thickness and material properties. In this case, the interface is referred as a *homogeneously imperfect interface*. In most cases of interest in composite mechanics, the interphase layer can be considered to be equal thickness with approximately uniform properties around the inclusion. Hence, the *homogeneously imperfect interface* model, based on the assumption that normal and tangential displacement discontinuities are proportional to the perspective traction components by spring constant-type material parameters (see, for example, Hashin, 1991), provides an adequate approximation to the behavior of the actual interphase layer between the matrix and inclusion. Therefore, in this thesis, we adopt this assumption and base our analysis on the *homogeneously imperfect interface* model.

It will be shown later, that the infinite values of the interface parameters m and n imply vanishing of displacement jumps and therefore correspond to perfect interface conditions; while zero values of the interface parameters imply vanishing of the corresponding interface tractions which corresponds to complete debonding. Any finite positive values of the interface parameters define an imperfect interface. At the same time, the imperfect interface parameters m and n will be characterized for convenience by the new parameters M and N , defined by $M = (m-n)/2$ and $N = (m+n)/2$. In addition, a dimensionless interface parameter N' is defined by $N' = N/(\mu_1/R)$. Since we analyze three different cases: 1) $m = n$; 2) $m = 3n$; and 3) the

case of a sliding interface, $N = (m+n)/2 \sim n$. Therefore, $N' \sim N/(\mu_i/R) \sim n/(\mu_i/R) = n \frac{R}{\mu_i}$, and $n \sim \frac{\mu_t}{t}$, here μ_t and t are the shear modulus and thickness of the interphase layer, respectively; then, we have $N' \sim \frac{R}{t} \frac{\mu_t}{\mu_i}$. For example, if $t=0.1R$ and $\mu_t=10\mu_i$, then, $N'=1$.

It is well known that the single-inclusion problem is the fundamental problem in a composite (Eshelby, 1957, 1959; Hashin, 1991). For example, Eshelby considered one single inclusion and Eshelby's tensor is a well-known solution in composite mechanics. In addition, the single-inclusion model is suitable for modeling composites with lower fiber volume fractions (Schmauder et al., 1992). Under this condition, the interaction among neighboring fibers and its influence on stress fields near the isolated fiber are small and therefore negligible. More importantly, the interaction between neighboring fibers and its influence on the fiber-matrix crack interaction can be described approximately using the effective medium models in which the role of other fibers is represented by the effective elastic constants. Hence, the study of the interaction between a single fiber and a matrix crack is of fundamental significance to understand the major factors affecting matrix cracking.

Furthermore, the single-inclusion model may be extended to the problem of thermal stress analysis. It is well-known that thermal mismatch induced stresses are considered as the main cause of failure in many materials and devices, such as metal-ceramic composites and passivated interconnect lines in integrated circuits

(see, for example, Gouldstone et al., 1998; Gleixner et al., 1997; Ru, 1998a; Ru et al., 1999; Wu, et al., 1996). Many practical problems require a systematical study of the effects of interphase layers on thermal mismatch induced stresses in inclusion/matrix systems. For example, the failure of interconnect lines due to thermal stress-induced voiding has become a major issue in the design of reliable integrated circuits (Gleixner et al., 1997; Gouldstone et al., 1998). In this case, the line is subjected to large tensile stresses upon cooling from high passivation deposition temperatures.

Several investigators have constructed composite models of osteonal cortical bone to study its mechanical properties. For example, Katz (1981) considered the anisotropy of cortical moduli using a hierarchical composite model of osteons made of hollow, right circular cylinders of concentric lamellae. His model describes well trends of elastic anisotropy. More recently, the finite element method has been used to develop osteonal cortical bone models (Hogan, 1992; Crolet, et al., 1993). Hogan studied the elastic moduli and their dependence on material properties of osteon, interstitial bone, and cement lines and found reasonable agreement with experimental data. Crolet et al. applied homogenization techniques to construct a hierarchical osteonal cortical bone model consisting of various levels of microstructure: osteons, interstitial bone, and layers of lamellae with collagen fibers and hydroxyapatite. Their results demonstrate a good agreement with the experimental data and, furthermore, using homogenization techniques allowed them to determine and evaluate the contribution of microstructure at varying levels of hierarchy and under different stress/strain environments.

1.4 THE LIMITATIONS OF THE DISLOCATION-DENSITY METHOD FOR CRACK-INCLUSION INTERACTION

A critical literature review shows that the solution of the interaction between a circular inclusion and a radial matrix crack under the perfect interface assumption, as in many crack problems, can be obtained through the superposition of two solutions. The first refers to the simple problem of a circular elastic inclusion inserted into a matrix without the crack. This problem can be easily solved under the given system of external loads. In the second problem, only the stress disturbance due to the existence of the crack in the matrix is considered. In this problem, the only external loads are the crack surface tractions which are equal in magnitude and opposite in sign to the stresses obtained in the first problem along the line which is the presumed location of the crack. The nonhomogeneous medium may be subjected to an arbitrary set of external loads (including quasi-static thermal loads) applied to the matrix and the inclusion. However, it is assumed that the dimensions of the matrix are sufficiently large so that in the second problem the interaction between the outer boundary of the matrix and the crack-inclusion combination may be neglected. Thus, in the second problem, which contains the singular part of the solution, the matrix will be assumed as being infinite.

The existing most popular method (dislocation-density method) assumes that the crack can be modeled as a distribution of dislocations with unknown

density functions (see, for example, Dundurs and Mura, 1964; Atkinson, 1972; Erdogan et al., 1974 and Guo et al., 1998). In this case, the derivation of the governing integral equations for the unknown density functions is based on the conditions that mechanical tractions vanish along the crack faces. Except for an earlier study concerning a slipping interface (Dundurs and Gangadharan, 1969), to our knowledge, the inclusion/crack interaction remains to be investigated in the case of imperfect bonding between the inclusion and the matrix. This can be attributed to the fact that the extension of the dislocation-density method to an imperfect interface meets two major difficulties: 1) The fundamental solution for the interaction between an isolated dislocation and a circular inclusion with a generally imperfect interface is not yet available; 2) Numerical solution of the resulting singular integral equation for imperfect interfaces would be extremely challenging.

In view of these two difficulties, the main objective of this project is to develop a simple series method (which makes use of analytic continuation) to study the interaction between a radial matrix crack and a circular inclusion under the assumption of imperfect bonding at the inclusion-matrix interface. The results obtained clearly demonstrate that the series method developed here is simple and effective in describing the influence of interface imperfections on the radial matrix crack in a range of different cases.

1.5 OBJECTIVE OF THE PRESENT WORK

The present research emphasizes the interaction between a radial matrix crack and a circular inclusion under the assumption of imperfect bonding at the inclusion-matrix interface. Since the existing dislocation-density method is not suitable for the study of an imperfect interface, our aim is to develop a simple series method to study the effects of imperfect bonding on stress intensity factors (SIFs) calculated at a radial matrix crack in a fiber (inclusion) composite subjected to various cases of mechanical loading.

In the present study, complex variable techniques are used and existing series methods are adapted and extended by analytic continuation to obtain series representations of deformation and stress fields in both the inclusion and the surrounding matrix in the presence of the crack. The interaction between the crack and the inclusion is demonstrated numerically for different elastic materials, geometries and varying degrees of bonding (represented by imperfect interface parameters) at the interface.

In this thesis, three cases of remote mechanical loading are considered in the absence of any eigenstrain inside the inclusion: 1) uniaxial loading normal to the crack, which is of significant practical interest; 2) purely shear loading and 3) uniaxial loading parallel to the crack.

The thesis is organized as follows: Chapter 2 develops the fundamental formulation of a series method. Chapter 3 studies the effect of imperfect bonding under uniaxial loading perpendicular to the crack. The conditions of uniaxial loading

parallel to the crack and pure shear loading are discussed in detail in Chapters 4 and 5, respectively. Chapter 6 provides some concluding remarks and suggestions for future research.

The results indicate that the inclusion can either promote or retard crack propagation in the matrix, depending not only on the ratio of the moduli, but also on the interface imperfection (Liu, et al., 2001). Some qualitatively new phenomena are predicted for radial matrix cracking, specifically the influence of imperfect bonding at the inclusion-matrix interface on the direction of crack growth. To the author's knowledge, these results provide, for the first time, a clear quantitative description of the relationship between interface imperfections and the direction of propagation of radial matrix cracks, and hence, useful information for the design of fiber-matrix interface of fiber composites against matrix cracking.

CHAPTER 2

FORMULATION OF A SERIES METHOD

2.1 INTRODUCTION

In Chapter 1, it was noted that the existing dislocation-density method is not suitable for the study of inclusion-matrix crack interaction in the presence of an imperfect interface. In this chapter, we will develop a simple series method (which makes use of analytic continuation) to study the interaction between a radial matrix crack and a circular inclusion under the assumption of imperfect bonding at the inclusion-matrix interface. Four analytic (potential) functions will be obtained in both the inclusion and the surrounding matrix in the presence of the matrix crack. The results show that the series method developed here is simple and effective in describing the influence of interface imperfections on the radial matrix crack in a range of different cases.

2.2 COMPLEX VARIABLE METHOD

2.2.1 Problem Formulation

One of the most widely used models of an imperfect interface (see, for example, Benveniste, 1984; Aboudi, 1987; Achenbach and Zhu, 1989, 1990;

Hashin, 1990, 1991; Gao, 1995 and Ru and Schiavone, 1997) is based on the assumption that tractions are continuous but displacements are discontinuous across the interface. More precisely, jumps in the displacement components are assumed to be proportional, in terms of ‘spring-factor-type’ interface parameters, to their respective interface traction components. This model of an imperfect interface is often referred to as a ‘spring-layer imperfect interface’.

Consider an infinite elastic plane (matrix) containing a circular inclusion centered at the origin. The circular inclusion is of radius R with shear modulus μ_2 and Poisson’s ratio ν_2 . The surrounding matrix is characterized by shear modulus μ_1 and Poisson’s ratio ν_1 . As illustrated in Figure 2.1, a finite radial matrix crack $L = [a, b]$ with length $2l$ is located outside the inclusion at a distance d from the inclusion-matrix interface. Let S_2 and S_1 be the regions occupied by the inclusion and the cracked matrix (containing the crack L), respectively and Γ the circular interface separating S_2 and S_1 . In what follows, the subscripts 1 and 2 are used to identify quantities in S_1 and S_2 , respectively.

In the case of plane deformations, the corresponding displacement and stress fields are given in terms of two complex potentials $\varphi(z)$ and $\psi(z)$ as follows (England, 1971):

$$\begin{aligned} 2\mu(u + iv) &= \kappa\varphi(z) - z\overline{\varphi'(z)} - \overline{\psi(z)}, \\ \sigma_{xx} + \sigma_{yy} &= 2[\varphi'(z) + \overline{\varphi'(z)}], \\ \sigma_{xx} - i\sigma_{xy} &= \varphi'(z) + \overline{\varphi'(z)} - z\overline{\varphi''(z)} - \psi'(z). \end{aligned} \tag{2.1}$$

Here, $z = x+iy$ is the complex coordinate, $\kappa = (3-4\nu)$ in the case of plane strain (assumed henceforth in this paper) and $(3-\nu)/(1+\nu)$ in the case of plane stress. If polar coordinates are introduced so that $z = x+iy = re^{i\theta}$, (2.1) takes the form:

$$\begin{aligned} 2\mu(u_r + iu_\theta) &= e^{-i\theta} [\kappa \varphi(z) - z \overline{\varphi'(z)} - \overline{\psi(z)}], \\ \sigma_{rr} + \sigma_{\theta\theta} &= 2[\varphi'(z) + \overline{\varphi'(z)}], \\ \sigma_{rr} - i\sigma_{r\theta} &= \varphi'(z) + \overline{\varphi'(z)} - e^{2i\theta} [\overline{z\varphi''(z)} + \psi'(z)]. \end{aligned} \quad (2.2)$$

Hence, all stress and displacement fields can be found from (2.1) or (2.2) once the complex potentials $\varphi(z)$ and $\psi(z)$ are known. Of course, the determination of $\varphi(z)$ and $\psi(z)$ depends on the boundary and interface conditions.

Assume that the circular inclusion is imperfectly bonded to the matrix along Γ by such an interface. The boundary value problem for the displacements in both the inclusion and the matrix can then be formulated in terms of the following interface conditions (Ru, 1998b):

$$\begin{aligned} \|\sigma_{rr} - i\sigma_{r\theta}\| &= 0, \\ \sigma_{rr} &= m \|u_r\| - m u_r^0, \quad \sigma_{r\theta} = n \|u_\theta\| - n u_\theta^0, \quad z \in \Gamma, \end{aligned} \quad (2.3)$$

while the crack-face conditions are given by,

$$\varphi_1(z) + z \overline{\varphi_1'(z)} + \overline{\psi_1(z)} = 0, \quad z \in L. \quad (2.4)$$

Here, m and n are two imperfect interface parameters (which are non-negative and constant along the entire interface), $\| * \| = (*)_1 - (*)_2$ denotes the jump across Γ and u^o is the additional displacement induced by the uniform eigenstrains $\{ \varepsilon_r^o, \varepsilon_v^o, \varepsilon_w^o \}$ prescribed within the inclusion. The first condition of (2.3) indicates that the normal and tangential tractions are continuous across the interface. The second condition of (2.3) indicates that the jump of the displacements across the interface. It is seen from (2.3) that infinite values of the interface parameters m and n imply vanishing of displacement jumps and therefore correspond to perfect interface conditions. On the other hand, zero values of the interface parameters imply vanishing of the corresponding interface tractions which corresponds to complete debonding. Any finite positive values of the interface parameters define an imperfect interface. As noted in Chapter 1, such interface imperfections may be due to the presence of an interphase layer or perhaps interface bond deterioration caused by, for example, fatigue damage or environmental and chemical effects.

The uniform remote loading is described by the conditions

$$\varphi_1(z) \equiv Az + o(1), \quad \psi_1(z) \equiv Bz + o(1), \quad |z| \rightarrow \infty, \quad (2.5)$$

where A (a given real number) and B (a given complex number) are determined by the uniform remote stresses. In the case of a uniaxial load σ^0 normal to the crack (see Figure 2.1), A and B are given by

$$A = \frac{\sigma^0}{4}, \quad B = \bar{B} = 2A = \frac{\sigma^0}{2}.$$

For purely shear loading σ_{xy}^0 , we have $A = 0$, $B = i\sigma_{xy}^0$. Finally, for uniaxial loading σ^0 parallel to the crack (in the x -direction), we have $A = \frac{\sigma^0}{4}$, $B = -2A = -\frac{\sigma^0}{2}$.

2.2.2 Analytic Continuation Theory

In the case of the interaction between a circular inclusion and a radial matrix crack under the perfect interface assumption, the existing most popular method (dislocation-density method) assumes that the crack can be modeled as a distribution of dislocations with unknown density functions (see, for example, Dundurs and Mura, 1964; Atkinson, 1972; Erdogan et al., 1974 and Guo et al., 1998), and the derivation of the governing integral equations for the unknown density functions is based on the conditions that mechanical tractions vanish along the crack faces. Except for an earlier study concerning a slipping interface (Dundurs and Gangadharan, 1969), to the author's knowledge, the inclusion/crack interaction remains to be investigated in the case of imperfect bonding between the inclusion and the matrix. This can be attributed to the fact that the extension of the

dislocation-density method to an imperfect interface meets two major difficulties:

1) The fundamental solution for the interaction between an isolated dislocation and a circular inclusion with a generally imperfect interface is not yet available; 2) Numerical solution of the resulting singular integral equation for imperfect interfaces would be extremely challenging.

A convenient method used to analyze the case of circular boundaries is the series method (England, 1971). However, in the case of the present problem, the domain S_1 contains a crack L so that $\varphi_1(z)$ and $\psi_1(z)$ are not analytic outside the circle Γ . As a result, $\varphi_1(z)$ and $\psi_1(z)$ cannot be expanded into standard Laurent series in S_1 . To overcome this difficulty, a method based on analytic continuation (Tamate, 1968; England, 1971) is employed below to express $\varphi_1(z)$ and $\psi_1(z)$ in terms of two new functions which are analytic outside the circle Γ where they can thus be expanded into standard Laurent series. To this end, denote by D the domain outside the circle Γ minus the matrix crack L (namely, D consists of the complex plane with the circular *hole* S_2 , but without the matrix crack L). Clearly, $\varphi_1(z)$ and $\psi_1(z)$ are analytic in S_1 , but not in D . Thus, the crack-face conditions (2.4) along the upper and lower faces of L given by:

$$\varphi_1(z)^+ + z \overline{\varphi_1'(z)^+} + \overline{\psi_1(z)^+} = 0, \quad z \in L^+,$$

$$\varphi_1(z)^- + z \overline{\varphi_1'(z)^-} + \overline{\psi_1(z)^-} = 0, \quad z \in L^-,$$

can be written into the equivalent form

$$\varphi_1(z)^+ + [z\bar{\varphi}'_1(z) + \overline{\psi_1(z)}]^- = 0, \quad z \in L, \quad (2.6)$$

$$\varphi_1(z)^- + [z\bar{\varphi}'_1(z) + \overline{\psi_1(z)}]^+ = 0, \quad z \in L.$$

It thus follows that

$$\varphi_1(z)^+ - [z\bar{\varphi}'_1(z) + \overline{\psi_1(z)}]^+ = \varphi_1(z)^- - [z\bar{\varphi}'_1(z) + \overline{\psi_1(z)}]^-, \quad z \in L. \quad (2.7)$$

Next, we define an analytic function $\Phi(z)$ in S_1 by:

$$\Phi(z) = \varphi_1(z) - [z\bar{\varphi}'_1(z) + \overline{\psi_1(z)}]. \quad (2.8)$$

(note that analytic continuation implies that both $\bar{\varphi}_1(z)$ and $\overline{\psi_1(z)}$ are analytic in S_1). The above continuity condition (2.7) implies that $\Phi(z)$ is continuous across L . Consequently, $\Phi(z)$ is analytic in D and can then be expanded into a Laurent series in D as

$$\Phi(z) = -\bar{B}z + \sum_{k=1}^{\infty} a_k z^{-k}, \quad z \in D, \quad (2.9)$$

where a_k ($k=1,2,\dots$) are unknown complex coefficients.

Furthermore, the remaining crack-face condition (2.6) can be rewritten as

$$[\varphi_1(z) + z\bar{\varphi}'_1(z) + \overline{\psi_1(z)}]^+ + [\varphi_1(z) + z\bar{\varphi}'_1(z) + \overline{\psi_1(z)}]^- = 0, \quad z \in L. \quad (2.10)$$

We introduce another analytic function $\Psi(z)$ in S_1 as follows:

$$\Psi(z) = \frac{\sqrt{(z-a)(z-b)}}{z} [\varphi_1(z) + z\bar{\varphi}'_1(z) + \bar{\psi}_1(z)]. \quad (2.11)$$

Then, since (England, 1971)

$$\sqrt{(z-a)(z-b)}^- = -\sqrt{(z-a)(z-b)}^+ \quad , \quad z \in L = [a, b],$$

condition (2.11) can be written in terms of $\Psi(z)$ as

$$\Psi(z)^+ - \Psi(z)^- = 0, \quad z \in L. \quad (2.12)$$

It follows that $\Psi(z)$ is continuous across L and analytic in D and can therefore be expanded into a Laurent series in D as follows:

$$\Psi(z) = (2A + \bar{B})z + \sum_{k=1}^{\infty} b_k z^{-k}, \quad (2.13)$$

where b_k ($k=1,2,\dots$) are unknown complex coefficients.

Now, $\varphi_1(z)$ and $\psi_1(z)$ can be expressed in terms of $\Phi(z)$ and $\Psi(z)$ as

$$\psi_1(z) = \bar{\varphi}_1(z) - z\varphi'_1(z) - \bar{\Phi}(z), \quad (2.14)$$

$$\varphi_1(z) = \frac{z\Psi(z)}{2\sqrt{(z-a)(z-b)}} + \frac{\Phi(z)}{2}. \quad (2.15)$$

On the other hand, $\varphi_2(z)$ and $\psi_2(z)$ are analytic within the circular inclusion and can then be expanded into their respective Maclaurin's series in S_2 :

$$\varphi_2(z) = \sum_{k=0}^{\infty} d_k z^k, \quad \psi_2(z) = \sum_{k=0}^{\infty} e_k z^k, \quad (2.16)$$

where d_k and e_k are complex coefficients. Hence, the problem reduces to determining the four sets of unknown coefficients a_k , b_k , d_k and e_k , such that the two interface conditions (2.3) can be satisfied on Γ .

The traction continuity conditions (2.3) give:

$$\begin{aligned} \varphi_1'(z) - z\varphi_1''(z) - \frac{\bar{z}^2}{R^2}\psi_1'(z) + \bar{\varphi}_1'\left(\frac{R^2}{z}\right) = \\ \varphi_2'(z) - z\varphi_2''(z) - \frac{\bar{z}^2}{R^2}\psi_2'(z) + \bar{\varphi}_2'\left(\frac{R^2}{z}\right) \end{aligned} \quad (2.17)$$

On the other hand, the remaining two displacement interface conditions (2.3) can be written in the complex form:

$$\sigma_{rr} - i\sigma_{r\theta} = \frac{m-n}{2}\|u_r + iu_\theta\| + \frac{m+n}{2}\|u_r - iu_\theta\| - [mu_r^0 - inu_\theta^0].$$

On using (2.2), the above displacement discontinuity conditions can be rewritten as follows:

$$\begin{aligned}
& \frac{m-n}{2} \left\{ \frac{R}{2\mu_1 z} [\kappa_1 \varphi_1(z) - z \overline{\varphi_1'}(\frac{R^2}{z}) - \overline{\psi_1}(\frac{R^2}{z})] - \frac{R}{2\mu_2 z} [\kappa_2 \varphi_2(z) - \right. \\
& \left. z \overline{\varphi_2'}(\frac{R^2}{z}) - \overline{\psi_2}(\frac{R^2}{z})] \right\} + \frac{m+n}{2} \left\{ \frac{z}{2\mu_1 R} [\kappa_1 \overline{\varphi_1}(\frac{R^2}{z}) - \overline{z \varphi_1'}(z) - \overline{\psi_1}(z)] - \right. \\
& \left. \frac{z}{2\mu_2 R} [\kappa_2 \overline{\varphi_2}(\frac{R^2}{z}) - \overline{z \varphi_2'}(z) - \overline{\psi_2}(z)] \right\} - mR\varepsilon_1 - (\frac{m+n}{2R})(\varepsilon_2 - i\varepsilon_3)z^2 - \\
& (\frac{m-n}{2z^2})R^3(\varepsilon_2 + i\varepsilon_3) = \varphi_2'(z) - z\varphi_2''(z) - \frac{z^2}{R^2}\psi_2'(z) + \overline{\varphi_2'}(\frac{R^2}{z})
\end{aligned} \tag{2.18}$$

where $\varepsilon_1 = \frac{\varepsilon_x^0 + \varepsilon_y^0}{2}$, $\varepsilon_2 = \frac{\varepsilon_x^0 - \varepsilon_y^0}{2}$ and $\varepsilon_3 = \varepsilon_{xy}^0$ (see, Ru, 1998). Hence, all

unknown coefficients a_k , b_k , d_k and e_k ($k=1,2,\dots$) can be determined by the interface conditions (2.17) and (2.18).

2.3 STRESS INTENSITY FACTOR

To derive the formulas for the stress intensity factor (SIF), it is noted from (2.1) that the stresses in the matrix are given by:

$$\sigma_{yy} = Re[\varphi_1'(z) + \overline{\varphi_1'(z)} + z \overline{\varphi_1''(z)} + \overline{\psi_1''(z)}],$$

$$\sigma_{xx} = Re[\varphi_1'(z) + \overline{\varphi_1'(z)} - z \overline{\varphi_1''(z)} - \overline{\psi_1''(z)}]$$

and

$$\sigma_{xy} = Im[\varphi_1'(z) + \overline{\varphi_1'(z)} - z \overline{\varphi_1''(z)} - \overline{\psi_1''(z)}].$$

On using

$$\psi_1(z) = \bar{\varphi}_1(z) - z\varphi'_1(z) - \bar{\Phi}(z),$$

the above expressions can be re-written as

$$\sigma_{yy} = Re[\varphi'_1(z) + \varphi'_1(\bar{z}) + (z - \bar{z})\overline{\varphi''_1(z)} - \Phi'(\bar{z})],$$

$$\sigma_{xx} = Re[\varphi'_1(z) - \varphi'_1(\bar{z}) + 2\overline{\varphi'_1(z)} + (\bar{z} - z)\overline{\varphi''_1(z)} + \Phi'(\bar{z})],$$

$$\sigma_{xy} = Im[\varphi'_1(z) - \varphi'_1(\bar{z}) + 2\overline{\varphi'_1(z)} + (\bar{z} - z)\overline{\varphi''_1(z)} + \Phi'(\bar{z})],$$

where $\varphi_1(z)$ is given by (2.15). Since the leading-order singularity is the inverse square-root singularity, it follows that

$$\Psi(a) = \Psi(b) = 0.$$

As expected, these conditions are verified by our numerical results obtained later. In following Chapters 3, 4 and 5, the stresses in the neighborhood of the crack tip $z = a$ and $z = b$ are given under different remote loading conditions, respectively.

2.4 CONCLUSIONS

To overcome the major difficulties of the existing dislocation-density method, a novel series method is presented. In this method, we use analytic continuation to obtain a representation (2.14) and (2.15) of the complex potentials $\varphi_1(z)$ and $\psi_1(z)$ in the matrix, in terms of two new functions $\Phi(z)$ and $\Psi(z)$ which are analytic outside the inclusion and can then be expanded into standard Laurent series (2.9) and (2.13). It is stressed that the crack face conditions (2.4) or (2.6) are automatically satisfied by (2.14) and (2.15), provided that $\Phi(z)$ and $\Psi(z)$ are

analytic outside the circular inclusion. On the other hand, because $\varphi_2(z)$ and $\psi_2(z)$ are analytic inside the circular inclusion they can be expanded into Taylor series (2.16) within the circular domain. Thus, four sets of the unknown coefficients a_k , b_k , d_k and e_k will be determined by the remaining interface conditions (2.17) and (2.18). In following chapters, these unknown coefficients will be determined and the interaction between the crack and the inclusion will be demonstrated numerically for different elastic materials, geometries and varying degrees of bonding (represented by imperfect interface parameters) at the interface. The effects of imperfect bonding on stress intensity factors (SIFs) calculated at a radial matrix crack in a fiber (inclusion) composite subjected to various cases of mechanical loading will be studied in Chapters 3, 4 and 5, respectively.

CHAPTER 3

EFFECT OF IMPERFECT BONDING ON RADIAL MATRIX CRACKING --UNIAXIAL LOADING NORMAL TO THE CRACK

3.1 DESCRIPTION OF THE PROBLEM

In the present chapter, we consider the problem of interaction between a radial matrix crack and a circular inclusion under the uniaxial remote loading perpendicular to the crack when the bonding at the inclusion-matrix interface is homogeneously imperfect. By adapting the potential functions derived in Chapter 2, we obtain series representations of deformation and stress fields in both the inclusion and the surrounding matrix in the presence of the crack. The interaction between the crack and the inclusion is demonstrated numerically for different elastic materials, geometries and varying degrees of bonding (represented by imperfect interface parameters) at the interface.

3.2 PROBLEM SOLUTIONS

3.2.1 Problem Formulation

Let us define $F(z)$ as:

$$F(z) = \frac{z}{2\sqrt{(z-a)(z-b)}}.$$

Because $F(z)$ is analytic in $S_2 + \Gamma$, it can be expanded into a Taylor series within a circular domain of radius larger than R but smaller than a and valid at the circular interface as:

$$F(z) = \sum_{k=1}^{\infty} c_k z^k.$$

where c_k are the known real coefficients. Here, we only give the first 11 coefficients of c_k as follows:

$$c_1 = -\frac{(ab)^{-\frac{1}{2}}}{2},$$

$$c_2 = -\frac{(ab)^{-\frac{3}{2}}(a+b)}{2 \times 2 \times 1!},$$

$$c_3 = -\frac{1}{2 \times 2!} \left[\frac{1 \times 3}{2^2} (ab)^{-\frac{5}{2}} (a+b)^2 - (ab)^{-\frac{3}{2}} \right]$$

$$c_4 = -\frac{1}{2 \times 3!} \left[\frac{1 \times 3 \times 5}{2^3} (ab)^{-\frac{7}{2}} (a+b)^3 - \frac{9}{2} (ab)^{-\frac{5}{2}} (a+b) \right]$$

$$c_5 = -\frac{1}{2 \times 4!} \left[\frac{1 \times 3 \times 5 \times 7}{2^4} (ab)^{-\frac{9}{2}} (a+b)^4 - \frac{1 \times 3 \times 5 \times 3}{2} (ab)^{-\frac{7}{2}} (a+b)^2 + 9(ab)^{-\frac{5}{2}} \right]$$

$$c_6 = -\frac{1}{2 \times 5!} \left[\frac{1 \times 3 \times 5 \times 7 \times 9}{2^5} (ab)^{-\frac{11}{2}} (a+b)^5 - \frac{1 \times 3 \times 5 \times 7 \times 5}{2^2} (ab)^{-\frac{9}{2}} (a+b)^3 + \frac{1 \times 3 \times 5 \times 5 \times 3}{2} (ab)^{-\frac{7}{2}} (a+b) \right]$$

.

$$c_7 = -\frac{1}{2 \times 6!} \left[\frac{1 \times 3 \times 5 \times 7 \times 9 \times 11}{2^6} (ab)^{\frac{13}{2}} (a+b)^6 - \frac{1 \times 3 \times 5 \times 7 \times 9 \times 5 \times 3}{2^4} (ab)^{\frac{11}{2}} (a+b)^4 + \frac{1 \times 3 \times 5 \times 7 \times 5 \times 3 \times 3}{2^2} (ab)^{\frac{9}{2}} (a+b)^2 - 1 \times 3 \times 5 \times 3 \times (ab)^{\frac{7}{2}} \right]$$

$$c_8 = -\frac{1}{2 \times 7!} \left[\frac{1 \times 3 \times 5 \times 7 \times 9 \times 11 \times 13}{2^7} (ab)^{\frac{15}{2}} (a+b)^7 - \frac{1 \times 3 \times 5 \times 7 \times 9 \times 11 \times 7 \times 3}{2^5} (ab)^{\frac{13}{2}} (a+b)^5 + \frac{1 \times 3 \times 5 \times 7 \times 9 \times 5 \times 3 \times 7}{2^3} (ab)^{\frac{11}{2}} (a+b)^3 - \frac{1 \times 3 \times 5 \times 7 \times 5 \times 3 \times 7}{2} (ab)^{\frac{9}{2}} (a+b) \right]$$

$$c_9 = -\frac{1}{2 \times 8!} \left[\frac{1 \times 3 \times 5 \times 7 \times 9 \times 11 \times 13 \times 15}{2^8} (ab)^{\frac{17}{2}} (a+b)^8 - \frac{1 \times 3 \times 5 \times 7 \times 9 \times 11 \times 13 \times 7 \times 4}{2^6} (ab)^{\frac{15}{2}} (a+b)^6 + \frac{1 \times 3 \times 5 \times 7 \times 9 \times 11 \times 15 \times 7}{2^4} (ab)^{\frac{13}{2}} (a+b)^4 - \frac{1 \times 3 \times 5 \times 7 \times 9 \times 15 \times 14}{2^2} (ab)^{\frac{11}{2}} (a+b)^2 + 1 \times 3 \times 5 \times 7 \times 15 \times 7 (ab)^{\frac{9}{2}} \right]$$

$$c_{10} = -\frac{1}{2 \times 9!} \left[\frac{1 \times 3 \times 5 \times 7 \times 9 \times 11 \times 13 \times 15 \times 17}{2^9} (ab)^{\frac{19}{2}} (a+b)^9 - \frac{1 \times 3 \times 5 \times 7 \times 9 \times 11 \times 13 \times 15 \times 9 \times 4}{2^7} (ab)^{\frac{17}{2}} (a+b)^7 + \frac{1 \times 3 \times 5 \times 7 \times 9 \times 11 \times 13 \times 7 \times 27}{2^5} (ab)^{\frac{15}{2}} (a+b)^5 - \frac{1 \times 3 \times 5 \times 7 \times 9 \times 11 \times 13 \times 15 \times 3}{2^3} (ab)^{\frac{13}{2}} (a+b)^3 + \frac{1 \times 3 \times 5 \times 7 \times 9 \times 25 \times 27}{2} (ab)^{\frac{11}{2}} (a+b) \right]$$

$$\begin{aligned}
c_{11} = & -\frac{1}{2 \times 10!} \left[\frac{1 \times 3 \times 5 \times 7 \times 9 \times 11 \times 13 \times 15 \times 17 \times 19}{2^{10}} (ab)^{\frac{21}{2}} (a+b)^{10} - \right. \\
& \frac{1 \times 3 \times 5 \times 7 \times 9 \times 11 \times 13 \times 15 \times 17 \times 9 \times 5}{2^8} (ab)^{\frac{19}{2}} (a+b)^8 + \\
& \frac{1 \times 3 \times 5 \times 7 \times 9 \times 11 \times 13 \times 15 \times 9 \times 7 \times 10}{2^6} (ab)^{\frac{17}{2}} (a+b)^6 - \\
& \frac{1 \times 3 \times 5 \times 7 \times 9 \times 11 \times 13 \times 9 \times 17 \times 10}{2^3} (ab)^{\frac{15}{2}} (a+b)^4 + \\
& \left. \frac{1 \times 3 \times 5 \times 7 \times 9 \times 11 \times 5 \times 27 \times 31}{2^2} (ab)^{\frac{13}{2}} (a+b)^2 - 1 \times 3 \times 5 \times \right. \\
& \left. 7 \times 9 \times 25 \times 27 (ab)^{\frac{11}{2}} \right]
\end{aligned}$$

If we retain the first 8 terms of $F(z)$ as an approximation to $F(z)$ and retain the first 4 terms (including z terms) for $\Phi(z)$ and $\Psi(z)$, while $\varphi_2(z)$ and $\psi_2(z)$ keep five terms (including z^0 terms), then, $\Phi(z)$, $\Psi(z)$, $\varphi_2(z)$ and $\psi_2(z)$ can be expressed as:

$$\Phi(z) = -\bar{B}z + a_1 z^{-1} + a_2 z^{-2} + a_3 z^{-3} + a_4 z^{-4};$$

$$\Psi(z) = (2A + \bar{B})z + b_1 z^{-1} + b_2 z^{-2} + b_3 z^{-3} + b_4 z^{-4};$$

$$\varphi_2(z) = d_0 + d_1 z + d_2 z^2 + d_3 z^3 + d_4 z^4;$$

$$\psi_2(z) = e_0 + e_1 z + e_2 z^2 + e_3 z^3 + e_4 z^4.$$

where a_k , b_k , d_k , e_k are unknown coefficients.

Substitute $F(z)$, $\Phi(z)$ and $\Psi(z)$ into Eq. (2.15) in Chapter 2, we have

$$\varphi_1(z) = F(z)\Psi(z) + \frac{\Phi(z)}{2} =$$

$$\begin{aligned} & c_8(2A + \bar{B})z^9 + c_7(2A + \bar{B})z^8 + [c_8b_1 + c_6(2A + \bar{B})]z^7 + [c_8b_2 + \\ & c_7b_1 + c_5(2A + \bar{B})]z^6 + [c_8b_3 + c_7b_2 + c_6b_1 + c_4(2A + \bar{B})]z^5 + [c_8b_4 + \\ & c_7b_3 + c_6b_2 + c_5b_1 + c_3(2A + \bar{B})]z^4 + [c_7b_4 + c_6b_3 + c_5b_2 + c_4b_1 + \\ & c_2(2A + \bar{B})]z^3 + [c_6b_4 + c_5b_3 + c_4b_2 + c_3b_1 + c_1(2A + \bar{B})]z^2 + (c_5b_4 + \\ & c_4b_3 + c_3b_2 + c_2b_1 - \frac{\bar{B}}{2})z + (c_4b_4 + c_3b_3 + c_2b_2 + c_1b_1) + (c_3b_4 + c_2b_3 + \\ & c_1b_2 + \frac{a_1}{2})z^{-1} + (c_2b_4 + c_1b_3 + \frac{a_2}{2})z^{-2} + (c_1b_4 + \frac{a_3}{2})z^{-3} + \frac{a_4}{2}z^{-4} \end{aligned}$$

$$\psi_1(z) = \bar{\varphi}_1(z) - z\varphi'_1(z) - \bar{\Phi}(z) =$$

$$\begin{aligned} & [c_8(2A + B) - 9c_8(2A + \bar{B})]z^9 + [c_7(2A + B) - 8c_7(2A + \bar{B})]z^8 + [c_8\bar{b}_1 + \\ & c_6(2A + B) - 7c_8\bar{b}_1 - 7c_7(2A + \bar{B})]z^7 + [c_8\bar{b}_2 + c_7\bar{b}_1 + c_5(2A + B) - \\ & 6c_8\bar{b}_2 - 6c_7\bar{b}_1 - 6c_6(2A + \bar{B})]z^6 + [c_8\bar{b}_3 + c_7\bar{b}_2 + c_6\bar{b}_1 + c_4(2A + B) - \\ & 5c_8\bar{b}_3 - 5c_7\bar{b}_2 - 5c_6\bar{b}_1 - 5c_4(2A + \bar{B})]z^5 + [c_8\bar{b}_4 + c_7\bar{b}_3 + c_6\bar{b}_2 + c_5\bar{b}_1 + \\ & c_3(2A + B) - 4c_8\bar{b}_4 - 4c_7\bar{b}_3 - 4c_6\bar{b}_2 - 4c_5\bar{b}_1 - 4c_3(2A + \bar{B})]z^4 + [c_7\bar{b}_4 + \\ & c_6\bar{b}_3 + c_5\bar{b}_2 + c_4\bar{b}_1 + c_2(2A + B) - 3c_7\bar{b}_4 - 3c_6\bar{b}_3 - 3c_5\bar{b}_2 - 3c_4\bar{b}_1 - \\ & 3c_2(2A + \bar{B})]z^3 + [c_6\bar{b}_4 + c_5\bar{b}_3 + c_4\bar{b}_2 + c_3\bar{b}_1 + c_1(2A + B) - 2c_6\bar{b}_4 - \\ & 2c_5\bar{b}_3 - 2c_4\bar{b}_2 - 2c_3\bar{b}_1 - 2c_1(2A + \bar{B})]z^2 + (c_5\bar{b}_4 + c_4\bar{b}_3 + c_3\bar{b}_2 + c_2\bar{b}_1 + \\ & \frac{B}{2} - c_5\bar{b}_4 - c_4\bar{b}_3 - c_3\bar{b}_2 - c_2\bar{b}_1 + \frac{\bar{B}}{2})z + (c_4\bar{b}_4 + c_3\bar{b}_3 + c_2\bar{b}_2 + c_1\bar{b}_1) + \\ & (c_3\bar{b}_4 + c_2\bar{b}_3 + c_1\bar{b}_2 - \frac{\bar{a}_1}{2} + c_3b_4 + c_2b_3 + c_1b_2 + \frac{a_1}{2})z^{-1} + (c_2\bar{b}_4 + c_1\bar{b}_3 - \\ & \frac{\bar{a}_2}{2} + 2c_2b_4 + 2c_1b_3 + a_2)z^{-2} + (c_1\bar{b}_4 - \frac{\bar{a}_3}{2} + 3c_1b_4 + \frac{3a_3}{2})z^{-3} + (2a_4 - \frac{\bar{a}_4}{2})z^{-4} \end{aligned}$$

Hence, substituting $\varphi_1(z)$, $\psi_1(z)$, $\varphi_2(z)$ and $\psi_2(z)$ into the traction continuity condition [(2.16) of Chapter 2] yields:

$$\begin{aligned}
& \{ 9c_8(2A + \bar{B})z^8 + 8c_7(2A + \bar{B})z^7 + 7[c_8b_1 + c_6(2A + \bar{B})]z^6 + 6[c_7b_1 + \\
& c_8b_2 + c_5(2A + \bar{B})]z^5 + 5[c_8b_3 + c_7b_2 + c_6b_1 + c_4(2A + \bar{B})]z^4 + 4[c_8b_4 + \\
& c_7b_3 + c_6b_2 + c_5b_1 + c_3(2A + \bar{B})]z^3 + 3[c_7b_4 + c_6b_3 + c_5b_2 + c_4b_1 + \\
& c_2(2A + \bar{B})]z^2 + 2[c_6b_4 + c_5b_3 + c_4b_2 + c_3b_1 + c_1(2A + \bar{B})]z + (c_5b_4 + \\
& c_4b_3 + c_3b_2 + c_2b_1 - \frac{\bar{B}}{2}) - (c_3b_4 + c_2b_3 + c_1b_2 + \frac{a_1}{2})z^{-1} - 2(c_2b_4 + \\
& c_1b_3 + \frac{a_2}{2})z^{-2} - (3c_1b_4 + \frac{3a_3}{2})z^{-3} - 2a_4z^{-4} \} - \left\{ 72c_8(2A + \bar{B})z^8 + \right. \\
& 56c_7(2A + \bar{B})z^7 + 42[c_8b_1 + c_6(2A + \bar{B})]z^6 + 30[c_7b_1 + c_8b_2 + \\
& c_5(2A + \bar{B})]z^5 + 20[c_8b_3 + c_7b_2 + c_6b_1 + c_4(2A + \bar{B})]z^4 + 12[c_8b_4 + \\
& c_7b_3 + c_6b_2 + c_5b_1 + c_3(2A + \bar{B})]z^3 + 6[c_7b_4 + c_6b_3 + c_5b_2 + c_4b_1 + \\
& c_2(2A + \bar{B})]z^2 + 2[c_6b_4 + c_5b_3 + c_4b_2 + c_3b_1 + c_1(2A + \bar{B})]z + \\
& 2(c_3b_4 + c_2b_3 + c_1b_2 + \frac{a_1}{2})z^{-1} + 6(c_2b_3 + c_1b_2 + \frac{a_2}{2})z^{-2} + 12(c_1b_4 + \\
& \frac{a_3}{2})z^{-3} + 10a_4z^{-4} \} - \frac{1}{R^2} \left\{ 9[c_8(2A + B) - 9c_8(2A + \bar{B})]z^{10} + 8[c_7(2A + B) - \right. \\
& 8c_7(2A + \bar{B})]z^9 + 7[c_8\bar{b}_1 + c_6(2A + B) - 7c_8b_1 - 7c_6(2A + \bar{B})]z^8 + \\
& 6[c_8\bar{b}_2 + c_7\bar{b}_1 + c_5(2A + B) - 6c_8b_2 - c_7b_1 - 6c_5(2A + \bar{B})]z^7 + 5[c_8\bar{b}_3 + \\
& c_7\bar{b}_2 + c_6\bar{b}_1 + c_4(2A + B) - 5c_8b_3 - 5c_7b_2 - 5c_6b_1 - 5c_4(2A + \bar{B})]z^6 + \\
& 4[c_8\bar{b}_4 + c_7\bar{b}_3 + c_6\bar{b}_2 + c_5\bar{b}_1 + c_3(2A + B) -
\end{aligned}$$

$$\begin{aligned}
& 4c_8 \bar{b}_4 - 4c_7 \bar{b}_3 - 4c_6 \bar{b}_2 - 4c_5 \bar{b}_1 - 4c_3 (2A + \bar{B})]z^5 + 3[c_7 \bar{b}_4 + c_6 \bar{b}_3 + c_5 \bar{b}_2 + \\
& c_4 \bar{b}_1 + c_2 (2A + B) - 3c_7 \bar{b}_4 - 3c_6 \bar{b}_3 - 3c_5 \bar{b}_2 - 3c_4 \bar{b}_1 - 3c_2 (2A + \bar{B})]z^4 + \\
& 2[c_6 \bar{b}_4 + c_5 \bar{b}_3 + c_4 \bar{b}_2 + c_3 \bar{b}_1 + c_1 (2A + B) - 2c_6 \bar{b}_4 - 2c_5 \bar{b}_3 - 2c_4 \bar{b}_2 - \\
& 2c_3 \bar{b}_1 - 2c_1 (2A + \bar{B})]z^3 + (c_5 \bar{b}_4 + c_4 \bar{b}_3 + c_3 \bar{b}_2 + c_2 \bar{b}_1 + \frac{B}{2} - c_5 \bar{b}_4 - \\
& c_4 \bar{b}_3 - c_3 \bar{b}_2 - c_2 \bar{b}_1 + \frac{\bar{B}}{2})z^2 - (c_3 \bar{b}_4 + c_2 \bar{b}_3 + c_1 \bar{b}_2 - \frac{\bar{a}_1}{2} + c_1 \bar{b}_2 + c_2 \bar{b}_3 + \\
& c_3 \bar{b}_4 + \frac{a_1}{2}) - 2(c_2 \bar{b}_4 + c_1 \bar{b}_3 - \frac{\bar{a}_2}{2} + 2c_2 \bar{b}_4 + 2c_1 \bar{b}_3 + a_2)z^{-1} - 3(c_1 \bar{b}_4 - \frac{\bar{a}_3}{2} + \\
& 3c_1 \bar{b}_4 + \frac{3a_3}{2})z^{-2} - 4(2a_4 - \frac{\bar{a}_4}{2})z^{-3} \} + \{ 9R^{10}c_3 (2A + B)z^{-4} + \\
& 8R^{14}c_1 (2A + B)z^{-7} + 7R^{12}[c_3 \bar{b}_1 + c_6 (2A + B)]z^{-6} + 6R^{10}[c_3 \bar{b}_2 + c_5 \bar{b}_1 + \\
& c_5 (2A + B)]z^{-5} + 5R^8[c_3 \bar{b}_3 + c_5 \bar{b}_2 + c_6 \bar{b}_1 + c_4 (2A + B)]z^{-4} + 4R^6[c_3 \bar{b}_4 + \\
& c_5 \bar{b}_3 + c_6 \bar{b}_2 + c_5 \bar{b}_1 + c_3 (2A + B)]z^{-3} + 3R^4[c_5 \bar{b}_4 + c_6 \bar{b}_3 + c_5 \bar{b}_2 + c_4 \bar{b}_1 + \\
& c_2 (2A + B)]z^{-2} + 2R^2[c_6 \bar{b}_4 + c_5 \bar{b}_3 + c_4 \bar{b}_2 + c_3 \bar{b}_1 + c_1 (2A + B)]z^{-1} + (c_5 \bar{b}_4 + \\
& c_4 \bar{b}_3 + c_3 \bar{b}_2 + c_2 \bar{b}_1 - \frac{B}{2}) - \frac{1}{R^4}(c_1 \bar{b}_2 + c_2 \bar{b}_3 + \frac{\bar{a}_1}{2} + c_3 \bar{b}_4)z^2 - \frac{2}{R^6}(c_1 \bar{b}_3 + \\
& c_2 \bar{b}_4 + \frac{\bar{a}_2}{2})z^3 - \frac{1}{R^8}(3c_1 \bar{b}_4 + \frac{3\bar{a}_3}{2})z^4 - \frac{2}{R^{10}}\bar{a}_4 z^5 \} = \\
& d_1 + 2d_2 z + 3d_3 z^2 + 4d_4 z^3 - 2d_2 z - 6d_3 z^2 - 12d_4 z^3 - \frac{1}{R^2}(e_1 z^2 + 2e_2 z^3 \\
& + 3e_3 z^4 + 4e_4 z^5) + (\bar{d}_1 + 2\bar{d}_2 R^2 z^{-1} + 3\bar{d}_3 R^4 z^{-2} + 4\bar{d}_4 R^6 z^{-3})
\end{aligned}$$

On the other hand, substituting $\varphi_1(z)$, $\psi_1(z)$, $\varphi_2(z)$ and $\psi_2(z)$ into displacement discontinuities condition [(2.17) of Chapter 2] gives:

$$\begin{aligned}
& \frac{m-n}{2} \left\{ \frac{R}{2\mu_1} \left\{ \left\{ \kappa_1 [c_3 b_2 + c_4 b_1 + c_5 (2A + \bar{B})] z^5 + \kappa_1 [c_3 b_3 + c_4 b_2 + c_5 b_1 + c_6 (2A + \bar{B})] z^4 \right. \right. \right. \\
& + \kappa_1 [c_3 b_4 + c_4 b_3 + c_5 b_2 + c_6 b_1 + c_7 (2A + \bar{B})] z^3 + \kappa_1 [c_3 b_4 + c_5 b_3 + c_6 b_2 + c_7 b_1 + \\
& c_8 (2A + \bar{B})] z^2 + \kappa_1 [c_6 b_4 + c_5 b_3 + c_4 b_2 + c_3 b_1 + c_1 (2A + \bar{B})] z + \kappa_1 [c_5 b_4 + c_4 b_3 + \\
& c_3 b_2 + c_2 b_1 - \frac{\bar{B}}{2}] + \kappa_1 (c_4 b_4 + c_3 b_3 + c_2 b_2 + c_1 b_1) z^{-1} + \kappa_1 (c_3 b_4 + c_2 b_3 + c_1 b_2 + \\
& \frac{a_1}{2}) z^{-2} + \kappa_1 (c_2 b_4 + c_1 b_3 + \frac{a_2}{2}) z^{-3} + \kappa_1 (c_1 b_4 + \frac{a_3}{2}) z^{-4} + \kappa_1 \frac{a_4}{2} z^{-5} \left. \right\} - \\
& \left\{ 5R^8 [c_3 \bar{b}_3 + c_4 \bar{b}_2 + c_5 \bar{b}_1 + c_6 (2A + B)] z^{-4} + 4R^6 [c_3 \bar{b}_4 + c_4 \bar{b}_3 + c_5 \bar{b}_2 + \right. \\
& c_6 \bar{b}_1 + c_7 (2A + B)] z^{-3} + 3R^4 [c_3 \bar{b}_4 + c_5 \bar{b}_3 + c_6 \bar{b}_2 + c_7 \bar{b}_1 + c_8 (2A + B)] z^{-2} + \\
& 2R^2 [c_6 \bar{b}_4 + c_5 \bar{b}_3 + c_4 \bar{b}_2 + c_3 \bar{b}_1 + c_1 (2A + B)] z^{-1} + (c_5 \bar{b}_4 + c_4 \bar{b}_3 + c_3 \bar{b}_2 + \\
& c_2 \bar{b}_1 - \frac{B}{2}) - \frac{1}{R^4} (c_1 \bar{b}_2 + c_2 \bar{b}_3 + \frac{\bar{a}_1}{2} + c_3 \bar{b}_4) z^2 - \frac{2}{R^6} (c_1 \bar{b}_3 + c_2 \bar{b}_4 + \frac{\bar{a}_2}{2}) z^3 - \\
& \frac{1}{R^8} (3c_1 \bar{b}_4 + \frac{3\bar{a}_1}{2}) z^4 - \frac{2\bar{a}_4}{R^{10}} z^5 \left. \right\} - \left\{ R^6 [c_3 b_4 + c_5 b_3 + c_6 b_2 + c_7 b_1 + c_8 (2A + \bar{B}) - \right. \\
& 3c_3 \bar{b}_4 - 3c_5 \bar{b}_3 - 3c_6 \bar{b}_2 - 3c_7 \bar{b}_1 - 3c_8 (2A + B)] z^{-4} + R^4 [c_6 b_4 + c_5 b_3 + c_4 b_2 + c_3 b_1 + \\
& c_1 (2A + \bar{B}) - 2c_6 \bar{b}_4 - 2c_5 \bar{b}_3 - 2c_4 \bar{b}_2 - 2c_3 \bar{b}_1 - 2c_1 (2A + B)] z^{-3} + R^2 (c_3 b_4 + c_4 b_3 + \\
& c_5 b_2 + c_6 b_1 + \frac{\bar{B}}{2} - c_3 \bar{b}_4 - c_4 \bar{b}_3 - c_5 \bar{b}_2 - c_6 \bar{b}_1 + \frac{B}{2}) z^{-2} + (c_3 b_3 + c_4 b_2 + c_1 b_1) z^{-1} + \\
& \frac{1}{R^2} (c_3 b_4 + c_2 b_3 + c_1 b_2 - \frac{a_1}{2} + c_3 \bar{b}_4 + c_2 \bar{b}_3 + c_1 \bar{b}_2 + \frac{\bar{a}_1}{2}) + \frac{1}{R^4} (c_2 b_4 + c_1 b_3 - \frac{a_2}{2} + \\
& 2c_2 \bar{b}_4 + 2c_1 \bar{b}_3 + \bar{a}_2) z + \frac{1}{R^6} (c_1 b_4 - \frac{a_3}{2} + 3c_1 \bar{b}_4 + \frac{3\bar{a}_1}{2}) z^2 + \frac{1}{R^8} (2\bar{a}_4 - \frac{a_4}{2}) z^3 \left. \right\} \} \\
& - \frac{R}{2\mu_2} [(\kappa_2 d_0 z^{-1} + \kappa_2 d_1 + \kappa_2 d_2 z + \kappa_2 d_3 z^2 + \kappa_2 d_4 z^3) - (\bar{d}_1 + 2R^2 \bar{d}_2 z^{-1} + \\
& 3R^4 \bar{d}_3 z^{-2} + 4R^6 \bar{d}_4 z^{-3}) - (e_0 z^{-1} + R^2 e_1 z^{-2} + R^4 e_2 z^{-3} + R^6 e_3 z^{-4} + R^8 e_4 z^{-5})] \left. \right\} +
\end{aligned}$$

$$\begin{aligned}
& \frac{m+n}{2} \left\{ \frac{1}{2\mu_1 R} \left\{ \left\{ \kappa_1 R^{10} [c_3 \bar{b}_3 + c_7 \bar{b}_2 + c_6 \bar{b}_1 + c_4 (2A+B)] z^{-4} + \right. \right. \right. \\
& \kappa_1 R^8 [c_3 \bar{b}_4 + c_7 \bar{b}_3 + c_6 \bar{b}_2 + c_5 \bar{b}_1 + c_3 (2A+B)] z^{-3} + \kappa_1 R^6 [c_7 \bar{b}_4 + \\
& c_6 \bar{b}_3 + c_5 \bar{b}_2 + c_4 \bar{b}_1 + c_2 (2A+B)] z^{-2} + \kappa_1 R^4 [c_6 \bar{b}_4 + c_5 \bar{b}_3 + c_4 \bar{b}_2 + \\
& c_3 \bar{b}_1 + c_1 (2A+B)] z^{-1} + \kappa_1 R^2 (c_5 \bar{b}_4 + c_4 \bar{b}_3 + c_3 \bar{b}_2 + c_2 \bar{b}_1 - \frac{B}{2}) + \\
& \kappa_1 (c_4 \bar{b}_4 + c_3 \bar{b}_3 + c_2 \bar{b}_2 + c_1 \bar{b}_1) z + \frac{\kappa_1}{R^2} (c_3 \bar{b}_4 + c_2 \bar{b}_3 + c_1 \bar{b}_2 + \\
& \frac{\bar{a}_1}{2}) z^2 + \frac{\kappa_1}{R^4} (c_2 \bar{b}_4 + c_1 \bar{b}_3 + \frac{\bar{a}_2}{2}) z^3 + \frac{\kappa_1}{R^6} (c_1 \bar{b}_4 + \frac{\bar{a}_3}{2}) z^4 + \kappa_1 \frac{\bar{a}_4}{2R^8} z^5 \left. \right\} - \\
& \left\{ 6R^2 [c_3 b_2 + c_7 b_1 + c_5 (2A+\bar{B})] z^5 + 5R^2 [c_3 b_3 + c_7 b_2 + c_6 b_1 + \right. \\
& c_4 (2A+\bar{B})] z^4 + 4R^2 [c_3 b_4 + c_7 b_3 + c_6 b_2 + c_5 b_1 + c_3 (2A+\bar{B})] z^3 + \\
& 3R^2 [c_7 b_4 + c_6 b_3 + c_5 b_2 + c_4 b_1 + c_2 (2A+\bar{B})] z^2 + 2R^2 [c_6 b_4 + c_5 b_3 + \\
& c_4 b_2 + c_3 b_1 + c_1 (2A+\bar{B})] z + R^2 (c_5 b_4 + c_4 b_3 + c_3 b_2 + c_2 b_1 - \frac{\bar{B}}{2}) - \\
& R^2 (c_3 b_4 + c_2 b_3 + c_1 b_2 + \frac{a_1}{2}) z^{-2} - 2R^2 (c_2 b_4 + c_1 b_3 + \frac{a_2}{2}) z^{-3} - R^2 (3c_1 b_4 + \\
& \frac{3a_3}{2}) z^{-4} - 2R^2 a_4 z^{-5} \left. \right\} - \{ [c_3 \bar{b}_4 + c_7 \bar{b}_3 + c_6 \bar{b}_2 + c_5 \bar{b}_1 + c_3 (2A+B) - \\
& 4c_5 b_4 - 4c_7 b_3 - 4c_6 b_2 - 4c_3 b_1 - 4c_3 (2A+\bar{B})] z^5 + [c_7 \bar{b}_4 + c_6 \bar{b}_3 + \\
& c_5 \bar{b}_2 + c_4 \bar{b}_1 + c_2 (2A+B) - 3c_7 b_4 - 3c_6 b_3 - 3c_5 b_2 - 3c_4 b_1 - 3c_2 (2A+\bar{B})] z^4 \\
& + [c_6 \bar{b}_4 + c_5 \bar{b}_3 + c_4 \bar{b}_2 + c_3 \bar{b}_1 + c_1 (2A+B) - 2c_6 b_4 - 2c_5 b_3 - 2c_4 b_2 - \\
& 2c_3 b_1 - 2c_1 (2A+\bar{B})] z^3 + (c_5 \bar{b}_4 + c_4 \bar{b}_3 + c_3 \bar{b}_2 + c_2 \bar{b}_1 + \frac{B}{2} - c_5 b_4 - c_4 b_3 -
\end{aligned}$$

$$\begin{aligned}
& c_3 \bar{b}_2 - c_2 \bar{b}_1 + \frac{\bar{B}}{2} z^2 + (c_1 \bar{b}_1 + c_2 \bar{b}_2 + c_3 \bar{b}_3) z + (c_3 \bar{b}_4 + c_2 \bar{b}_3 + c_1 \bar{b}_2 - \frac{\bar{a}_1}{2} + \\
& c_3 \bar{b}_4 + c_2 \bar{b}_3 + c_1 \bar{b}_2 + \frac{a_1}{2}) + (c_2 \bar{b}_4 + c_1 \bar{b}_3 - \frac{\bar{a}_2}{2} + 2c_1 \bar{b}_3 + 2c_2 \bar{b}_4 + a_2) z^{-1} + \\
& (c_1 \bar{b}_4 - \frac{\bar{a}_3}{2} + 3c_1 \bar{b}_4 + \frac{3a_3}{2}) z^{-2} + (2a_4 - \frac{\bar{a}_4}{2}) z^{-3} \} \} - \frac{1}{2\mu_2 R} [(\kappa_2 \bar{d}_0 z + \\
& \kappa_2 R^2 \bar{d}_1 + \kappa_2 R^4 \bar{d}_2 z^{-1} + \kappa_2 R^6 \bar{d}_3 z^{-2} + \kappa_2 R^8 \bar{d}_4 z^{-3}) - (R^2 d_1 + 2R^2 d_2 z + \\
& 3R^2 d_3 z^2 + 4R^2 d_4 z^3) - (e_0 z + e_1 z^2 + e_2 z^3 + e_3 z^4 + e_4 z^5)] \} - \\
& mR\epsilon_1 - (\frac{m+n}{2R})(\epsilon_2 - i\epsilon_3)z^2 - (\frac{m-n}{2z^2})R^2(\epsilon_2 + i\epsilon_3) = -\frac{4e_4}{R^2} z^5 - \frac{3e_3}{R^2} z^4 - \\
& (8d_4 + \frac{2e_2}{R^2})z^3 - (3d_3 + \frac{e_1}{R^2})z^2 + d_1 + \bar{d}_1 + 2R^2 \bar{d}_2 z^{-1} + 3R^4 \bar{d}_3 z^{-2} + 4R^6 \bar{d}_4 z^{-3}
\end{aligned}$$

Comparing coefficients of powers of z , we can obtain coupled linear equations for the unknown coefficients a_k , b_k ($k=1, 2, 3, 4$) and d_k , e_k ($k=0, 1, 2, 3, 4$). The detailed calculations can be found in Appendix 1.

Noting that the interface model [Eq. (2.3) of Chapter 2] can be used to represent an adhesive layer, we remark that the two interface parameters m and n depend on the thickness and modulus of the layer. If only a single adhesive material is assumed to make up the layer, the ratio of m/n is usually taken to be a material constant, independent of the thickness of the adhesive layer. For example, the ratio m/n can take the (approximate) value 1 for a layer modeled by a series of distributed springs (see, for example, Achenbach and Zhu, 1989, 1990), or the value 3 for an

elastic interphase layer (see, for example, Hashin, 1991). Consequently, in this chapter, we analyze three different cases:

- 1) $m = n$ (the spring layer);
- 2) $m = 3n$ (an elastic interphase layer)

and

- 3) $m = \infty$ and $n = 0$ (the sliding interface, see Mura, et al., 1996). Here, the Poisson's ratios of both the inclusion and the matrix are held constant ($\nu_1 = \nu_2 = 1/3$).

3.2.2 The Spring-layer Interface ($m=n$)

First, consider the case of $m=n$. There are altogether 18 unknown coefficients a_k , b_k ($k=1, 2, 3, 4$) and d_k , e_k ($k=0, 1, 2, 3, 4$). As one of the e_0 and d_0 can be chosen arbitrarily without changing the displacement field (Muskhelishvili, 1963), we arbitrarily choose $e_0=0$. So only 17 unknown coefficients remain to be solved. The equations A.19 to A.35 in Appendix 1 give the final 17 coupled linear algebraic equations.

3.2.3 The Elastic Interphase Layer ($m=3n$)

Second, consider the case of $m=3n$. As mentioned in 3.2.2, there are 17 unknown coefficients and equations A.36 to A.52 in Appendix 1 list all required linear equations.

3.2.4 The Sliding Interface ($m=\infty, n=0$)

Finally, sliding interface ($m = \infty$, $n=0$) is considered. Following the same procedures as shown in Sections 3.2.2 and 3.2.3, equations A.53 to A.69 in Appendix 1 show the final 17 linear algebraic equations.

3.3 NUMERICAL RESULTS AND DISCUSSIONS

In the case of a uniaxial load σ^0 normal to the crack, the stresses in the neighborhood of the crack tip $z = a$ are given by:

$$\sigma_{xx} = -\frac{\sqrt{l}}{\sqrt{2r_1}} \sigma^0 \frac{a}{l} \left(\frac{3}{4} \sin \frac{\theta_1}{2} + \frac{1}{4} \sin 5 \frac{\theta_1}{2} \right) \left[1 - \frac{1}{2a\sigma^0} \sum_{k=1}^{\infty} kb_{k+1} a^{-(k+1)} \right] + O(r_1^0),$$

$$\sigma_{yy} = -\frac{\sqrt{l}}{\sqrt{2r_1}} \sigma^0 \frac{a}{l} \left(\frac{5}{4} \sin \frac{\theta_1}{2} - \frac{1}{4} \sin 5 \frac{\theta_1}{2} \right) \left[1 - \frac{1}{2a\sigma^0} \sum_{k=1}^{\infty} kb_{k+1} a^{-(k+1)} \right] + O(r_1^0),$$

$$\sigma_{xy} = -\frac{\sqrt{l}}{\sqrt{2r_1}} \sigma^0 \frac{a}{l} \left(\frac{1}{4} \cos \frac{\theta_1}{2} - \frac{1}{4} \cos 5 \frac{\theta_1}{2} \right) \left[1 - \frac{1}{2a\sigma^0} \sum_{k=1}^{\infty} kb_{k+1} a^{-(k+1)} \right] + O(r_1^0),$$

where $z - a = r_1 e^{i\theta_1}$ ($0 \leq \theta_1 \leq 2\pi$). Similarly, the stress field around the crack tip $z = b$ is given by

$$\sigma_{xx} = \frac{\sqrt{l}}{\sqrt{2r_2}} \sigma^0 \frac{b}{l} \left(\frac{3}{4} \cos \frac{\theta_2}{2} + \frac{1}{4} \cos 5 \frac{\theta_2}{2} \right) \left[1 - \frac{1}{2b\sigma^0} \sum_{k=1}^{\infty} kb_{k+1} a^{-(k+1)} \right] + O(r_2^0),$$

$$\sigma_{yy} = \frac{\sqrt{l}}{\sqrt{2r_2}} \sigma^0 \frac{b}{l} \left(\frac{5}{4} \cos \frac{\theta_2}{2} - \frac{1}{4} \cos 5 \frac{\theta_2}{2} \right) \left[1 - \frac{1}{2b\sigma^0} \sum_{k=1}^{\infty} kb_{k+1} a^{-(k+1)} \right] + O(r_2^0),$$

$$\sigma_{xy} = -\frac{\sqrt{l}}{\sqrt{2r_2}} \sigma^0 \frac{b}{l} \left(\frac{1}{4} \sin \frac{\theta_2}{2} - \frac{1}{4} \sin 5 \frac{\theta_2}{2} \right) \left[1 - \frac{1}{2b\sigma^0} \sum_{k=1}^{\infty} kb_{k+1} a^{-(k+1)} \right] + O(r_2^0),$$

where $z - b = r_2 e^{i\theta_2}$ ($-\pi \leq \theta_1 \leq \pi$). In the above equations, the first term of each equation represents the leading order singular stress near the crack tips, inversely proportional to the square-root of the radial distance from the crack tip. The square-bracketed terms represent the influence of the inclusion and the imperfect interface on the SIF.

Figures 3.1 and 3.2 show, for the case of $m = n$ and the fixed crack length $2l$ ($l=R$), the SIF ratio at the nearby and distant crack tips. This ratio is defined by K_I/K_I^0 (where K_I is the actual mode-I SIF and $K_I^0 = \sigma^0 \sqrt{\pi l}$ is the mode-I SIF for the same crack in a homogeneous matrix material without the inclusion). Clearly, the inclusion has a significant effect on K_I (a) but not on K_I (b). On the other hand, the effect of the inclusion decreases with d/R . For the case of an inclusion stiffer than the surrounding matrix (Figure 3.1), $K_I(a)$ increases as the imperfect interface parameter N' decreases. It is clear that the presence of the inclusion with imperfect interface can either increase the SIF at the nearby crack tip (for example, when $N'=0.01, 0.1$ or 1), or reduce it significantly (for example, when $N'=10$ or 100), as compared to $\sigma^0 \sqrt{\pi l}$. For the case of an inclusion softer than the surrounding matrix (Figure 3.2), the SIF at the nearby crack tip increases sharply when the crack approaches the inclusion. On the other hand, $K_I(a)$ increases when the imperfect interface parameter N' decreases and, most importantly, the SIF at the nearby crack tip is always larger than that at the distant crack tip.

In particular, it is seen from Figure 3.1 that, for a stiffer inclusion, the SIF at the nearby crack tip is smaller than that at the distant crack tip for a larger imperfect interface parameter but larger than the SIF at the distant crack tip for smaller values

of the imperfect interface parameter. Hence, for any given inclusion composed of material stiffer than the surrounding matrix, there is a corresponding critical value of the imperfect interface parameter at which $K_I(a)=K_I(b)$. Clearly, this critical value of the imperfect interface parameter depends on the ratio of shear moduli. For a fixed value of d/R , Figures 3.3 and 3.4 illustrate the shear moduli ratios of inclusion to matrix determined by the condition $K_I(a)=K_I(b)$ for different imperfect interface parameters. In Figure 3.3, four curves are drawn for different ratios d/R . These curves correspond to the fixed crack length $l/R = 1$. Figure 3.4 deals with the case of $l/R = 0.1$. These curves show that, for the fixed interface parameter N' , the ratio of μ_2/μ_1 , determined by the condition $K_I(a)=K_I(b)$, increases as d/R becomes larger. On the other hand, for the fixed ratio μ_2/μ_1 , the interface parameter N' , determined by the condition $K_I(a)=K_I(b)$, becomes larger when d/R increases. In both Figures 3.3 and 3.4, each curve defines a minimum critical value of N' , referred to as N^* , below which the condition $K_I(a)=K_I(b)$ cannot be satisfied by any ratio μ_2/μ_1 (more precisely, below which $K_I(a)$ is always larger than $K_I(b)$ for any ratio μ_2/μ_1). For example, the minimum critical values in Figure 3.3 are $N^*= 0.05, 0.1, 5.6$ and 8.7 when $d/R = 0.01, 0.05, 0.5$ and 1 , respectively. In Figure 3.4, the minimum critical values are $N^*=0.01, 0.08, 5.2$ and 6.9 when $d/R = 0.01, 0.05, 0.5$ and 1 , respectively. In any case, if the imperfect interface parameter is smaller than the corresponding critical value N^* , we have $K_I(a)>K_I(b)$ and the radial matrix crack will grow toward the interface leading to interface debonding for any ratio μ_2/μ_1 . It is therefore possible to predict and control the direction of matrix cracking and therefore interfacial debonding by designing the inclusion-matrix interface accordingly.

In the case of $m=3n$, Figures 3.5 to 3.8 illustrate mode-I stress intensity factor at the nearby and distant crack tips for both softer ($\mu_1/\mu_2=2$) and stiffer inclusion ($\mu_1/\mu_2=0.5$). It can be seen from our calculations that there is no significant difference from the case $m = n$ discussed above. This is probably due to the fact that the shear imperfect interface parameter n has a minor effect on stress fields subjected uniaxial loading.

It should be noted that a consequence of the imperfect interface model employed in this paper is the prediction of possible overlapping of the two materials at the interface (a negative normal displacement jump across the interface; see, Achenbach and Zhu, 1989; Hashin, 1991). As explained by Hashin (1991), under the assumptions of this interface model, the matrix or the inclusion can be moved toward the interface by a small distance less than or equal to the initial interphase thickness without any physical overlapping of materials. With this interpretation, a small negative normal displacement jump is permissible so that the imperfect interface model used here does not, in fact, lead to any physical contradiction, at least for cases of relatively lower order remote loading.

An interesting special case of the imperfect interface is the so-called “sliding interface” characterized by $m = \infty$, $n=0$ (see, for example, Benveniste, 1984; Mura et al., 1996). In Figure 3.9, the sliding interface is considered and the mode-I stress intensity factor ratio (defined as for Figure 3.1) is drawn as a function of the distance d for both a softer inclusion ($\mu_1/\mu_2=2$) and a stiffer inclusion ($\mu_1/\mu_2=0.5$). For the softer inclusion, the SIF at the nearby crack tip increases when the distance d becomes smaller. Figure 3.9 shows that the SIF at the nearby crack tip is always

larger than that at the distant crack tip, which implies that the crack grows towards the inclusion. On the other hand, for the stiffer inclusion, the SIF at the nearby crack tip increases monotonically if the distance d increases and the SIF at the nearby crack tip is always smaller than that at the distant crack tip. This means that the stiffer inclusion with sliding interface always resists crack propagation towards the inclusion. Clearly, the SIF at the distant crack tip is not sensitive to the distance d/R for both softer and stiffer inclusions.

As mentioned previously, the present imperfect interface model describes perfect bonding when $m = n = \infty$ and complete debonding when $m = n = 0$. Hence, for the sake of comparison, the SIFs calculated by the present method for very large or very small interface parameters are compared with known results for the perfect interface and traction-free holes, respectively. For example, the calculated SIF at the nearby and distant crack tips under uniaxial loading normal to the crack ($m=n$) for $N'=100$ are compared with SIFs corresponding to perfect bonding (see Tamate, 1968; Guo, et al. 1998). The results are shown in Tables 3.1 and 3.2, respectively.

Table 3.1. Comparison between the calculated nearby SIF with very large interface parameter and the SIF corresponding to perfect bonding.

	$\mu_2/\mu_1=0.5$				2			
	$d/R=0.1$	0.2	0.5	1	0.1	0.2	0.5	1
$N'=100$	1.2876	1.2269	1.1154	1.0365	0.7546	0.8483	0.9435	0.9708
Perfect bond	1.30	1.23	1.12	1.04	0.73	0.83	0.94	0.97

Table 3.2. Comparison between the calculated distant SIF with very large interface parameter and the SIF corresponding to perfect bonding.

	$\mu_2/\mu_1=0.5$			2		
	$d/R=0.1$	0.2	1	0.1	0.2	1
$N'=100$	1.0332	1.0267	1.0051	0.9402	0.9467	0.9801
Perfect bond	1.035	1.028	1.005	0.93	0.94	0.98

Similarly, in Table 3.3, we compare the SIFs for near-by and distant crack tips with very small interface parameter ($N'=0.01$) with the SIFs for the traction free-hole (see, Sih, 1973).

Table 3.3. Comparison between the calculated nearby and distant SIF and SIF corresponding to traction-free hole.

$\mu_2/\mu_1=0.5$	Nearby SIF				Distant SIF		
	$d/R=0.1$	0.2	0.5	1	0.1	0.2	1
$N'=0.01$	1.8624	1.724	1.3434	1.1434	1.2069	1.1667	1.0551
Traction free hole	1.893	1.74	1.35	1.145	1.22	1.18	1.055

All comparisons show that the perfect interface can be described by very large imperfect interface parameters (for example $N'>100$). Similarly, traction-free debonding can be described by very small interface parameters (for example

$N' < 0.01$). In particular, these results confirm the validity of the present series method.

3.4 CONCLUSIONS

This chapter studies the effect of imperfect bonding on radial matrix cracking under uniaxial loading normal to the crack. In the case of a perfect interface, as we know, one of the main results concerning an inclusion/crack interaction is that, the SIF at the nearby tip of a radial matrix crack is greater (smaller) than the SIF at the distant crack tip, if and only if the inclusion is more compliant (stiffer) than the matrix (see, for example, Tamate, 1968; Atkinson, 1972 and Guo et al., 1998). This result is of major importance since it determines whether the radial crack grows towards or away from the inclusion. However, our present study shows that this conclusion is qualitatively invalid when imperfect bonding is present at the inclusion/matrix interface. In total, three cases of interface conditions are considered in this chapter. The major conclusions are as follows:

1. In contrast to the case of a perfect interface for which the SIF at the nearby crack tip is greater than the SIF at the distant crack tip only when the inclusion is more compliant than the matrix, the imperfect bonding condition allows for the possibility of a SIF at the nearby crack tip greater than that at the distant crack tip even when the inclusion is stiffer than the matrix. In fact, for any given inclusion stiffer than the surrounding matrix, there is a corresponding critical

value of the imperfect interface parameter below which a radial matrix crack grows toward the interface leading to interface debonding. In particular, for given crack length and distance from the interface, there is a minimum critical value of the imperfect interface parameter (defined by N^* in Section 3.1) below which (that is, when $N' < N^*$) the SIF in the nearby crack tip is always greater than that at the distant crack tip for any shear modulus ratio of the inclusion and the matrix.

2. For the special case of a perfectly bonded or entirely debonded interface, the present results are consistent with the known results in the literature.
3. For the case of elastic interphase ($m=3n$), our results show that there is no significant difference from the case $m = n$. This is probably due to the fact that the shear imperfect interface parameter n has a minor effect on stress fields subjected uniaxial loading.
4. For the case of sliding interface ($m = \infty$, $n=0$), our results indicate that for the softer inclusion, the SIF at the nearby crack tip is always larger than that at the distant crack tip, which implies that the crack grows towards the inclusion. On the other hand, for the stiffer inclusion, the SIF at the nearby crack tip is always smaller than that at the distant crack tip. This means that the stiffer inclusion with sliding interface always resists crack propagation towards the inclusion.
5. The interface imperfection has significant effect on SIFs especially when the crack is close to the inclusion. The results indicate inclusion can either promote or retard crack propagation in matrix, depending not only on the ratio of the modulus of inclusion to that of the matrix, but also on the interface imperfection.

The present semi-analytic power-series method is effective to investigate the inclusion-crack interaction with imperfect interface.

CHAPTER 4

EFFECT OF IMPERFECT BONDING ON RADIAL MATRIX CRACKING--UNIAXIAL LOADING PARALLEL TO THE CRACK

4.1 DESCRIPTION OF THE PROBLEM

In this chapter, we will consider uniaxial loading parallel to the crack for the case of $m=3n$, where uniaxial loading σ^0 is in the x -direction. In this case, we have

$$A = \frac{\sigma^0}{4}, \quad B = -2A = -\frac{\sigma^0}{2}.$$

4.2 PROBLEM SOLUTIONS

4.2.1 The Elastic Interphase Layer ($m=3n$)

By adopting the same steps as described in Chapter 3, using the two interface conditions in Chapter 2 and comparing the coefficients for like powers of z , we can obtain coupled linear equations for the unknown coefficients a_k , b_k ($k=1, 2, 3, 4$) and d_k , e_k ($k=0, 1, 2, 3, 4$). As one of the e_0 and d_0 can be chosen arbitrarily without

changing the displacement field (Muskhelishvili, 1963), we arbitrarily choose $e_0=0$.

The final equations for uniaxial loading parallel to the crack are given as:

$$\frac{a'_3}{2} + (5c_6R^0 - 2c_4R^4)b'_1 + (5c_7R^7 - 2R^5c_5)b'_2 + (5c_8R^8 - 2c_6R^6)b'_3 + (c_1R - 2c_7R^7)b'_4 - e'_3 = 0, \quad (4.1)$$

$$a'_2 + (4c_5R^5 - c_3R^3)b'_1 + (4c_6R^6 - c_4R^4)b'_2 + (4c_7R^7 - c_5R^5 + c_1R)b'_3 + (4c_8R^8 - c_6R^6 + c_2R^2)b'_4 - 4d'_4 - e'_2 = 0, \quad (4.2)$$

$$a'_1 + 3c_4R^4b'_1 + c_1Rb'_2 + (3c_6R^6 + c_2R^2)b'_3 + (3c_7R^7 + c_3R^3)b'_4 - 3d'_3 - e'_1 - 2R^4A = 0, \quad (4.3)$$

$$c_2R^2b'_1 + (c_3R^3 + c_1R)b'_2 + (c_4R^4 + c_2R^2)b'_3 + (c_5R^5 + c_3R^3)b'_4 - d'_1 + R^4A = 0, \quad (4.4)$$

$$a'_2 + R^3c_3b'_1 + R^4c_4b'_2 + (R^5c_5 + 3Rc_1)b'_3 + (R^6c_6 + 3R^2c_2)b'_4 - d'_2 = 0, \quad (4.5)$$

$$a'_1 - a'_3 - R^4c_4b'_1 + (Rc_1 - R^5c_5)b'_2 + (R^2c_2 - R^6c_6)b'_3 + (R^3c_3 - R^7c_7 - 4Rc_1)b'_4 + d'_3 = 0, \quad (4.6)$$

$$2a'_2 - \frac{3a'_4}{2} - R^5c_5b'_1 - R^6c_6b'_2 + (2Rc_1 - R^7c_7)b'_3 + (2R^2c_2 - R^3c_3)b'_4 + d'_4 = 0, \quad (4.7)$$

.

$$a'_4 + (12R^7c_7 - 6R^5c_5)b'_1 + (12R^8c_8 - 6R^6c_6)b'_2 - 6R^7c_7b'_3 - 6R^8c_8b'_4 - 2e'_4 = 0, \quad (4.8)$$

$$\begin{aligned} & \frac{(3/2 + \kappa_1)}{4}a'_3 + \left(\frac{\kappa_1}{4}R^0c_6 - \frac{5}{2}R^0c_6 + R^4c_4\right)b'_1 + \left(\frac{\kappa_1}{4}R^7c_7 - \frac{5}{2}R^7c_7 + R^5c_5\right)b'_2 + \left(\frac{\kappa_1}{4}c_8R^8 - \frac{5}{2}R^8c_8 + R^6c_6\right)b'_3 + \left(\frac{3}{4}Rc_1 + \frac{\kappa_1}{2}Rc_1 + R^7c_7\right)b'_4 + \left(\frac{1}{2}\frac{\mu_1}{\mu_2} + \frac{3}{N'}\right)e'_3 = 0, \end{aligned} \quad (4.9)$$

$$\begin{aligned} & \frac{(1 + \kappa_1)}{2}a'_2 - \frac{3}{4}a'_4 + \left(\frac{\kappa_1}{4}R^5c_5 + \frac{1}{2}R^3c_3 - 2R^5c_5\right)b'_1 + \left(\frac{\kappa_1}{4}R^0c_6 + \frac{1}{2}R^4c_4 - 2R^0c_6\right)b'_2 + \left(\frac{\kappa_1}{4}R^7c_7 + \frac{1}{2}Rc_1 + \frac{\kappa_1}{2}Rc_1 - 2R^7c_7 + \frac{1}{2}R^5c_5\right)b'_3 + \left(\frac{\kappa_1}{4}R^8c_8 + \frac{1}{2}R^2c_2 + \frac{\kappa_1}{2}R^2c_2 - 2R^8c_8 + \frac{1}{2}R^0c_6\right)b'_4 + \left(2\frac{\mu_1}{\mu_2} - \frac{\kappa_2\mu_1}{4\mu_2} + \frac{8}{N'}\right)d'_4 + \left(\frac{1}{2}\frac{\mu_1}{\mu_2} + \frac{2}{N'}\right)e'_2 = 0, \end{aligned} \quad (4.10)$$

$$\begin{aligned} & \frac{(1/2 + \kappa_1)}{2}a'_1 - \frac{1}{4}a'_3 + \left(\frac{\kappa_1}{4} - \frac{3}{2}\right)R^4c_4b'_1 + \left(\frac{\kappa_1}{4}R^5c_5 + \frac{1}{4}Rc_1 + \frac{\kappa_1}{2}Rc_1 - \frac{3}{2}R^5c_5\right)b'_2 + \left(\frac{\kappa_1}{4}R^0c_6 + \frac{1}{4}R^2c_2 + \frac{\kappa_1}{2}R^2c_2 - \frac{3}{2}R^0c_6\right)b'_3 + \left(\frac{\kappa_1}{4}R^7c_7 + \frac{1}{4}R^3c_3 - Rc_1 + \frac{\kappa_1}{2}R^3c_3 - \frac{3}{2}R^7c_7\right)b'_4 + \left(\frac{3}{2}\frac{\mu_1}{\mu_2} - \frac{\kappa_2}{4}\frac{\mu_1}{\mu_2} + \frac{3}{N'}\right)d'_3 + \left(\frac{1}{2}\frac{\mu_1}{\mu_2} + \frac{1}{N'}\right)e'_1 + R^4A = 0, \end{aligned} \quad (4.11)$$

$$\begin{aligned}
& -\frac{1}{4}a'_2 + \left(\frac{\kappa_1}{4}R^3c_3 + \frac{\kappa_1}{2}Rc_1 - R^3c_3 - \frac{1}{2}Rc_1\right)b'_1 + \left(\frac{\kappa_1}{4}R^4c_4 + \right. \\
& \left. \frac{\kappa_1}{2}R^2c_2 - R^4c_4 - \frac{1}{2}R^2c_2\right)b'_2 + \left(\frac{\kappa_1}{4}R^5c_5 - \frac{3}{4}Rc_1 + \frac{\kappa_1}{2}R^3c_3 - \right. \\
& \left. R^5c_5 - \frac{1}{2}R^3c_3\right)b'_3 + \left(\frac{\kappa_1}{4}R^6c_6 - \frac{3}{4}R^2c_2 + \frac{\kappa_1}{2}R^4c_4 - R^6c_6 - \right. \\
& \left. \frac{1}{2}R^4c_4\right)b'_4 - \frac{\kappa_2}{2}\frac{\mu_1}{\mu_2}d'_0 + \left(1 - \frac{\kappa_2}{4}\right)\frac{\mu_1}{\mu_2}d'_2 = 0,
\end{aligned} \tag{4.12}$$

$$\begin{aligned}
& \left(\frac{\kappa_1}{4}R^2c_2 - \frac{1}{4}R^2c_2 + \frac{\kappa_1}{2}R^2c_2 - \frac{1}{2}R^2c_2\right)b'_1 + \left(\frac{\kappa_1}{4}R^3c_3 - \frac{1}{4}R^3c_3 - \right. \\
& \left. \frac{1}{2}Rc_1 + \frac{\kappa_1}{2}R^3c_3 - \frac{R^3c_3}{2} - Rc_1\right)b'_2 + \left(\frac{\kappa_1}{4}R^4c_4 - \frac{1}{4}R^4c_4 - \frac{1}{2}R^2c_2 + \right. \\
& \left. \frac{\kappa_1}{2}R^4c_4 - \frac{R^4c_4}{2} - R^2c_2\right)b'_3 + \left(\frac{\kappa_1}{4}R^5c_5 - \frac{1}{4}R^5c_5 - \frac{1}{2}R^3c_3 + \frac{\kappa_1}{2}R^5c_5 - \right. \\
& \left. \frac{R^5c_5}{2} - R^3c_3\right)b'_4 + \left(\frac{3\mu_1}{4\mu_2} - \kappa_2\frac{3\mu_1}{4\mu_2} - \frac{2}{N'}\right)d'_1 + \left(\frac{3\kappa_1}{4} - \frac{3}{4}\right)R^4A = 0,
\end{aligned} \tag{4.13}$$

$$\begin{aligned}
& -\frac{1}{2}a'_2 + \left(\frac{\kappa_1}{4}Rc_1 - \frac{R^3}{2}c_3 - \frac{1}{4}Rc_1 + \frac{\kappa_1}{2}R^3c_3\right)b'_1 + \left(\frac{\kappa_1}{4}R^2c_2 - \frac{R^4}{2}c_4 - \right. \\
& \left. \frac{1}{4}R^2c_2 + \frac{\kappa_1}{2}R^4c_4\right)b'_2 + \left(\frac{\kappa_1}{4}R^3c_3 - \frac{R^5}{2}c_5 - \frac{1}{4}R^3c_3 + \frac{\kappa_1}{2}R^5c_5 - \right. \\
& \left. \frac{3}{2}Rc_1\right)b'_3 + \left(\frac{\kappa_1}{4}R^4c_4 - \frac{R^6}{2}c_6 - \frac{1}{4}R^4c_4 + \frac{\kappa_1}{2}R^6c_6 - \frac{3}{2}R^2c_2\right)b'_4 - \\
& \frac{\kappa_2}{4}\frac{\mu_1}{\mu_2}d'_0 + \left(\frac{1}{2}\frac{\mu_1}{\mu_2} - \frac{\kappa_2}{2}\frac{\mu_1}{\mu_2} - \frac{2}{N'}\right)d'_2 = 0,
\end{aligned} \tag{4.14}$$

$$\begin{aligned}
& \frac{(1+\kappa_1/2)}{2}a'_1 - \frac{1}{2}a'_3 + \left(\frac{\kappa_1}{2} - \frac{3}{4}\right)R^4c_4b'_1 + \left(\frac{\kappa_1}{4}Rc_1 + \frac{\kappa_1}{2}R^5c_5 + \right. \\
& \left. \frac{1}{2}Rc_1\right)b'_2 + \left(\frac{\kappa_1}{4}R^2c_2 - \frac{3}{4}R^6c_6 + \frac{\kappa_1}{2}R^6c_6 + \frac{1}{2}R^2c_2\right)b'_3 + \left(\frac{\kappa_1}{4}R^3c_3 - \right. \\
& \left. \frac{3}{4}R^7c_7 + \frac{\kappa_1}{2}R^7c_7 + \frac{1}{2}R^3c_3 - 2Rc_1\right)b'_4 + \left(\frac{3}{4}\frac{\mu_1}{\mu_2} - \frac{\kappa_2}{2}\frac{\mu_1}{\mu_2} - \frac{3}{N'}\right)d'_3 + \\
& \frac{1}{4}\frac{\mu_1}{\mu_2}e'_1 + \frac{1}{2}R^4A = 0,
\end{aligned} \tag{4.15}$$

$$\begin{aligned}
& (1 + \kappa_1 / 4) a'_2 - \frac{3}{4} a'_4 + \left(\frac{1}{4} R^3 c_3 - R^5 c_5 + \frac{\kappa_1}{2} R^5 c_5 \right) b'_1 + \left(\frac{1}{4} R^4 c_4 - \right. \\
& R^6 c_6 + \frac{\kappa_1}{2} R^6 c_6 \left. \right) b'_2 + \left(\frac{\kappa_1}{4} R c_1 + \frac{1}{4} R^5 c_5 - R^7 c_7 + \frac{\kappa_1}{2} R^7 c_7 + \right. \\
& R c_1 \left. \right) b'_3 + \left(\frac{\kappa_1}{4} R^2 c_2 + \frac{1}{4} R^6 c_6 - R^8 c_8 + \frac{\kappa_1}{2} R^8 c_8 + R^2 c_2 \right) b'_4 + \\
& \left(\frac{\mu_1}{\mu_2} - \frac{\kappa_2}{2} \frac{\mu_1}{\mu_2} - \frac{4}{N'} \right) d'_4 + \frac{1}{4} \frac{\mu_1}{\mu_2} e'_2 = 0,
\end{aligned} \tag{4.16}$$

and

$$\begin{aligned}
& \left(\frac{1}{2} + \frac{\kappa_1}{4} \right) a'_4 + \left(\frac{\kappa_1}{4} R^7 c_7 - 3 R^7 c_7 + \frac{3}{2} R^5 c_5 \right) b'_1 + \left(\frac{\kappa_1}{4} R^8 c_8 - \right. \\
& 3 R^8 c_8 + \frac{3}{2} R^6 c_6 \left. \right) b'_2 + \frac{3}{2} R^7 c_7 b'_3 + \frac{3}{2} R^8 c_8 b'_4 + \left(\frac{1}{2} \frac{\mu_1}{\mu_2} + \frac{4}{N'} \right) e'_4 = 0.
\end{aligned} \tag{4.17}$$

4.3 NUMERICAL RESULTS AND DISCUSSIONS

In the present case, the stresses in the neighborhood of the crack tip $z = a$ are given by:

$$\sigma_{xx} = \frac{\sqrt{l}}{2\sqrt{2}r_1} \sigma^0 \frac{a}{l} \left(\frac{3}{4} \sin \frac{\theta_1}{2} + \frac{1}{4} \sin 5 \frac{\theta_1}{2} \right) \left[\frac{1}{a \sigma^0} \sum_{k=1}^{\infty} k b_{k+1} a^{-(k+1)} \right] + O(r_1^0),$$

$$\sigma_{yy} = \frac{\sqrt{l}}{2\sqrt{2}r_1} \sigma^0 \frac{a}{l} \left(\frac{5}{4} \sin \frac{\theta_1}{2} - \frac{1}{4} \sin 5 \frac{\theta_1}{2} \right) \left[\frac{1}{a \sigma^0} \sum_{k=1}^{\infty} k b_{k+1} a^{-(k+1)} \right] + O(r_1^0),$$

$$\sigma_{xy} = \frac{\sqrt{l}}{2\sqrt{2}r_1} \sigma^0 \frac{a}{l} \left(\frac{1}{4} \cos \frac{\theta_1}{2} - \frac{1}{4} \cos 5 \frac{\theta_1}{2} \right) \left[\frac{1}{a \sigma^0} \sum_{k=1}^{\infty} k b_{k+1} a^{-(k+1)} \right] + O(r_1^0),$$

where $z - a = r_1 e^{i\theta_1}$ ($0 \leq \theta_1 \leq 2\pi$). Similarly, the stress field around the crack tip $z = b$ is given by

$$\sigma_{xx} = -\frac{\sqrt{l}}{2\sqrt{2}r_2} \sigma^0 \frac{b}{l} \left(\frac{3}{4} \cos \frac{\theta_2}{2} + \frac{1}{4} \cos 5 \frac{\theta_2}{2} \right) \left[\frac{1}{b\sigma^0} \sum_{k=1}^{\infty} k b_{k+1} a^{-(k+1)} \right] + O(r_2^0),$$

$$\sigma_{yy} = -\frac{\sqrt{l}}{2\sqrt{2}r_2} \sigma^0 \frac{b}{l} \left(\frac{5}{4} \cos \frac{\theta_2}{2} - \frac{1}{4} \cos 5 \frac{\theta_2}{2} \right) \left[\frac{1}{b\sigma^0} \sum_{k=1}^{\infty} k b_{k+1} a^{-(k+1)} \right] + O(r_2^0),$$

$$\sigma_{xy} = \frac{\sqrt{l}}{2\sqrt{2}r_2} \sigma^0 \frac{b}{l} \left(\frac{1}{4} \sin \frac{\theta_2}{2} - \frac{1}{4} \sin 5 \frac{\theta_2}{2} \right) \left[\frac{1}{b\sigma^0} \sum_{k=1}^{\infty} k b_{k+1} a^{-(k+1)} \right] + O(r_2^0),$$

where $z - b = r_2 e^{i\theta_2}$ ($-\pi \leq \theta_2 \leq \pi$).

Figures 4.1 to 4.4 illustrate mode-I stress intensity factor ratios at the nearby crack tip for the case of $m=3n$, while Figures 4.5 to 4.8 show those at the distant crack tip. This ratio is defined by K_I/K_I^0 (where K_I is the actual mode-I SIF and $K_I^0 = \sigma^0 \sqrt{\pi l}$ is the mode-I SIF for the same crack in a homogeneous matrix material without the inclusion). It is seen from Figures 4.1 to 4.8 that imperfect bonding could make the SIF at the nearby and distant tips significantly large as compared to that corresponding to the perfect interface. Here, in order to have a clear idea of the effect of the interface imperfections on the SIF, four different modulus ratios, $\mu_1/\mu_2 = 10, 2, 0.5$ and 0.1 are considered for both SIFs at the nearby and distant crack tips.

It is clear from our results that the imperfect interface parameter has a significant effect on the SIF at the nearby crack tip. For stiffer inclusions as shown in Figures 4.1 and 4.3, when the imperfect interface parameter N' varies from 1000

(approximately perfect bonding) to 0.01 (approximately complete debonding), there is a significant increase in the SIF for the fixed length d/R . Considering the influence of the distance d , if we fix the interface parameter N' , the SIF will decrease as d/R increases.

Comparing Figure 4.1 with Figure 4.3, when the modulus ratios μ_1/μ_2 become smaller (from 0.5 to 0.1), that is, the inclusion becomes much stiffer, the relevant SIF ratios increase for the fixed distance d and imperfect interface parameter N' . On the other hand, for the softer inclusions shown in Figures 4.2 and 4.4, when the imperfect interface parameter N' varies from 1000 to 0.01, there is also a significant increase in the SIF for the fixed length d/R . Considering the influence of the distance d , if we fix the interface parameter N' , the SIF will decrease as d/R increases. Comparing Figure 4.2 with Figure 4.4, when the modulus ratios μ_1/μ_2 become larger (from 2 to 10), that is, when the inclusion becomes much softer, the relevant SIF ratios increase for the fixed distance d and imperfect interface parameter N' .

It can be seen from Figures 4.5 to 4.8 illustrating stress intensity factors at the distant crack tip, for the fixed length d/R , when the imperfect interface parameter N' varies from 1000 to 0, there is a significant increase in the SIF for both softer and stiffer inclusions. Considering the influence of the distance d , if we fix the interface parameter N' , the SIF will decrease as d/R increases. Clearly, the stress intensity factor at the nearby crack tip is larger than that at the distant crack tip for the same imperfect interface parameter N' and geometrical parameters.

4.4 CONCLUSIONS

This chapter presents a semi-analytic solution of the problem of uniaxial loading parallel to the crack. The numerical computations and analysis of the subsequent results have led to the following conclusions:

1. The imperfect bonding makes the SIF at the nearby and distant crack tips significantly large as compared to that corresponding to the perfect interface.
2. Considering the case of SIF at the nearby crack tip, for a stiffer inclusion, when the imperfect interface parameter N' varies from approximately perfect bonding to approximately complete debonding, there is a significant increase in the SIF for the fixed length d/R . For the fixed interface parameter N' , the SIF will decrease as d/R increases.
3. For a softer inclusion, when the imperfect interface parameter changes from perfect bonding to complete debonding, there is a significant increase in the SIF for fixed d/R . On the other hand, the SIF will decrease when d/R increases.
4. Considering the case of SIF at the distant crack tip, for both stiffer and softer inclusions, when the imperfect interface parameter varies from approximately perfect bonding to approximately complete debonding,
5. From all the aforementioned, it can be seen that the imperfect interface parameter has a significant effect on the SIF.

CHAPTER 5

EFFECT OF IMPERFECT BONDING ON RADIAL MATRIX CRACKING--PURE SHEAR LOADING

5.1 DESCRIPTION OF THE PROBLEM

In this chapter, pure shear loading σ_{xy}^0 for the cases of sliding interface ($m = \infty, n = 0$) and $m=3n$ will be considered, respectively. For purely shear loading, we have $A = 0$, $B = i\sigma_{xy}^0$.

5.2 PROBLEM SOLUTIONS

In this section, we will consider two cases of interface parameters: the sliding interface and elastic interphase layer.

5.2.1 The Sliding Interface ($m=\infty, n=0$)

As mentioned in Chapter 4, there are 17 unknown coefficients and equations B.18 to B.34 in Appendix 2 give all the required final linear equations as follows:

$$\frac{a'_3}{2} + (4c_4R^4 - 5c_6R^0)b'_1 + (4R^5c_5 - 5c_7R^7)b'_2 + (4c_6R^6 - 5c_8R^8)b'_3 + (c_1R + 4c_7R^7)b'_4 + e'_3 = (4R^2c_2 - 5R^4c_4)R^4B, \quad (5.1)$$

$$a'_2 + (3c_3R^3 - 4c_5R^5)b'_1 + (3c_4R^4 - 4c_6R^6)b'_2 + (3c_5R^5 - 4c_7R^7 + c_1R)b'_3 + (3c_6R^6 - 4c_8R^8 + c_2R^2)b'_4 + 4d'_4 + e'_2 = (3c_1R - 4c_3R^3A)R^4B, \quad (5.2)$$

$$a'_1 + (3c_4R^4 - 2c_2R^2)b'_1 + (3c_5R^5 - 2c_3R^3 - c_1R)b'_2 + (3c_6R^6 - 2c_4R^4 - c_2R^2)b'_3 + (3c_7R^7 - 2c_5R^5 - c_3R^3)b'_4 - 3d'_3 - e'_1 = 3c_2R^2R^4B, \quad (5.3)$$

$$a'_1 = 0, \quad (5.4)$$

$$3a'_2 - R^3c_3b'_1 - R^4c_4b'_2 + (Rc_1 - R^5c_5)b'_3 + (R^2c_2 - R^6c_6)b'_4 + d'_2 = -Rc_1R^4B, \quad (5.5)$$

$$a'_1 - 2a'_3 - R^4c_4b'_1 + (Rc_1 - R^5c_5)b'_2 + (R^2c_2 - R^6c_6)b'_3 + (R^3c_3 - R^7c_7 - 2Rc_1)b'_4 + d'_3 = -R^2c_2R^4B, \quad (5.6)$$

$$2a'_2 - \frac{5a'_4}{2} + R^5c_5b'_1 + R^6c_6b'_2 + (2Rc_1 + R^7c_7)b'_3 + (2R^2c_2 + R^8c_8)b'_4 - d'_4 = R^3c_3R^4B, \quad (5.7)$$

$$a'_4 + (10R^5c_5 - 12R^7c_7)b'_1 + (10R^6c_6 - 12R^8c_8)b'_2 + 10R^7c_7b'_3 + 10R^8c_8b'_4 - 2e'_4 = (10c_3R^3 - 12c_5R^5)R^4B, \quad (5.8)$$

$$\begin{aligned}
& -\frac{(3+\kappa_1)}{4}a'_3 + \left(\frac{\kappa_1}{2}R^0c_6 - \frac{5}{2}R^0c_6 + 2R^4c_4\right)b'_1 + \left(\frac{\kappa_1}{2}R^7c_7 - \frac{5}{2}R^7c_7 + \right. \\
& 2R^5c_5)b'_2 + \left(\frac{\kappa_1}{2}c_8R^8 - \frac{5}{2}R^8c_8 + 2R^6c_6\right)b'_3 + \left(2R^7c_7 - \frac{3}{4}Rc_1 - \frac{\kappa_1}{2}Rc_1\right)b'_4 + \\
& \left(\frac{1}{2}\frac{\mu_1}{\mu_2} + \frac{3}{N'}\right)e'_3 = \left[\frac{(\kappa_1-5)}{2}R^4c_4 + 2R^2c_2\right]R^4B,
\end{aligned} \tag{5.9}$$

$$\begin{aligned}
& -\frac{(2+\kappa_1)}{2}a'_2 + \frac{5}{4}a'_4 + \left(\frac{\kappa_1}{2}R^5c_5 + \frac{3}{2}R^3c_3 - 2R^5c_5\right)b'_1 + \left(\frac{\kappa_1}{2}R^0c_6 + \frac{3}{2}R^4c_4 - \right. \\
& 2R^0c_6)b'_2 + \left(\frac{\kappa_1}{2}R^7c_7 + \frac{3}{2}R^5c_5 - 2R^7c_7 - Rc_1 - \frac{\kappa_1}{2}Rc_1\right)b'_3 + \left(\frac{\kappa_1}{2}R^8c_8 + \right. \\
& \left.\frac{3}{2}R^0c_6 - 2R^8c_8 - R^2c_2 - \frac{\kappa_1}{2}R^2c_2\right)b'_4 + \left(2\frac{\mu_1}{\mu_2} - \frac{\kappa_2\mu_1}{4\mu_2} + \frac{8}{N'}\right)d'_4 + \\
& \left(\frac{1}{2}\frac{\mu_1}{\mu_2} + \frac{2}{N'}\right)e'_2 = \left(\frac{\kappa_1}{2}R^3c_3 - 2R^3c_3 + \frac{3}{2}Rc_1\right)R^4B,
\end{aligned} \tag{5.10}$$

$$\begin{aligned}
& \frac{(\kappa_1-1)}{2}a'_1 + a'_3 + \left(\frac{\kappa_1}{2}R^4c_4 - \frac{3}{2}R^4c_4 + R^2c_2\right)b'_1 + \left(\frac{\kappa_1}{2}R^5c_5 - \right. \\
& \left.\frac{3}{2}R^5c_5 + R^3c_3 - \frac{1}{2}Rc_1 - \frac{\kappa_1}{2}Rc_1\right)b'_2 + \left(\frac{\kappa_1}{2}R^0c_6 - \frac{3}{2}R^0c_6 + R^4c_4 - \right. \\
& \left.\frac{1}{2}R^2c_2 - \frac{\kappa_1}{2}R^2c_2\right)b'_3 + \left(\frac{\kappa_1}{2}R^7c_7 - \frac{3}{2}R^7c_7 + R^5c_5 - \frac{1}{2}R^3c_3 - \right. \\
& \left.\frac{\kappa_1}{2}R^3c_3 + Rc_1\right)b'_4 + \left(\frac{3}{2}\frac{\mu_1}{\mu_2} - \frac{\kappa_2}{4}\frac{\mu_1}{\mu_2} + \frac{3}{N'}\right)d'_3 + \left(\frac{1}{2}\frac{\mu_1}{\mu_2} + \frac{1}{N'}\right)e'_1 = \\
& -\left(\frac{\kappa_1}{2}R^2c_2 + \frac{3}{2}R^2c_2\right)R^4B,
\end{aligned} \tag{5.11}$$

$$\begin{aligned}
& \frac{3}{2}a'_2 + \left(\frac{\kappa_1}{2}R^3c_3 - \frac{\kappa_1}{2}Rc_1 - R^3c_3 + \frac{1}{2}Rc_1\right)b'_1 + \left(\frac{\kappa_1}{2}R^4c_4 - \frac{\kappa_1}{2}R^2c_2 - \right. \\
& \left. R^4c_4 + \frac{1}{2}R^2c_2\right)b'_2 + \left(\frac{\kappa_1}{2}R^5c_5 - \frac{\kappa_1}{2}R^3c_3 - R^5c_5 + \frac{1}{2}R^3c_3 + \frac{1}{2}Rc_1\right)b'_3 + \\
& \left(\frac{\kappa_1}{2}R^6c_6 - \frac{\kappa_1}{2}R^4c_4 - R^6c_6 + \frac{1}{2}R^4c_4 + \frac{1}{2}R^2c_2\right)b'_4 + \frac{\kappa_2}{2}\frac{\mu_1}{\mu_2}d'_0 + \\
& \left(1 - \frac{\kappa_2}{4}\right)\frac{\mu_1}{\mu_2}d'_2 = \left(\frac{\kappa_1}{2}Rc_1 - Rc_1\right)R^4B,
\end{aligned} \tag{5.12}$$

$$a'_1 - \frac{\mu_1}{\mu_2}\kappa_2d'_1 = 0, \tag{5.13}$$

$$\begin{aligned}
& -\frac{3}{2}a'_2 + \left(\frac{\kappa_1}{2}Rc_1 + R^3c_3 - \frac{1}{2}Rc_1 - \frac{\kappa_1}{2}R^3c_3\right)b'_1 + \left(\frac{\kappa_1}{2}R^2c_2 + R^4c_4 - \right. \\
& \left. \frac{1}{2}R^2c_2 - \frac{\kappa_1}{2}R^4c_4\right)b'_2 + \left(\frac{\kappa_1}{2}R^3c_3 + R^5c_5 - \frac{1}{2}R^3c_3 - \frac{\kappa_1}{2}R^5c_5 - \right. \\
& \left. \frac{1}{2}Rc_1\right)b'_3 + \left(\frac{\kappa_1}{2}R^4c_4 + R^6c_6 - \frac{1}{2}R^4c_4 - \frac{\kappa_1}{2}R^6c_6 - \frac{1}{2}R^2c_2\right)b'_4 - \\
& \frac{\kappa_2}{2}\frac{\mu_1}{\mu_2}d'_0 - \left(\frac{\mu_1}{\mu_2} - \frac{\kappa_2}{2}\frac{\mu_1}{\mu_2} - \frac{2}{N'}\right)d'_2 = (1 - \kappa_1/2)Rc_1R^4B,
\end{aligned} \tag{5.14}$$

$$\begin{aligned}
& \frac{(1 + \kappa_1)}{2}a'_1 - a'_3 + \left(\frac{3}{2}R^4c_4 - R^2c_2 - \frac{\kappa_1}{2}R^4c_4\right)b'_1 + \left(\frac{\kappa_1}{2}Rc_1 + \right. \\
& \left. \frac{3}{2}R^5c_5 - R^3c_3 - \frac{\kappa_1}{2}R^5c_5 + \frac{1}{2}Rc_1\right)b'_2 + \left(\frac{\kappa_1}{2}R^2c_2 + \frac{3}{2}R^6c_6 - \right. \\
& \left. R^4c_4 - \frac{\kappa_1}{2}R^6c_6 + \frac{1}{2}R^2c_2\right)b'_3 + \left(\frac{\kappa_1}{2}R^3c_3 + \frac{3}{2}R^7c_7 - R^5c_5 - \right. \\
& \left. \frac{\kappa_1}{2}R^7c_7 + \frac{1}{2}R^3c_3 - Rc_1\right)b'_4 - \left(\frac{3}{2}\frac{\mu_1}{\mu_2} - \frac{\kappa_2}{2}\frac{\mu_1}{\mu_2} - \frac{3}{N'}\right)d'_3 - \frac{1}{2}\frac{\mu_1}{\mu_2}e'_1 \\
& = \left(\frac{3}{2}R^2c_2 - \frac{\kappa_1}{2}R^2c_2\right)R^4B,
\end{aligned} \tag{5.15}$$

$$\begin{aligned}
& (1 + \kappa_1/2)a'_2 - \frac{5}{4}a'_4 + (2R^5c_5 - \frac{3}{2}R^3c_3 - \frac{\kappa_1}{2}R^5c_5)b'_1 + (2R^6c_6 - \\
& \frac{3}{2}R^4c_4 - \frac{\kappa_1}{2}R^6c_6)b'_2 + (\frac{\kappa_1}{2}Rc_1 + 2R^7c_7 - \frac{3}{2}R^5c_5 - \frac{\kappa_1}{2}R^7c_7 + \\
& Rc_1)b'_3 + (\frac{\kappa_1}{2}R^2c_2 + 2R^8c_8 - \frac{3}{2}R^6c_6 - \frac{\kappa_1}{2}R^8c_8 + R^2c_2)b'_4 - \\
& (2\frac{\mu_1}{\mu_2} - \frac{\kappa_2}{2}\frac{\mu_1}{\mu_2} - \frac{4}{N'})d'_4 - \frac{1}{2}\frac{\mu_1}{\mu_2}e'_2 = (R^3c_3 - \frac{3}{2}Rc_1 - \frac{\kappa_1}{2}R^3c_3)R^4B,
\end{aligned} \tag{5.16}$$

and

$$\begin{aligned}
& -(1 + \frac{\kappa_1}{4})a'_4 + (\frac{\kappa_1}{2}R^7c_7 - 3R^7c_7 + \frac{5}{2}R^5c_5)b'_1 + (\frac{\kappa_1}{2}R^8c_8 - \\
& 3R^8c_8 + \frac{5}{2}R^6c_6)b'_2 + \frac{5}{2}R^7c_7b'_3 + \frac{5}{2}R^8c_8b'_4 + (\frac{1}{2}\frac{\mu_1}{\mu_2} + \frac{4}{N'})e'_4 = \\
& (\frac{\kappa_1}{2}R^5c_5 - 3R^5c_5 + \frac{5}{2}R^3c_3)R^4B.
\end{aligned} \tag{5.17}$$

5.2.2 The Elastic Interphase Layer ($m=3n$)

The relevant 17 final linear algebraic equations for the elastic interphase layer given from B.35 to B.51 in Appendix B are shown as follows:

$$\begin{aligned}
& \frac{a'_3}{2} + (4c_4R^4 - 5c_6R^6)b'_1 + (4R^5c_5 - 5c_7R^7)b'_2 + (4c_6R^6 - 5c_8R^8)b'_3 + \\
& (c_1R + 4c_7R^7)b'_4 + e'_3 = (4R^2c_2 - 5R^4c_4)R^4B,
\end{aligned} \tag{5.18}$$

$$\begin{aligned}
& a'_2 + (3c_3R^3 - 4c_5R^5)b'_1 + (3c_4R^4 - 4c_6R^6)b'_2 + (3c_5R^5 - 4c_7R^7 + \\
& c_1R)b'_3 + (3c_6R^6 - 4c_8R^8 + c_2R^2)b'_4 + 4d'_4 + e'_2 = (3c_1R - 4c_3R^3)R^4B,
\end{aligned} \tag{5.19}$$

$$\begin{aligned}
& a'_1 + (3c_4R^4 - 2c_2R^2)b'_1 + (3c_5R^5 - 2c_3R^3 - c_1R)b'_2 + (3c_6R^6 - 2c_4R^4 - \\
& c_2R^2)b'_3 + (3c_7R^7 - 2c_5R^5 - c_3R^3)b'_4 - 3d'_3 - e'_1 = 3c_2R^2R^4B,
\end{aligned} \tag{5.20}$$

$$a'_1 = 0, \quad (5.21)$$

$$3a'_2 - R^3 c_3 b'_1 - R^4 c_4 b'_2 + (Rc_1 - R^5 c_5) b'_3 + (R^2 c_2 - R^6 c_6) b'_4 + d'_2 = -Rc_1 R^4 B, \quad (5.22)$$

$$a'_1 - 2a'_3 - R^4 c_4 b'_1 + (Rc_1 - R^5 c_5) b'_2 + (R^2 c_2 - R^6 c_6) b'_3 + (R^3 c_3 - R^7 c_7 - 2Rc_1) b'_4 + d'_3 = -R^2 c_2 R^4 B, \quad (5.23)$$

$$2a'_2 - \frac{5a'_4}{2} + R^5 c_5 b'_1 + R^6 c_6 b'_2 + (2Rc_1 + R^7 c_7) b'_3 + (2R^2 c_2 + R^8 c_8) b'_4 - d'_4 = R^3 c_3 R^4 B, \quad (5.24)$$

$$a'_4 + (10R^5 c_5 - 12R^7 c_7) b'_1 + (10R^6 c_6 - 12R^8 c_8) b'_2 + 10R^7 c_7 b'_3 + 10R^8 c_8 b'_4 - 2e'_4 = (10c_3 R^3 - 12c_5 R^5) R^4 B, \quad (5.25)$$

$$\begin{aligned} & -\frac{(3/2 + \kappa_1)}{4} a'_3 + \left(\frac{\kappa_1}{4} R^6 c_6 - \frac{5}{2} R^6 c_6 + 2R^4 c_4\right) b'_1 + \left(\frac{\kappa_1}{4} R^7 c_7 - \frac{5}{2} R^7 c_7 + \right. \\ & \left. 2R^5 c_5\right) b'_2 + \left(\frac{\kappa_1}{4} c_8 R^8 - \frac{5}{2} R^8 c_8 + 2R^6 c_6\right) b'_3 + \left(2R^7 c_7 - \frac{3}{4} Rc_1 - \frac{\kappa_1}{2} Rc_1\right) b'_4 + \\ & \left(\frac{1}{2} \frac{\mu_1}{\mu_2} + \frac{3}{N'}\right) e'_3 = \left[\frac{(\kappa_1 - 10)}{4} R^4 c_4 + 2R^2 c_2\right] R^4 B, \end{aligned} \quad (5.26)$$

$$\begin{aligned}
& -\frac{(1+\kappa_1)}{2}a'_2 + \frac{5}{8}a'_4 + \left(\frac{\kappa_1}{4}R^5c_5 + \frac{3}{2}R^3c_3 - 2R^5c_5\right)b'_1 + \left(\frac{\kappa_1}{4}R^6c_6 + \frac{3}{2}R^4c_4 - \right. \\
& \left. 2R^6c_6\right)b'_2 + \left(\frac{\kappa_1}{4}R^7c_7 + \frac{3}{2}R^5c_5 - 2R^7c_7 - \frac{1}{2}Rc_1 - \frac{\kappa_1}{2}Rc_1\right)b'_3 + \left(\frac{\kappa_1}{4}R^8c_8 + \right. \\
& \left. \frac{3}{2}R^6c_6 - 2R^8c_8 - \frac{1}{2}R^2c_2 - \frac{\kappa_1}{2}R^2c_2\right)b'_4 + \left(2\frac{\mu_1}{\mu_2} - \frac{\kappa_2\mu_1}{4\mu_2} + \frac{8}{N'}\right)d'_4 + \\
& \left(\frac{1}{2}\frac{\mu_1}{\mu_2} + \frac{2}{N'}\right)e'_2 = \left(\frac{\kappa_1}{4}R^3c_3 - 2R^3c_3 + \frac{3}{2}Rc_1\right)R^4B,
\end{aligned} \tag{5.27}$$

$$\begin{aligned}
& \frac{(\kappa_1 - 1/2)}{2}a'_1 + \frac{3}{2}a'_3 + \left(\frac{\kappa_1}{4}R^4c_4 - \frac{3}{2}R^4c_4 + R^2c_2\right)b'_1 + \left(\frac{\kappa_1}{4}R^5c_5 - \right. \\
& \left. \frac{3}{2}R^5c_5 + R^3c_3 - \frac{1}{4}Rc_1 - \frac{\kappa_1}{2}Rc_1\right)b'_2 + \left(\frac{\kappa_1}{4}R^6c_6 - \frac{3}{2}R^6c_6 + R^4c_4 - \right. \\
& \left. \frac{1}{4}R^2c_2 - \frac{\kappa_1}{2}R^2c_2\right)b'_3 + \left(\frac{\kappa_1}{4}R^7c_7 - \frac{3}{2}R^7c_7 + R^5c_5 - \frac{1}{4}R^3c_3 - \right. \\
& \left. \frac{\kappa_1}{2}R^3c_3 + \frac{Rc_1}{2}\right)b'_4 + \left(\frac{3}{2}\frac{\mu_1}{\mu_2} - \frac{\kappa_2}{4}\frac{\mu_1}{\mu_2} + \frac{3}{N'}\right)d'_3 + \left(\frac{1}{2}\frac{\mu_1}{\mu_2} + \frac{1}{N'}\right)e'_1 = \\
& -\left(\frac{\kappa_1}{4}R^2c_2 + \frac{3}{2}R^2c_2\right)R^4B,
\end{aligned} \tag{5.28}$$

$$\begin{aligned}
& \frac{3}{4}a'_2 + \left(\frac{\kappa_1}{4}R^3c_3 - \frac{\kappa_1}{2}Rc_1 - R^3c_3 + \frac{1}{2}Rc_1\right)b'_1 + \left(\frac{\kappa_1}{4}R^4c_4 - \frac{\kappa_1}{2}R^2c_2 - \right. \\
& \left. R^4c_4 + \frac{1}{2}R^2c_2\right)b'_2 + \left(\frac{\kappa_1}{4}R^5c_5 - \frac{\kappa_1}{2}R^3c_3 - R^5c_5 + \frac{1}{2}R^3c_3 + \frac{1}{4}Rc_1\right)b'_3 + \\
& \left(\frac{\kappa_1}{4}R^6c_6 - \frac{\kappa_1}{2}R^4c_4 - R^6c_6 + \frac{1}{2}R^4c_4 + \frac{1}{4}R^2c_2\right)b'_4 + \frac{\kappa_2}{2}\frac{\mu_1}{\mu_2}d'_0 + \\
& \left(1 - \frac{\kappa_2}{4}\right)\frac{\mu_1}{\mu_2}d'_2 = \left(\frac{\kappa_1}{4}Rc_1 - 4Rc_1\right)R^4B,
\end{aligned} \tag{5.29}$$

$$\begin{aligned}
& \frac{a'_1}{2} + \left(\frac{\kappa_1}{4} R^2 c_2 + \frac{1}{4} R^2 c_2 - \frac{\kappa_1}{2} R^2 c_2 - \frac{1}{2} R^2 c_2 \right) b'_1 + \left(\frac{\kappa_1}{4} R^3 c_3 + \frac{1}{4} R^3 c_3 - \right. \\
& \left. \frac{\kappa_1}{2} R^3 c_3 - \frac{R^3 c_3}{2} \right) b'_2 + \left(\frac{\kappa_1}{4} R^4 c_4 - \frac{1}{4} R^4 c_4 - \frac{\kappa_1}{2} R^4 c_4 - \frac{R^4 c_4}{2} \right) b'_3 + \\
& \left(\frac{\kappa_1}{4} R^5 c_5 - \frac{1}{4} R^5 c_5 - \frac{\kappa_1}{2} R^5 c_5 - \frac{R^5 c_5}{2} \right) b'_4 + \left(\frac{\mu_1}{4\mu_2} - \kappa_2 \frac{3\mu_1}{4\mu_2} \right) d'_1 = \\
& \left(\frac{\kappa_1}{8} + \frac{1}{8} \right) R^4 B,
\end{aligned} \tag{5.30}$$

$$\begin{aligned}
& -\frac{3}{2} a'_2 + \left(\frac{\kappa_1}{4} R c_1 + \frac{R^3}{2} c_3 - \frac{1}{2} R c_1 - \frac{\kappa_1}{2} R^3 c_3 \right) b'_1 + \left(\frac{\kappa_1}{4} R^2 c_2 + \frac{R^4}{2} c_4 - \right. \\
& \left. \frac{1}{2} R^2 c_2 - \frac{\kappa_1}{2} R^4 c_4 \right) b'_2 + \left(\frac{\kappa_1}{4} R^3 c_3 + \frac{R^5}{2} c_5 - \frac{1}{2} R^3 c_3 - \frac{\kappa_1}{2} R^5 c_5 - \right. \\
& \left. \frac{1}{2} R c_1 \right) b'_3 + \left(\frac{\kappa_1}{4} R^4 c_4 + \frac{R^6}{2} c_6 - \frac{1}{2} R^4 c_4 - \frac{\kappa_1}{2} R^6 c_6 - \frac{1}{2} R^2 c_2 \right) b'_4 - \\
& \frac{\kappa_2}{4} \frac{\mu_1}{\mu_2} d'_0 - \left(\frac{1}{2} \frac{\mu_1}{\mu_2} - \frac{\kappa_2}{2} \frac{\mu_1}{\mu_2} - \frac{2}{N'} \right) d'_2 = \frac{(1-\kappa_1)}{2} R c_1 R^4 B,
\end{aligned} \tag{5.31}$$

$$\begin{aligned}
& \frac{(1+\kappa_1/2)}{2} a'_1 - a'_3 + \left(\frac{3}{4} R^4 c_4 - \frac{1}{2} R^2 c_2 - \frac{\kappa_1}{2} R^4 c_4 \right) b'_1 + \left(\frac{\kappa_1}{4} R c_1 + \right. \\
& \left. \frac{3}{4} R^5 c_5 - \frac{1}{2} R^3 c_3 - \frac{\kappa_1}{2} R^5 c_5 + \frac{1}{2} R c_1 \right) b'_2 + \left(\frac{\kappa_1}{4} R^2 c_2 + \frac{3}{4} R^6 c_6 - \right. \\
& \left. \frac{1}{2} R^4 c_4 - \frac{\kappa_1}{2} R^6 c_6 + \frac{1}{2} R^2 c_2 \right) b'_3 + \left(\frac{\kappa_1}{4} R^3 c_3 + \frac{3}{4} R^7 c_7 - \frac{1}{2} R^5 c_5 - \right. \\
& \left. \frac{\kappa_1}{2} R^7 c_7 + \frac{1}{2} R^3 c_3 - R c_1 \right) b'_4 - \left(\frac{3}{4} \frac{\mu_1}{\mu_2} - \frac{\kappa_2}{2} \frac{\mu_1}{\mu_2} - \frac{3}{N'} \right) d'_3 - \frac{1}{4} \frac{\mu_1}{\mu_2} e'_1 \\
& = \left(\frac{3}{4} R^2 c_2 - \frac{\kappa_1}{2} R^2 c_2 \right) R^4 B,
\end{aligned} \tag{5.32}$$

$$\begin{aligned}
& (1 + \kappa_1 / 4) a'_2 - \frac{5}{4} a'_4 + (R^5 c_5 - \frac{3}{4} R^3 c_3 - \frac{\kappa_1}{2} R^5 c_5) b'_1 + (R^6 c_6 - \\
& \frac{3}{4} R^4 c_4 - \frac{\kappa_1}{2} R^6 c_6) b'_2 + (\frac{\kappa_1}{4} R c_1 + R^7 c_7 - \frac{3}{4} R^5 c_5 - \frac{\kappa_1}{2} R^7 c_7 + \\
& R c_1) b'_3 + (\frac{\kappa_1}{4} R^2 c_2 + R^8 c_8 - \frac{3}{4} R^6 c_6 - \frac{\kappa_1}{2} R^8 c_8 + R^2 c_2) b'_4 - \\
& (\frac{\mu_1}{\mu_2} - \frac{\kappa_2}{2} \frac{\mu_1}{\mu_2} - \frac{4}{N'}) d'_4 - \frac{1}{4} \frac{\mu_1}{\mu_2} e'_2 = (R^3 c_3 - \frac{3}{4} R c_1 - \frac{\kappa_1}{2} R^3 c_3) R^4 B,
\end{aligned} \tag{5.33}$$

and

$$\begin{aligned}
& -(\frac{1}{2} + \frac{\kappa_1}{4}) a'_4 + (\frac{\kappa_1}{4} R^7 c_7 - 3 R^7 c_7 + \frac{5}{2} R^5 c_5) b'_1 + (\frac{\kappa_1}{4} R^8 c_8 - \\
& 3 R^8 c_8 + \frac{5}{2} R^6 c_6) b'_2 + \frac{5}{2} R^7 c_7 b'_3 + \frac{5}{2} R^8 c_8 b'_4 + (\frac{1}{2} \frac{\mu_1}{\mu_2} + \frac{4}{N'}) e'_4 = \\
& (\frac{\kappa_1}{4} R^5 c_5 - 3 R^5 c_5 + \frac{5}{2} R^3 c_3) R^4 B.
\end{aligned} \tag{5.34}$$

5.2 NUMERICAL RESULTS AND DISCUSSIONS

In the present case, the stresses acting in the neighborhood of the crack tip $z = a$ are:

$$\sigma_{xx} = \frac{\sqrt{l}}{\sqrt{2r_1}} \sigma_{xy}^0 \frac{a}{l} \left(\frac{3}{4} \sin \frac{\theta_1}{2} + \frac{1}{4} \sin 5 \frac{\theta_1}{2} \right) \left[1 + \frac{1}{2a\sigma_{xy}^0} \sum_{k=1}^{\infty} k b_{k+1} a^{-(k+1)} \right] + O(r_1^0),$$

$$\sigma_{yy} = \frac{\sqrt{l}}{\sqrt{2r_1}} \sigma_{xy}^0 \frac{a}{l} \left(\frac{5}{4} \sin \frac{\theta_1}{2} - \frac{1}{4} \sin 5 \frac{\theta_1}{2} \right) \left[1 + \frac{1}{2a\sigma_{xy}^0} \sum_{k=1}^{\infty} k b_{k+1} a^{-(k+1)} \right] + O(r_1^0),$$

$$\sigma_{xy} = \frac{\sqrt{l}}{\sqrt{2r_1}} \sigma_{xy}^0 \frac{a}{l} \left(\frac{1}{4} \cos \frac{\theta_1}{2} - \frac{1}{4} \cos 5 \frac{\theta_1}{2} \right) \left[1 + \frac{1}{2a\sigma_{xy}^0} \sum_{k=1}^{\infty} k b_{k+1} a^{-(k+1)} \right] + O(r_1^0),$$

where $z - a = r_1 e^{i\theta_1}$ ($0 \leq \theta_1 \leq 2\pi$). The half length of crack $\frac{b-a}{2}$ is denoted by l .

Similarly, the stress state around the crack tip $z = b$ is given by

$$\sigma_{xx} = -\frac{\sqrt{l}}{\sqrt{2r_2}} \sigma_{xy}^0 \frac{b}{l} \left(\frac{3}{4} \cos \frac{\theta_2}{2} + \frac{1}{4} \cos 5 \frac{\theta_2}{2} \right) \left[1 + \frac{1}{2b\sigma_{xy}^0} \sum_{k=1}^{\infty} kb_{k+1} a^{-(k+1)} \right] + O(r_2^0),$$

$$\sigma_{yy} = -\frac{\sqrt{l}}{\sqrt{2r_2}} \sigma_{xy}^0 \frac{b}{l} \left(\frac{5}{4} \cos \frac{\theta_2}{2} - \frac{1}{4} \cos 5 \frac{\theta_2}{2} \right) \left[1 + \frac{1}{2b\sigma_{xy}^0} \sum_{k=1}^{\infty} kb_{k+1} a^{-(k+1)} \right] + O(r_2^0),$$

$$\sigma_{xy} = \frac{\sqrt{l}}{\sqrt{2r_2}} \sigma_{xy}^0 \frac{b}{l} \left(\frac{1}{4} \sin \frac{\theta_2}{2} - \frac{1}{4} \sin 5 \frac{\theta_2}{2} \right) \left[1 + \frac{1}{2b\sigma_{xy}^0} \sum_{k=1}^{\infty} kb_{k+1} a^{-(k+1)} \right] + O(r_2^0),$$

where $z - b = r_2 e^{i\theta_2}$ ($-\pi \leq \theta_2 \leq \pi$).

First, we study the mode-II stress intensity factor ratio, which is defined by K_{II}/K_{II}^0 (where K_{II} is the actual mode-II SIF and $K_{II}^0 = \sigma_{xy}^0 \sqrt{\pi l}$ is the mode-II SIF for the same crack in a homogeneous matrix material), at the nearby crack tip (Figure 5.1) for the case of a sliding interface ($m=\infty$, $n=0$) under purely shear loading. Compared with Figure 3.9 which corresponds to the sliding interface under uniaxial loading, Figure 5.1 shows that the SIF at the nearby crack tip increases when the distance d decreases for both softer and stiffer inclusions. As shown in Figure 5.1, inclusions with sliding interfaces always have increasing SIFs at the nearby crack tip as compared to $\sigma_{xy}^0 \sqrt{\pi l}$. Apparently, the sliding interface has a significant effect on the SIF at the nearby crack tip.

Figures 5.2 and 5.3 show the influence of the interface parameters ($m=3n$) on the behavior of mode-II stress intensity factor ratios under pure shear loading, whereas Figures 5.4 and 5.5 show the influence on mode-I stress intensity factor ratios under the same loading conditions. In Figures 5.2 and 5.3, the effects of the imperfect interface parameter N' on K_{II} at the nearby crack tip are investigated for softer and stiffer inclusions. For the softer inclusion, as shown in Figure 5.2, K_{II} increases monotonically for the fixed imperfect interface parameter N' when d/R becomes smaller, while K_{II} decreases with increasing N' for the fixed distance. On the other hand, for the stiffer inclusion, $K_{II}(a)$ decreases when d/R becomes larger, while $K_{II}(a)$ increases as the imperfect interface parameter N' decreases. When N' varies from 0.01 to 100, the inclusion with an imperfect interface ($m=3n$) can lead to either an increase in the SIF at the nearby crack tip or a significant reduction when compared to $\sigma_{xy}^0 \sqrt{\pi d}$. Hence, in both cases, interface imperfections have a significant effect on K_{II} .

In particular, Figures 5.4 and 5.5 illustrate the effects of the imperfect interface parameters on K_I at the nearby crack tip under pure shear loading. Owing to the presence of the inclusion and the imperfect interface, K_I is non-zero even under pure shear loading and therefore cannot be ignored. It is clear that the curves in Figures 5.4 and 5.5, for either softer or stiffer inclusions, are quite similar. For example, when the imperfect interface parameter N' is fixed, K_I increases monotonically when d/R becomes smaller while the SIF decreases with increasing N' when d/R is fixed.

5.3 CONCLUSIONS

This Chapter presents a study of the effects of imperfect bonding for pure shear loading. The numerical calculations and analysis of the subsequent results have led to the following conclusions:

1. The sliding interface has a significant effect on mode-II SIF at the nearby crack tip for pure shear loading.
2. The SIF at the nearby crack tip increases when the distance d decreases for both softer and stiffer inclusions, and inclusions with sliding interfaces always have increasing SIFs at the nearby crack tip.
3. For an elastic interphase layer ($m=3n$), the interface imperfections have significant effects on both mode-I and mode-II SIFs.
4. For a softer inclusion, K_{II} increases monotonically for the fixed imperfect interface parameter N' when d/R becomes smaller, while K_{II} decreases with increasing N' for the fixed distance. For the stiffer inclusion, $K_{II}(a)$ decreases when d/R becomes larger, while $K_{II}(a)$ increases as the imperfect interface parameter N' decreases. When N' varies from 0.01 to 100, the inclusion with an imperfect interface ($m=3n$) can lead to either an increase in the SIF at the nearby crack tip or a significant reduction.

5. The presence of imperfect interface makes the mode-I SIF significantly large at the nearby crack tip and cannot be ignored.

CHAPTER 6

CONCLUSIONS AND FUTURE WORK

6.1 CONCLUSIONS

In this thesis, the problem of the interaction between a circular inclusion with an imperfect interface and a radial matrix crack, subjected to several different types of loading, is studied using a homogeneously imperfect interface model. Such an imperfect interface model allows displacement discontinuities across the inclusion/matrix interface. Using analytic continuation, a novel series method is developed to find the stress intensity factors (SIFs) at the tips of the radial matrix crack. Numerical results show that the interface imperfection has a significant effect on the SIFs especially when the crack is close to the inclusion.

In the present research, the interphase is modeled by a distribution of mechanical springs. The constants m and n are the coefficients of these springs. Within this approach, the composite is modeled as a two-phase material with imperfect interfacial conditions applied along the interface between the single inclusion and its surrounding matrix. The single-inclusion model adopted in the analysis is a much simpler model than other available multi-inclusion composite models used by others. This model, as discussed by Schmauder et al., 1992, is suitable for modeling composites with lower fiber volume fractions. Under this condition, the interaction among neighboring fibers and its influence on the stress

fields of the overall composite system can be neglected. Therefore, a single fiber model should describe the stress and displacement fields inside and around the inclusion reliably for lower fiber volume content composites.

It was noticed in Section 3.3 of Chapter 3, that a possible negative normal displacement jump is an issue of major concern for the present imperfect interface model. There are two different methods available to address this issue. The first one is to modify the imperfect interface model by assuming the continuity of normal displacement at all points where a compressive normal traction occurs (Achenbach and Zhu, 1989, 1990). The second tolerates a limited negative normal displacement jump bounded by the original thickness of the interphase layer (Hashin, 1991). As explained in Section 3.3 of Chapter 3, the interphase layer can sustain a tensile normal traction as well as a compressive normal traction. Consequently, a negative normal displacement jump is acceptable provided it is smaller than the original interphase thickness.

In summary, the problem of the interaction between a circular inclusion and a radial matrix crack with a homogeneously imperfect interface, subjected to several different types of mechanical loading, is studied. A spring-type imperfect interface model is proposed and complex variable techniques are used to obtain the analytic potential functions. Numerical calculations are presented and the major conclusions can be drawn from these results studied in this research:

- For inclusions softer than the matrix, the radial matrix crack always propagates towards the inclusion regardless of the values of the imperfect interface parameters.
- However, for inclusions stiffer than matrix, the radial matrix crack can propagate either toward or away from the inclusion, depending on the values of the imperfect interface parameters. It is therefore crucial to quantify the effect of interface imperfection on the interaction between a circular inclusion and a radial matrix crack.
- Remarkably, in contrast to the case of a perfect interface for which the SIF at the nearby crack tip is greater than the SIF at the distant crack tip only when the inclusion is more compliant than the matrix, the imperfect bonding condition allows for the possibility of a SIF at the nearby crack tip greater than that at the distant crack tip even when the inclusion is stiffer than the matrix. In fact, for any given inclusion stiffer than the surrounding matrix, there is a corresponding critical value of the imperfect interface parameter below which a radial matrix crack grows toward the interface leading to interface debonding.
- In particular, for given crack length and distance from the interface, there is a minimum critical value of the imperfect interface parameter (defined by N^* in Section 3.1) below which (that is, when $N' < N^*$) the SIF in the nearby crack tip is always greater than that at the distant crack tip for any shear modulus ratio of the inclusion and the matrix.
- All these results provide, for the first time, a clear quantitative relation between interface imperfection and the direction of growth of radial matrix cracks. It is

therefore possible to predict and control the direction of matrix cracking and therefore interfacial debonding by designing the inclusion-matrix interface accordingly.

- In particular, for the special case of a perfectly bonded or entirely debonded interface, the present results are consistent with the known results for a radial matrix crack near a circular inclusion or a circular hole, available in the literature.
- All of the aforementioned results show that the present series method provides a simple and effective way of investigating an inclusion-crack interaction involving an imperfect interface.

6.2 THE FUTURE WORK

In the present study, only simpler mechanical loading conditions are considered for a two-phase composite material. The further possible development of the research might include the following aspects:

- 1) To experimentally determine the values of two imperfect interface parameters m and n for the applications of the model to practical problems.
- 2) *Three-phase circular inclusion* with an interior, intermediate or exterior radial crack.
- 3) *Void or rigid inclusion/matrix*, as simpler cases, in order to simplify the analysis.
- 4) *Thermal loading* due to thermal mismatch or some eigenstrains.

- 5) A radial crack in *touch with the interface*, from the inside or outside.
- 6) Other radial line defect (e.g. rigid-line inclusion, or radial crack with partial closure or friction).

REFERENCES

- Aboudi, J., 1987, "Damage in composite-modeling of imperfect bounding," *Compos. Sci. Tech.* 28, 103-128.
- Achenbach, J.D., and Zhu, H., 1989, "Effect of Interfacial Zone on Mechanical Behavior and Failure of Fiber-Reinforced Composites," *Journal of the Mechanics and Physics of Solids*, Vol. 37, pp. 381-393.
- Achenbach, J.D., and Zhu, H., 1990, "Effect of interphases on micro and macromechanical behavior of hexagonal-array fiber composites," *ASME Journal of Applied Mechanics*, Vol. 57, pp. 956-963.
- Agarwal, B. D., and Bansal, R. K., 1979, "Effect of an interfacial layer on the properties of composites," *Fiber Science and Technology*, Vol. 12, pp. 149-158.
- Atkinson, C., 1972, "The interaction between a crack and an inclusion," *International Journal of Engineering science*, Vol. 10, pp. 127-136.
- Benveniste, Y., 1984, "On the effect of debonding on the overall behavior of composite materials," *Mechanics of Materials*, Vol. 3, pp. 349-358.
- Benveniste, Y., Dvorak, G. J., and Chen, T., 1989, "Stress fields in composites with coated inclusions," *Mechanics of Materials*, Vol. 7, pp. 305-317.
- Bigoni, D, Serkov, S.K., Valentini, M. and Movchan, A.B., 1998, "Asymptotic model of dilute composite with imperfectly bonded inclusions," *International Journal of Solids and Structures*, Vol. 35, pp. 3239-3258.

- Budiansky, B., Hutchinson, J.W., and Evans, A.G., 1986, "Matrix fracture in fiber-reinforced ceramics," *Journal of the Mechanics and Physics of Solids*, Vol. 34, pp. 167-189.
- Budiansky, B., Evans, A.G., and Hutchinson, J.W., 1995, "Fiber-matrix debonding defects on cracking in aligned fiber ceramic composites," *International Journal of Solids and Structures*, Vol. 32, pp. 315-328.
- Crolet, J. M., Aoubiza, B., and Meunier, A., 1993, "Compact bone: numerical simulation of mechanical characteristics," *Journal of Biomechanics*, Vol. 26, pp. 677-687.
- Dundurs, J., and Zienkiewicz, O. C., 1964, "Stresses around circular inclusion due to thermal gradients with particular reference to reinforced concrete," *Journal of The American Concrete Institute*, pp. 1523-1533.
- Dundurs, J., and Mura, T., 1964, "Interaction between an edge dislocation and a circular inclusion," *The Journal of the Mechanics and Physics of Solids*, Vol. 12, pp. 177-189.
- Dundurs, J., and Gangadharan, A.C., 1969, "Edge dislocation near an inclusion with a slipping interface," *Journal of the Mechanics and Physics of Solids*, Vol. 47, pp. 1873-1892.
- Dundurs, J., 1989, "Cavities vis-à-vis rigid inclusions and some related general results in plane elasticity," *ASME Journal of Applied Mechanics*, Vol. 56, pp. 786-790.
- England, A.H., 1971, *Complex Variable Method in Elasticity*. Wiley Interscience, London.

- Erdogan, F., Gupta, G.D., and Ratwani, M., 1974, "Interaction between a circular inclusion and an arbitrarily oriented crack," *ASME Journal of Applied Mechanics*, Vol. 41, pp. 1007-1013.
- Eshelby, J. D., 1957, "The determination of the elastic field of an ellipsoidal inclusion and related problems," *Proc. R. Soc. Lond., A*, 241, pp. 376-396.
- Eshelby, J. D., 1959, "The elastic field outside an ellipsoidal inclusion," *Proc. R. Soc. Lond., A*, 252, pp. 561-569.
- Gao, J., 1995, "A Circular Inclusion With Imperfect Interface: Eshelby's Tensor and Related Problems," *ASME Journal of Applied Mechanics*, Vol. 62, pp. 860-866.
- Ghosh, S., Ling, Y., Majumdar, B., and Kim, R., 2000, 'Interfacial debonding analysis in multiple fiber reinforced composites,' *Mechanics of Materials*, Vol. 32, pp. 561-591.
- Gleixner, R. J., Clements, B. M. and Nix, W. D., 1997, "Void nucleation in passivated interconnect lines: Effect of site geometries, interfaces, and interface flaws," *J. of Mater. Res.*, 12(8), pp. 2081-2090.
- Goto, K., and Kagawa, Y., 1994, "Crack-fiber interaction and interfacial failure modes in fiber-reinforced ceramics," *Materials Science and Engineering*, A176, pp. 357-361.
- Gouldstone, A., Shen, Y-L, Suresh, S. and Thompson, C. V., 1998, "Evolution of stress in passivated and unpassivated metal interconnects," *J. of Mater. Res.*, 13(7), pp. 1956-1966.

- Guo, X.E., Liang, L.G., and Goldstein, S.A., 1998, "Micromechanics of osteonal cortical bone fracture," *ASME Journal of Biomechanical Engineering*, Vol. 120, pp. 112-117.
- Hashin, Z., 1990, "Thermoelastic properties of fiber composite with imperfect interface," *Mechanics of Materials*, Vol. 8, pp. 333-348.
- Hashin, Z., 1991, "The spherical Inclusion with imperfect interface," *ASME Journal of Applied Mechanics*, Vol. 58, pp. 444-449.
- Hogan, H.A., 1992, "Micromechanics modeling of haversian cortical bone properties," *Journal of Biomechanics*, Vol. 25, pp. 549-556.
- Honein, T., and Herrmann, C., 1990, "On bonded inclusion with circular or straight boundaries in plane elastostatics," *ASME Journal of Applied Mechanics*, Vol. 57, pp. 850-856.
- Jasiuk, I., Chen, J., and Thorpe, M. F., 1992, "Elastic moduli of composites with rigid sliding inclusions," *Journal of The Mechanics and Physics of Solids*, Vol. 40, No. 2, pp. 373-391.
- Jayaraman, K., Gao, Z., and Reifsnider, K. L., 1992, "The interphase in unidirectional fiber-reinforced epoxies: Effect on local stress fields," *Journal of Composite Technology and Research*, Vol. 16, No. 1, pp. 21-31.
- Katz, J. L., 1981, "Composite material models for cortical bone properties," *ASME AMD*, Vol. 45, 171-184.
- Lenci, S., and Menditto, G., 2000, "Weak interface in long fiber composites," *International Journal of Solids and Structures*, Vol. 37, pp. 4239-4260.

Liu, Y., Ru, C.Q., Schiavone, P., and Mioduchowski, A., "New Phenomena Concerning the Effect of Imperfect Bonding on Radial Matrix Cracking in Fiber Composites," *International Journal of Engineering Science*. (Accepted for publication, 32 manuscript pages).

Liu, Y. J., Xu, N., and Luo, J.F., 2000, "Modeling of interphases in fiber-reinforced composites under transverse loading using the boundary element method," *ASME Journal of Applied Mechanics*, Vol. 67, pp. 41-49.

Muskhelishvili, N.I., 1963, *Some Basic Problem of the Mathematical Theory of Elasticity*. P. Noordhoff Ltd., Groningen, Netherlands.

Pagano, N. J., and Tandon, G. P., 1990, "Modeling of imperfect bonding in fiber reinforced brittle matrix composites," *Mechanics of Materials*, Vol. 9, pp. 49-64.

Reifsnider, K. L., and Talug, A., 1980, "Analysis of fatigue damage in composite laminates," *Int. J. Fatigue*, 2 (1), 3.

Ru, C.Q., and Schiavone, P., 1996, "On the elliptic inclusion in antiplane shear," *Math. Mech. Solids*, 1, pp. 327-333.

Ru, C.Q., and Schiavone, P., 1997, "A circular inclusion with circumferentially inhomogeneous interface in antiplane shear," *Pro. R. Soc. Lond.*, Vol. 453, pp. 2551-2572.

Ru, C.Q., 1998a, "Effect of interface layers on thermal stresses within an Elliptical inclusion," *Journal of Applied Physics*, 84, pp. 4872-4879.

Ru, C.Q., 1998b, "A circular inclusion with circumferentially inhomogeneous sliding interface in plane elastostatics," *ASME Journal of Applied Mechanics*, Vol. 65, pp.

Ru, C.Q., Schiavone, P., and Mioduchowski, A., 1999, "Uniformity of stresses within a three-phase elliptic inclusion in anti-plane shear," *Journal of Elasticity*, Vol. 52, pp. 121-128.

Schmauder, S., Muller, W.H., and McMeeking, R.M., 1992, *Residual Stresses at Interfaces in Fiber Reinforced Composites. Residual Stresses-III* Science and Technology, H., Fujiwara, T. Abe and K. Tanaka Eds., pp. 589-594, Elsevier Applied Science, London.

Sih, G.C., 1973, *Methods of analysis and solution of crack problem*, pp. 57-160, Noordhoff International Publishing, Leyden, the Netherlands.

Tamate, O., 1968, "The effect of a circular inclusion on the stress around a line crack in a sheet under tension," *International Journal of Fracture Mechanics*, Vol. 4, pp. 257-265.

Tandon, G.P., and Pagano, N.J., 1996, "Effect thermoelastic moduli of a unidirectional fiber composite containing interfacial arc microcracks," *ASME Journal of Applied Mechanics*, Vol. 63, pp. 210-217.

Wu, C. C., Kahn, M. and Moy, W., 1996, "Piezoelectric Ceramics with functional gradients: a new application in material design," *J. of Am. Ceram. Soc.*, 79, pp. 809-812.

Xiao, Z.M., and Chen, B.J., 2000, "A screw dislocation interacting with a coated fiber," *Mechanics of Materials*, Vol. 32, pp. 485-494.

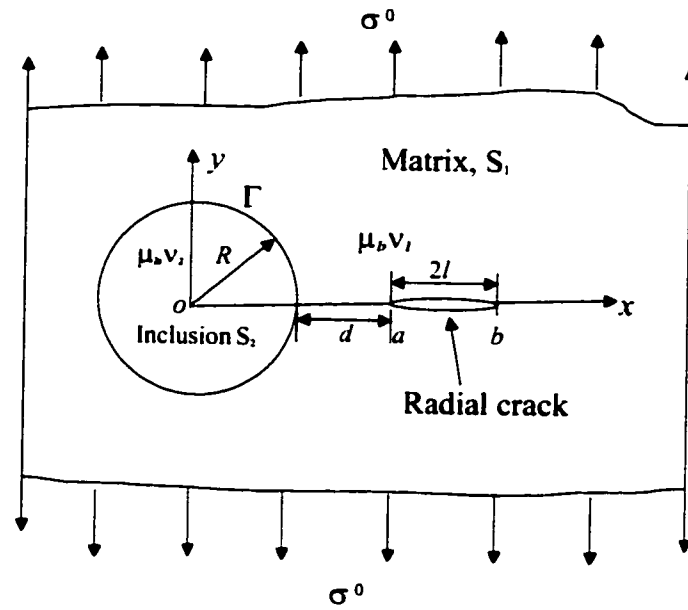


Figure 2.1. A circular inclusion with a radial matrix crack

Figure 3.1 The SIFs of crack tips via interface parameter N' (uniaxial load perpendicular to crack, $m=n$, $u_1/u_2=0.5$, $l/R=1$)

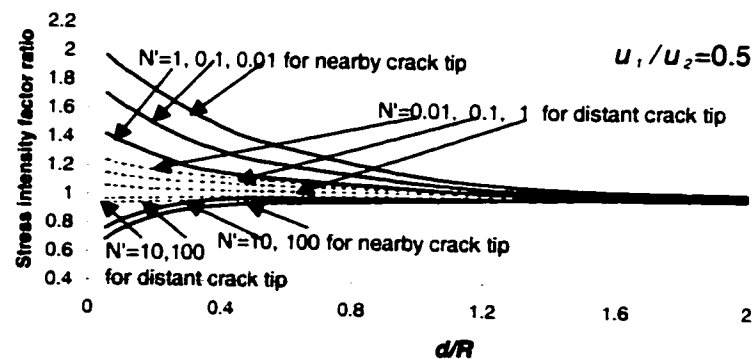


Figure 3.2 The SIFs of crack tips via interface parameter N' (uniaxial load perpendicular to crack, $m=n$, $u_1/u_2=2$, $l/R=1$)

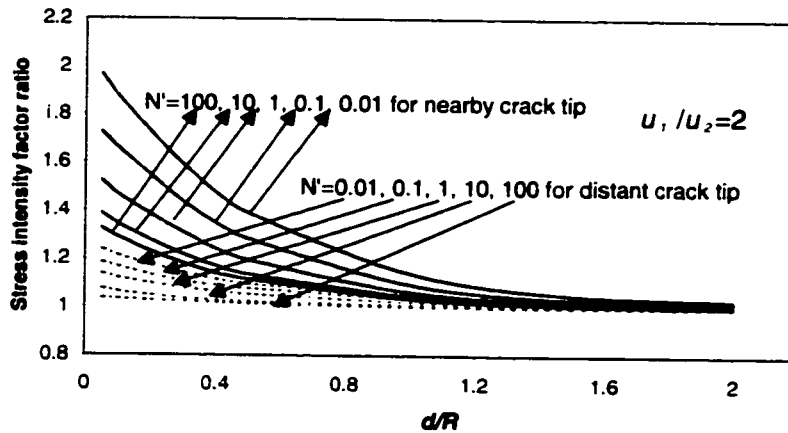


Figure 3.3 The shear modulus ratio of inclusion to matrix determined by the condition $K_1(a)=K_1(b)$ for different interface parameters ($m=n$, $l/R=1$)

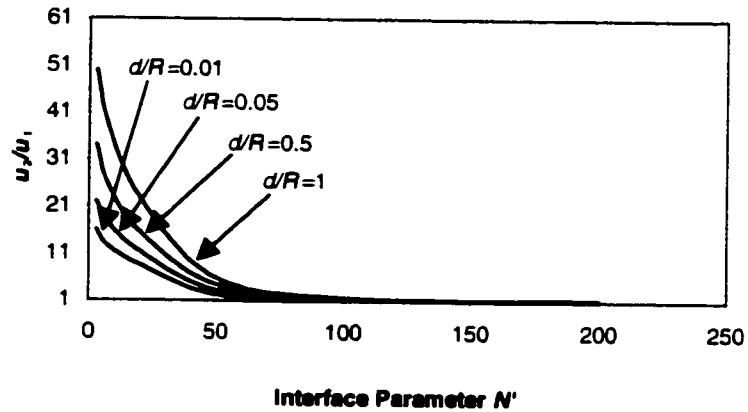


Figure 3.4 The shear modulus ratio of inclusion to matrix determined by the condition $K_I(a)=K_I(b)$ for different interface parameters ($m=n$, $l/R=0.1$)

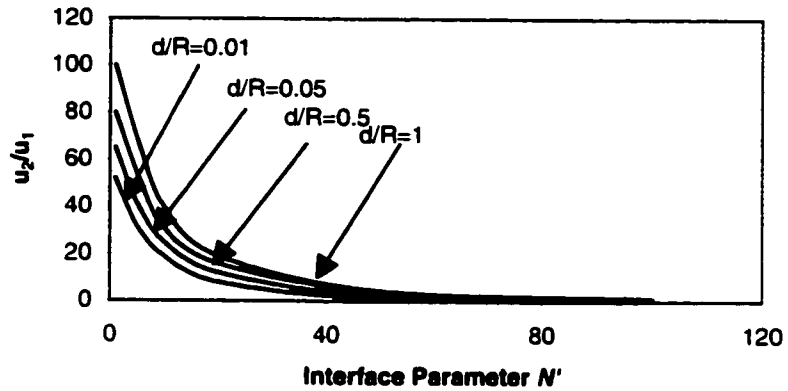


Figure 3.5 Near-by crack tip stress intensity factor versus interface parameter (uniaxial load perpendicular to crack, $m=3$, $u_1/u_2=2$, $l/R=1$)

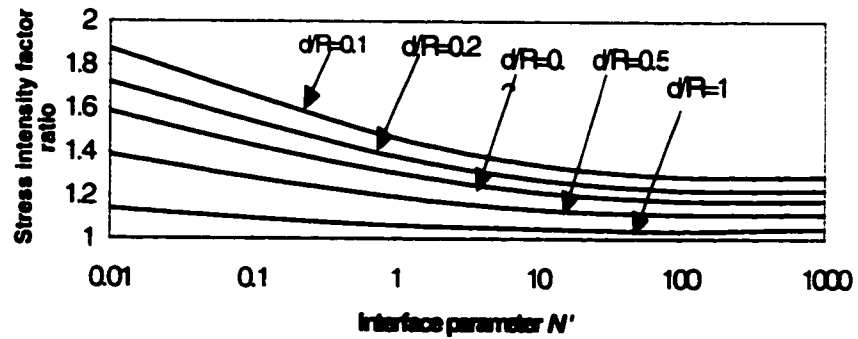


Figure 3.6 Near-by crack tip stress intensity factor versus interface parameter (uniaxial load perpendicular to crack, $m=3n$, $u_1/u_2=0.5$, $l/R=1$)

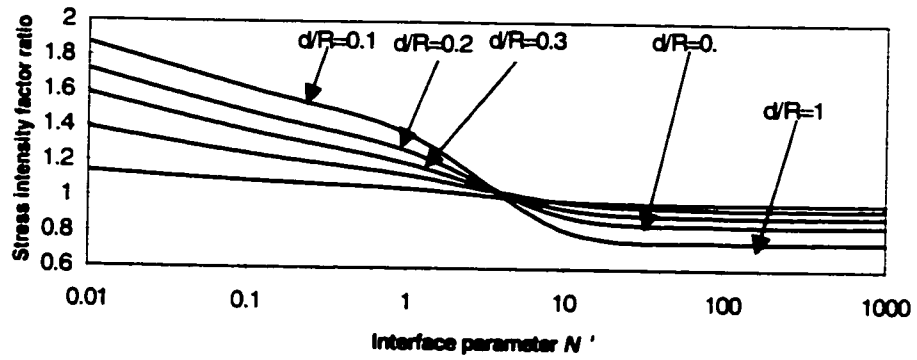


Figure 3.7 Distant crack tip stress intensity factor versus interface parameter (uniaxial load perpendicular to crack, $m=3n$, $u_1/u_2=2$, $l/R=1$)

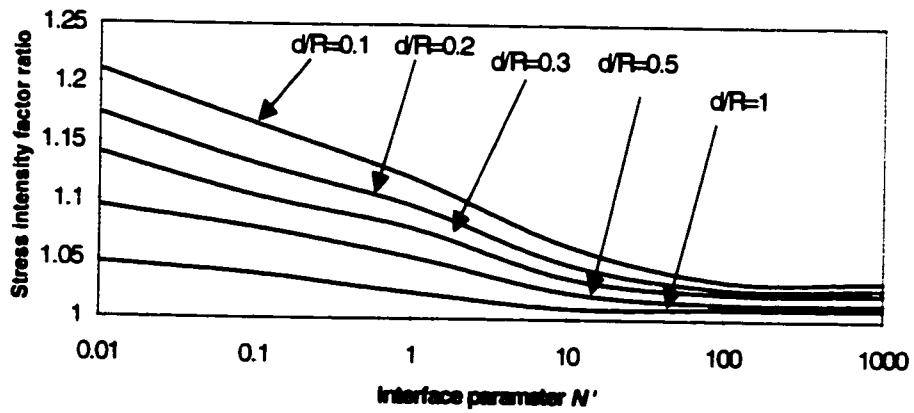


Figure 3.8 Distant crack tip stress intensity factor versus interface parameter (uniaxial load perpendicular to crack, $m=3n$, $u_1/u_2=0.5$, $l/R=1$)

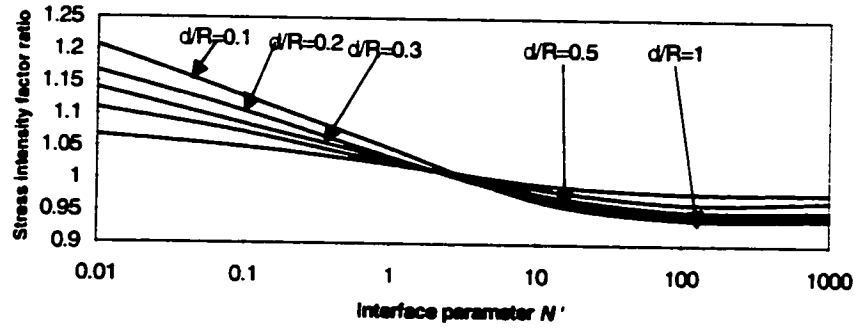


Figure 3.9 The mode-I SIFs via the distance d/R for different modulus ratio (sliding interface, uniaxial load perpendicular to the crack, $l/R=1$)

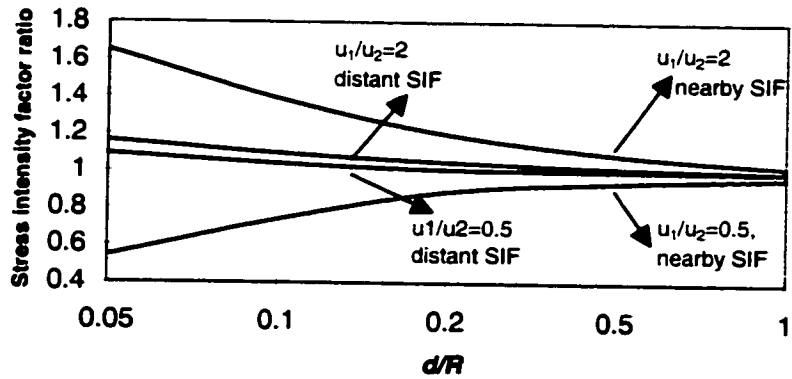


Figure 4.1 Nearby crack tip stress intensity factor versus interface parameter (uniaxial load parallel to crack, $m=3n$, $u_1/u_2=0.5$, $l/R=1$)

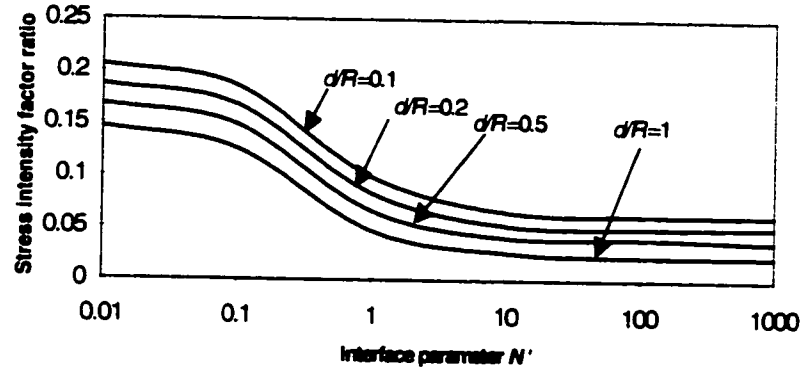


Figure 4.2 Near-by crack tip stress intensity factor versus interface parameter (uniaxial load parallel to crack, $m=3n$, $u_1/u_2=2$, $l/R=1$)

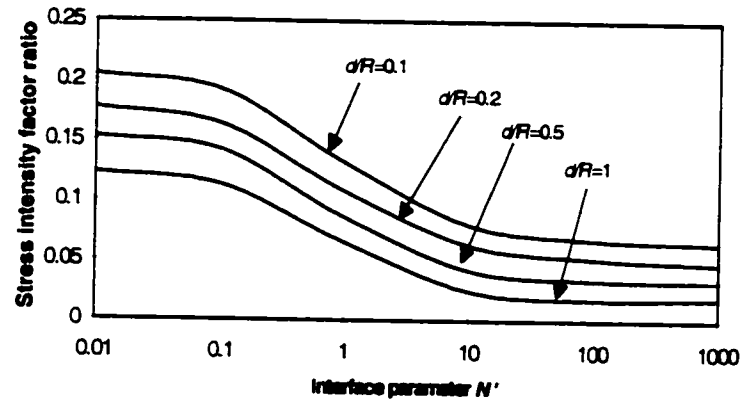


Figure 4.3 Near-by crack tip stress intensity factor versus interface parameter (uniaxial load parallel to crack, $m=3n$, $u_1/u_2=0.1$, $l/R=1$)

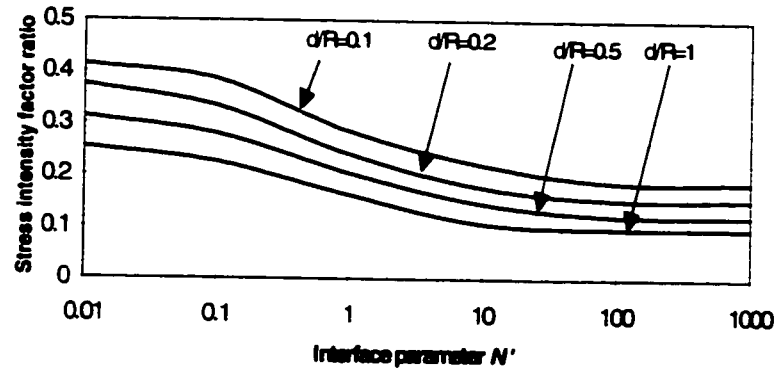


Figure 4.4 Nearby crack tip stress intensity factor versus interface parameter (uniaxial load parallel to crack, $m=3n$, $u_1/u_2=10$, $l/R=1$)

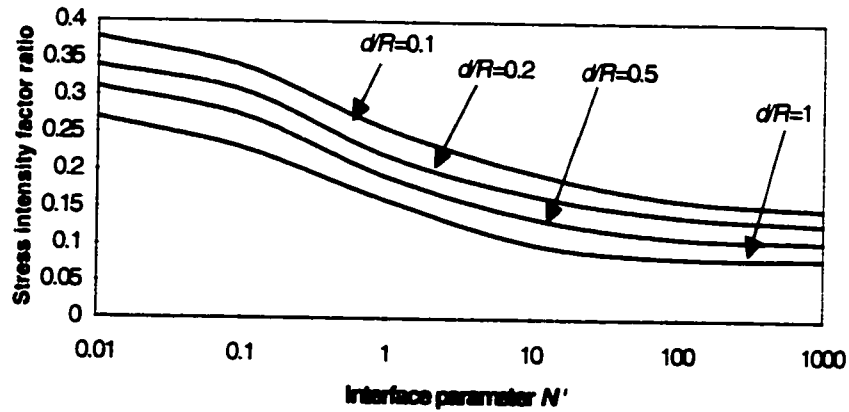


Figure 4.5 Distant crack tip stress intensity factor versus interface parameter (uniaxial load parallel to crack, $u_1/u_2=0.5$, $VR=1$)

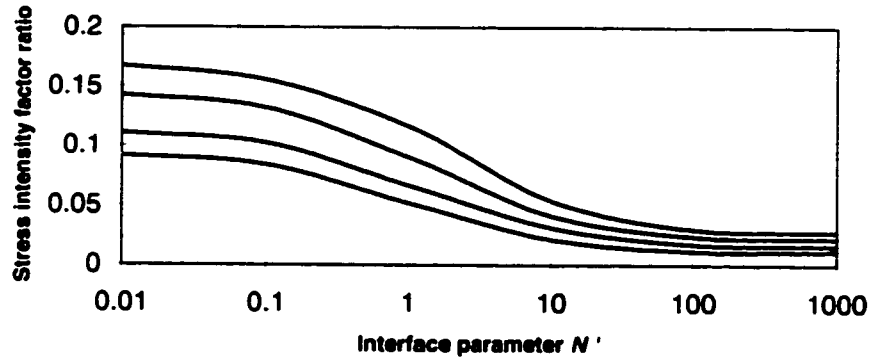
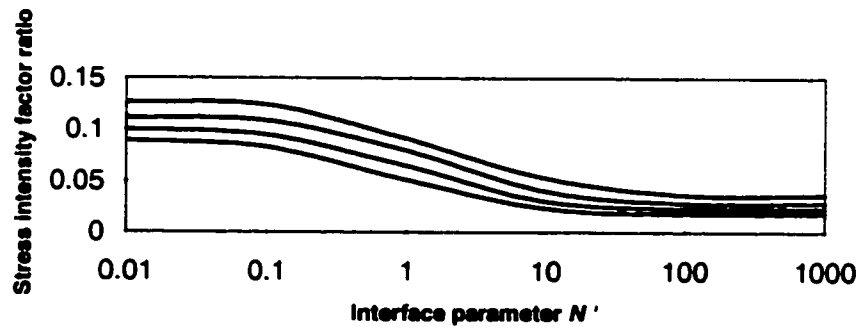


Figure 4.6 Distant crack tip stress intensity factor versus interface parameter (uniaxial load parallel to crack, $u_1/u_2=2$, $VR=1$)



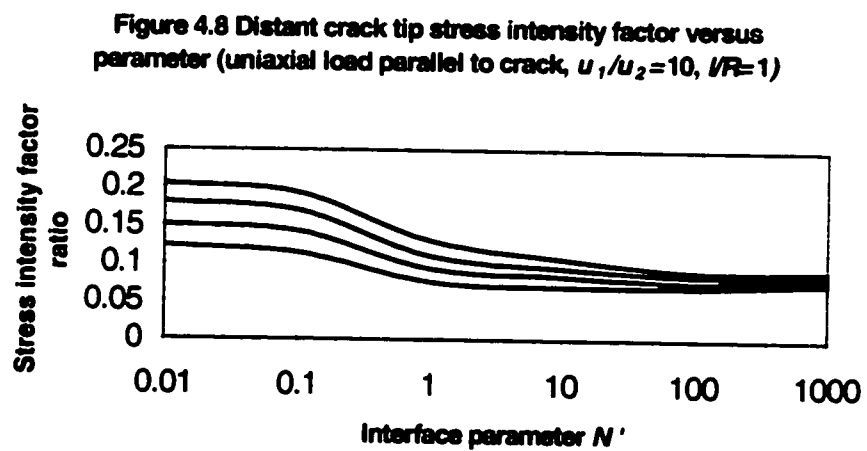
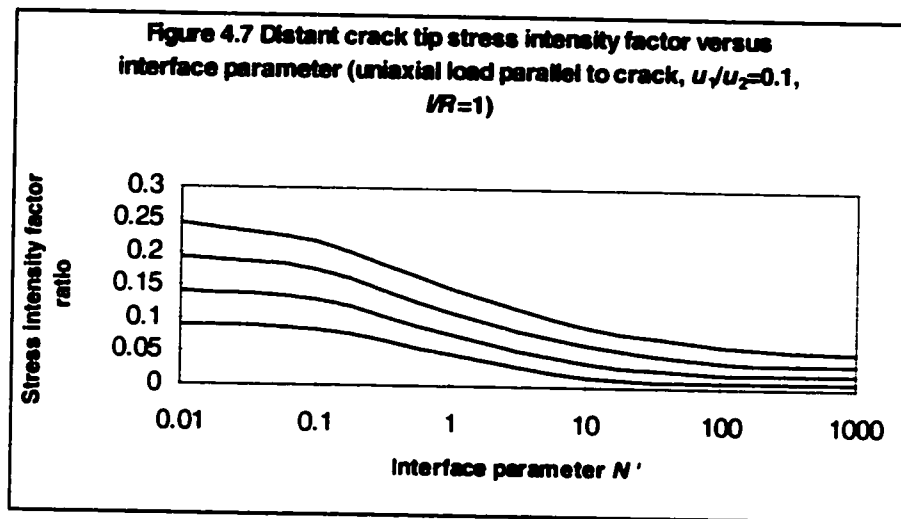


Figure 5.1 The mode-II nearby SIFs via the distance d/R for different modulus ratio (sliding interface, pure shear load, $\nu/R=1$)

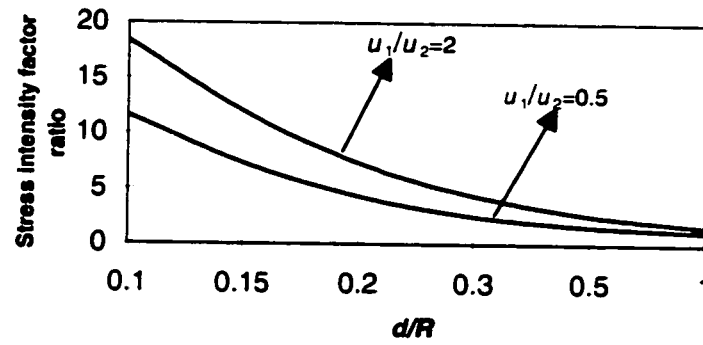


Figure 5.2 Mode-II nearby crack tip SIF versus interface parameter (pure shear loading, $m=3n$, $u_1/u_2=2$, $\nu/R=1$)

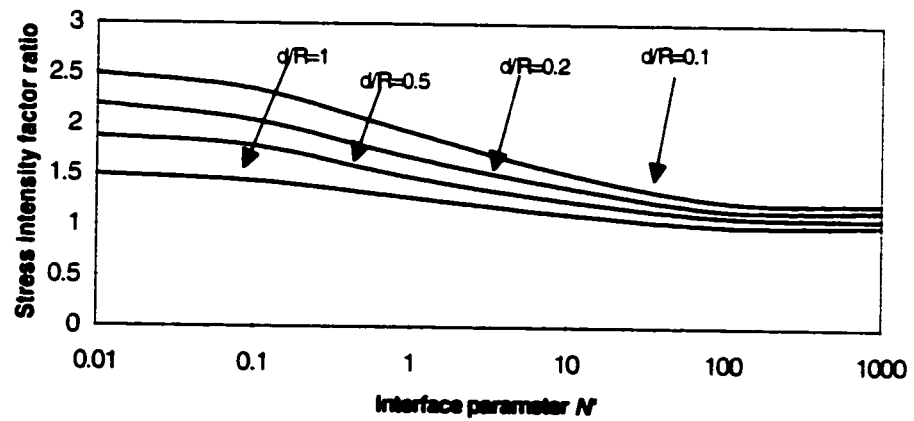


Figure 5.3 Mode-II nearby crack tip SIF versus interface parameter (pure shear loading, $m=3n$, $u_1/u_2=0.5$, $l/R=1$)

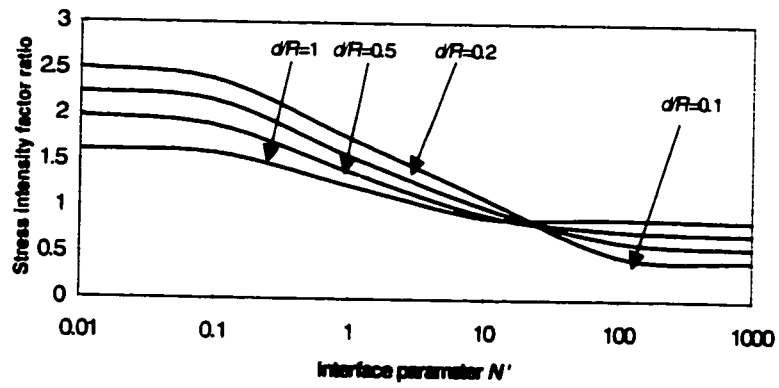


Figure 5.4 Mode-I nearby crack tip SIF versus interface parameter (pure shear loading, $m=3n$, $u_1/u_2=2$, $l/R=1$)

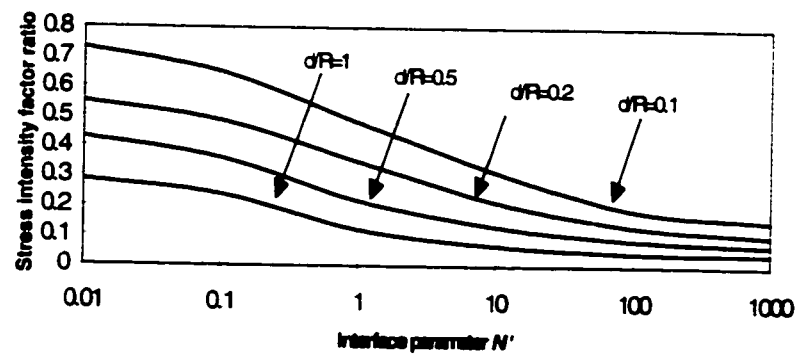
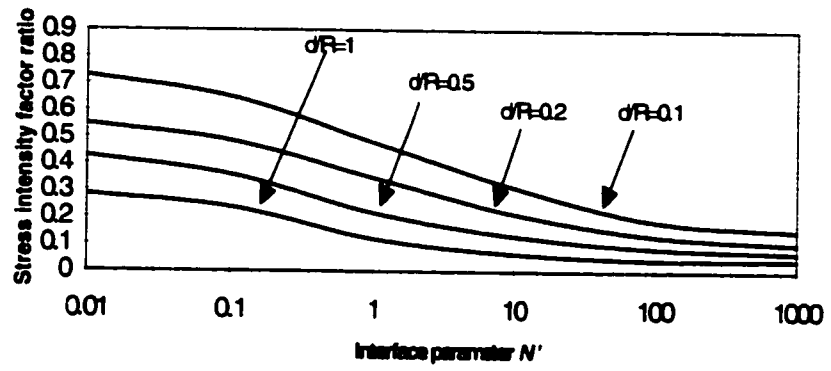


Figure 5.5 Mode-I nearby crack tip SIF versus interface parameter (pure shear loading, $m=3n$, $u_1/u_2=0.5$, $l/R=1$)



APPENDIX 1

For the interface condition (2.16), we obtain the following 9 equations:

Coefficients of z^j term, equation (A.1):

$$\begin{aligned}
 & -24[c_7 b_1 + c_8 b_2 + c_9(2A + \bar{B})] - \frac{1}{R^2}[4c_8 \bar{b}_4 + 4c_7 \bar{b}_3 + 4c_6 \bar{b}_2 + \\
 & 4c_5 \bar{b}_1 + 4c_3(2A + B) - 16c_3 b_4 - 16c_7 b_3 - 16c_6 b_2 - 16c_5 b_1 - \\
 & 16c_3(2A + \bar{B}) - 4e_4] - \frac{2}{R^{10}} \bar{a}_4 = 0,
 \end{aligned} \tag{A.1}$$

Coefficients of z^j term, equation (A.2):

$$\begin{aligned}
 & -15[c_8 b_3 + c_7 b_2 + c_6 b_1 + c_4(2A + \bar{B})] - \frac{3}{R^2}[c_7 \bar{b}_4 + c_6 \bar{b}_3 + c_5 \bar{b}_2 + \\
 & c_4 \bar{b}_1 + c_2(2A + B) - 3c_7 b_4 - 3c_6 b_3 - 3c_5 b_2 - 3c_4 \bar{b}_1 - 3c_2(2A + \bar{B})] - \\
 & \frac{3\bar{a}_3}{2R^3} - \frac{3c_1 \bar{b}_4}{R^3} + \frac{3e_3}{R^2} = 0,
 \end{aligned} \tag{A.2}$$

Coefficients of z^j term, equation (A.3):

$$\begin{aligned}
 & -8[c_8 b_4 + c_7 b_3 + c_6 b_2 + c_5 b_1 + c_3(2A + \bar{B})] - \frac{2}{R^2}[c_6 \bar{b}_4 + c_5 \bar{b}_3 + \\
 & c_4 \bar{b}_2 + c_3 \bar{b}_1 + c_1(2A + B) - 2c_6 b_4 - 2c_5 b_3 - 2c_4 b_2 - 2c_3 b_1 - \\
 & 2c_1(2A + \bar{B})] - \frac{1}{R^6}(2c_1 \bar{b}_3 + 2c_2 \bar{b}_4 + \bar{a}_2) + \frac{2e_2}{R^2} + 8d_4 = 0,
 \end{aligned} \tag{A.3}$$

Coefficients of z^2 term, equation (A.4):

$$\begin{aligned}
 & -3[c_7 b_4 + c_6 b_3 + c_5 b_2 + c_4 b_1 + c_3 (2A + \bar{B})] - \frac{1}{R^2} (c_5 \bar{b}_4 + c_4 \bar{b}_3 + \\
 & c_3 \bar{b}_2 + c_2 \bar{b}_1 + \frac{B}{2} - c_5 b_4 - c_4 b_3 - c_3 b_2 - c_2 b_1 + \frac{\bar{B}}{2}) - \frac{1}{R^4} (c_3 \bar{b}_4 + \\
 & c_2 \bar{b}_3 + c_1 \bar{b}_2 + \frac{\bar{a}_1}{2}) + \frac{e_1}{R^2} + 3d_3 = 0,
 \end{aligned} \tag{A.4}$$

Coefficients of z term, equation (A.5):

$$\begin{aligned}
 & 2[c_6 b_4 + c_5 b_3 + c_4 b_2 + c_3 b_1 + c_1 (2A + \bar{B})] - 2[c_6 \bar{b}_4 + c_5 \bar{b}_3 + \\
 & c_4 \bar{b}_2 + c_3 \bar{b}_1 + c_1 (2A + \bar{B})] = 0,
 \end{aligned} \tag{A.5}$$

(The left-hand side of equation is identical to zero).

Coefficients of z^0 term, equation (A.6):

$$\begin{aligned}
 & (c_5 b_4 + c_4 b_3 + c_3 b_2 + c_2 b_1 - \frac{\bar{B}}{2}) + \frac{1}{R^2} (c_1 \bar{b}_4 + c_2 \bar{b}_3 + c_1 \bar{b}_2 - \\
 & \frac{\bar{a}_1}{2} + c_1 b_4 + c_2 b_3 + c_1 b_2 + \frac{a_1}{2}) + (c_5 \bar{b}_4 + c_4 \bar{b}_3 + c_3 \bar{b}_2 + c_2 \bar{b}_1 - \\
 & \frac{B}{2}) - \bar{d}_1 - d_1 = 0,
 \end{aligned} \tag{A.6}$$

Coefficients of z^{-1} term, equation (A.7):

$$\begin{aligned}
 & \frac{1}{R^2} (2c_2 \bar{b}_4 + 2c_1 \bar{b}_3 - \bar{a}_2 + 4c_2 b_4 + 4c_1 b_3 + 2a_2) + 2R^2 [c_6 \bar{b}_4 + \\
 & c_5 \bar{b}_3 + c_4 \bar{b}_2 + c_3 \bar{b}_1 + c_1 (2A + B)] - 2R^2 \bar{d}_2 = 0,
 \end{aligned} \tag{A.7}$$

Coefficients of z^{-2} term, equation (A.8):

$$\begin{aligned}
& -3(c_3 b_4 + c_2 b_3 + c_1 b_2 + \frac{a_1}{2}) + \frac{3}{R^2}(c_1 \bar{b}_4 - \frac{\bar{a}_3}{2} + 3c_1 b_4 + \frac{3a_3}{2}) + \\
& 3R^4[c_7 \bar{b}_4 + c_6 \bar{b}_3 + c_5 \bar{b}_2 + c_4 \bar{b}_1 + c_2(2A + B)] - 3R^4 \bar{d}_3 = 0,
\end{aligned} \tag{A.8}$$

Coefficients of z^j term, equation (A.9):

$$\begin{aligned}
& -8c_1 b_3 - 8c_2 b_4 - 4a_2 + 4R^0[c_3 \bar{b}_4 + c_7 \bar{b}_3 + c_6 \bar{b}_2 + c_5 \bar{b}_1 + \\
& c_3(2A + B)] - 4R^0 \bar{d}_4 + \frac{1}{R^2}(8a_4 - 2\bar{a}_4) = 0.
\end{aligned} \tag{A.9}$$

If we represent $\frac{m-n}{2}$, $\frac{m+n}{2}$ by M and N respectively, then, for the interface condition (2.17), we obtain the following 9 equations:

Coefficients of z^j term, equation (A.10):

$$\begin{aligned}
& \frac{MR\kappa_1}{2\mu_1}[c_3 b_2 + c_7 b_1 + c_5(2A + \bar{B})] + \frac{M\bar{a}_4}{\mu_1 R^9} + \frac{N\kappa_1 \bar{a}_4}{4\mu_1 R^9} - \frac{3NR}{\mu_1}[c_3 b_2 + \\
& c_7 b_1 + c_5(2A + \bar{B})] - \frac{N}{2\mu_1 R}[c_3 \bar{b}_4 + c_7 \bar{b}_3 + c_6 \bar{b}_2 + c_5 \bar{b}_1 + c_3(2A + B) - \\
& 4c_3 b_4 - 4c_7 b_3 - 4c_6 b_2 - 4c_5 \bar{b}_1 - 4c_3(2A + \bar{B})] + \frac{Ne_4}{2\mu_1 R} + \frac{4e_4}{R^2} = 0,
\end{aligned} \tag{A.10}$$

Coefficients of z^j term, equation (A.11):

$$\begin{aligned}
& \frac{MR}{2\mu_1} \left\{ \kappa_1 [c_3 b_3 + c_7 b_2 + c_6 b_1 + c_4 (2A + \bar{B})] + \frac{3}{R^3} (c_1 \bar{b}_4 + \frac{1}{2} \bar{a}_3) \right\} + \\
& \left[\frac{N\kappa_1}{2\mu_1 R^7} (c_1 \bar{b}_4 + \frac{\bar{a}_3}{2}) - \frac{5NR}{2\mu_1} [c_3 b_3 + c_7 b_2 + c_6 b_1 + c_4 (2A + \bar{B})] - \right. \\
& \frac{N}{2\mu_1 R} [c_7 \bar{b}_4 + c_6 \bar{b}_3 + c_5 \bar{b}_2 + c_4 \bar{b}_1 + c_2 (2A + B) - 3c_7 b_4 - 3c_6 b_3 - \\
& \left. 3c_5 b_2 - 3c_4 b_1 - 3c_2 (2A + \bar{B})] + \frac{Ne_3}{2\mu_2 R} + \frac{3e_3}{R^2} = 0, \tag{A.11}
\end{aligned}$$

Coefficients of z^1 term, equation (A.12):

$$\begin{aligned}
& \frac{MR}{2\mu_1} \left\{ \kappa_1 [c_3 b_4 + c_7 b_3 + c_6 b_2 + c_5 b_1 + c_3 (2A + \bar{B})] + \frac{2}{R^3} (c_1 \bar{b}_3 + c_2 \bar{b}_4 + \right. \\
& \left. \frac{\bar{a}_2}{2}) - \frac{(2\bar{a}_4 - \frac{a_4}{2})}{R^3} \right\} - \frac{MR}{2\mu_2} \kappa_2 d_4 + \frac{N\kappa_1}{2\mu_1 R^3} (c_1 \bar{b}_3 + c_2 \bar{b}_4 + \frac{\bar{a}_2}{2}) - \\
& \frac{2NR}{\mu_1} [c_3 b_4 + c_7 b_3 + c_6 b_2 + c_5 b_1 + c_3 (2A + \bar{B})] - \frac{N}{2\mu_1 R} [c_6 \bar{b}_4 + \\
& c_5 \bar{b}_3 + c_4 \bar{b}_2 + c_3 \bar{b}_1 + c_1 (2A + B) - 2c_6 b_4 - 2c_5 b_3 - 2c_4 b_2 - 2c_3 b_1 - \\
& \left. 2c_1 (2A + \bar{B})] + \frac{2NR d_4}{\mu_2} + \frac{Ne_2}{2\mu_2 R} + 8d_4 + \frac{2e_2}{R^2} = 0, \tag{A.12}
\end{aligned}$$

Coefficients of z^1 term, equation (A.13):

$$\begin{aligned}
& \frac{MR\kappa_1}{2\mu_1} [c_7 b_4 + c_6 b_3 + c_5 b_2 + c_4 b_1 + c_2 (2A + B)] + \frac{M}{2\mu_1 R^3} (c_3 \bar{b}_4 + \\
& c_2 \bar{b}_3 + c_1 \bar{b}_2 + \frac{\bar{a}_1}{2}) - \frac{M}{2\mu_1 R^5} (c_1 b_4 - \frac{a_3}{2} + 3c_1 \bar{b}_4 + \frac{3\bar{a}_3}{2}) - \frac{MR \kappa_2}{2\mu_2} d_3 + \\
& \frac{N\kappa_1}{2\mu_1 R^3} (c_1 \bar{b}_2 + c_2 \bar{b}_3 + \frac{\bar{a}_1}{2} + c_3 \bar{b}_4) - \frac{3NR}{2\mu_1} [c_7 b_4 + c_6 b_3 + c_5 b_2 + c_4 b_1 + \\
& c_2 (2A + \bar{B})] - \frac{N}{2\mu_1 R} (c_5 \bar{b}_4 + c_4 \bar{b}_3 + c_3 \bar{b}_2 + c_2 \bar{b}_1 + \frac{B}{2} - c_5 b_4 - c_4 b_3 - c_3 b_2 - \\
& c_2 b_1 + \frac{\bar{B}}{2}) + \frac{3NR}{2\mu_2} d_3 + \frac{Ne_1}{2\mu_2 R} - \frac{N}{R} (\epsilon_2 - i\epsilon_3) + 3d_3 + \frac{e_1}{R^2} = 0,
\end{aligned} \tag{A.13}$$

Coefficients of z term, equation (A.14):

$$\begin{aligned}
& \frac{MR\kappa_1}{2\mu_1} [c_6 b_4 + c_5 b_3 + c_4 b_2 + c_3 b_1 + c_1 (2A + \bar{B})] - \frac{M}{2\mu_1 R^3} (c_2 b_4 + \\
& c_1 b_3 - \frac{a_2}{2} + 2c_1 \bar{b}_3 + 2c_2 \bar{b}_4 + \bar{a}_2) - \frac{MR \kappa_2}{2\mu_2} d_2 + \frac{N\kappa_1}{2\mu_1 R} (c_4 \bar{b}_4 + \\
& c_3 \bar{b}_3 + c_2 \bar{b}_2 + c_1 \bar{b}_1) - \frac{NR}{\mu_1} [c_6 b_4 + c_5 b_3 + c_4 b_2 + c_3 b_1 + c_1 (2A + \bar{B})] - \\
& \frac{N}{2\mu_1 R} (c_4 \bar{b}_4 + c_3 \bar{b}_3 + c_2 \bar{b}_2 + c_1 \bar{b}_1) - \frac{N\kappa_2}{2\mu_2 R} \bar{d}_0 + \frac{NR}{\mu_2} d_2 + \frac{Ne_0}{2\mu_2 R} = 0,
\end{aligned} \tag{A.14}$$

Coefficients of z'' term, equation (A.15):

$$\begin{aligned}
& \frac{MR\kappa_1}{2\mu_1}(c_5 \bar{b}_4 + c_4 \bar{b}_3 + c_3 \bar{b}_2 + c_2 \bar{b}_1 - \frac{\bar{B}}{2}) - \frac{MR}{2\mu_1}(c_5 \bar{b}_4 + c_4 \bar{b}_3 + \\
& c_3 \bar{b}_2 + c_2 \bar{b}_1 - \frac{B}{2}) - \frac{M}{2\mu_1 R}(c_1 \bar{b}_2 + c_2 \bar{b}_3 + c_3 \bar{b}_4 - \frac{a_1}{2} + c_1 \bar{b}_2 + \\
& c_2 \bar{b}_3 + c_3 \bar{b}_4 + \frac{\bar{a}_1}{2}) - \frac{MR\kappa_2}{2\mu_2} \bar{d}_1 + \frac{MR}{2\mu_2} \bar{d}_1 + \frac{NR\kappa_1}{2\mu_1}(c_5 \bar{b}_4 + c_4 \bar{b}_3 + \\
& c_3 \bar{b}_2 + c_2 \bar{b}_1 - \frac{B}{2}) - \frac{NR}{2\mu_1}(c_5 \bar{b}_4 + c_4 \bar{b}_3 + c_3 \bar{b}_2 + c_2 \bar{b}_1 - \frac{\bar{B}}{2}) - \frac{N}{2\mu_1 R} \\
& (c_1 \bar{b}_2 + c_2 \bar{b}_3 + c_3 \bar{b}_4 - \frac{\bar{a}_1}{2} + c_1 \bar{b}_2 + c_2 \bar{b}_3 + c_3 \bar{b}_4 + \frac{a_1}{2}) - \frac{NR\kappa_2}{2\mu_2} \bar{d}_1 + \\
& \frac{NRd_1}{2\mu_2} - mR\epsilon_1 - (d_1 + \bar{d}_1) = 0,
\end{aligned} \tag{A.15}$$

Coefficients of z' term, equation (A.16):

$$\begin{aligned}
& \frac{MR\kappa_1}{2\mu_1}(c_4 \bar{b}_4 + c_3 \bar{b}_3 + c_2 \bar{b}_2 + c_1 \bar{b}_1) - \frac{MR^3}{\mu_1}[c_6 \bar{b}_4 + c_5 \bar{b}_3 + c_4 \bar{b}_2 + \\
& c_3 \bar{b}_1 + c_1(2A + B)] - \frac{MR}{2\mu_1}(c_4 \bar{b}_4 + c_3 \bar{b}_3 + c_2 \bar{b}_2 + c_1 \bar{b}_1) - \frac{MR\kappa_2}{2\mu_2} \bar{d}_0 + \\
& \frac{MR^3}{\mu_2} \bar{d}_2 + \frac{MR}{2\mu_2} \bar{e}_0 + \frac{NR^3\kappa_1}{2\mu_1}[c_6 \bar{b}_4 + c_5 \bar{b}_3 + c_4 \bar{b}_2 + c_3 \bar{b}_1 + c_1(2A + B)] - \\
& \frac{N}{2\mu_1 R}(c_1 \bar{b}_3 + c_2 \bar{b}_4 - \frac{\bar{a}_2}{2} + 2c_1 \bar{b}_3 + 2c_2 \bar{b}_4 + a_2) - \frac{NR^3\kappa_2}{2\mu_2} \bar{d}_2 - 2\bar{d}_2 R^2 = 0,
\end{aligned} \tag{A.16}$$

Coefficients of z'' term, equation (A.17):

$$\begin{aligned}
& \frac{MR\kappa_1}{2\mu_1}(c_3 b_4 + c_2 b_3 + c_1 b_2 + \frac{a_1}{2}) - \frac{3MR^5}{2\mu_1}[c_7 \bar{b}_4 + c_6 \bar{b}_3 + \\
& c_5 \bar{b}_2 + c_4 \bar{b}_1 + c_2(2A + B)] - \frac{MR^3}{2\mu_1}(c_5 b_4 + c_4 b_3 + c_3 b_2 + \\
& c_2 b_1 + \frac{\bar{B}}{2} - c_5 \bar{b}_4 - c_4 \bar{b}_3 - c_3 \bar{b}_2 - c_2 \bar{b}_1 + \frac{B}{2}) + \frac{3MR^5}{2\mu_2} \bar{d}_3 + \\
& \frac{MR^3}{2\mu_2} \bar{e}_1 + \frac{NR^5 \kappa_1}{2\mu_1}[c_7 \bar{b}_4 + c_6 \bar{b}_3 + c_5 \bar{b}_2 + c_4 \bar{b}_1 + c_2(2A + B)] + \\
& \frac{NR}{2\mu_1}(c_1 b_2 + c_2 b_3 + c_3 b_4 + \frac{a_1}{2}) - \frac{N}{2\mu_1 R}(c_1 \bar{b}_4 - \frac{\bar{a}_3}{2} + 3c_1 b_4 + \\
& \frac{3a_3}{2}) - \frac{N\kappa_2 R^5 \bar{d}_3}{2\mu_2} - MR^2(\epsilon_2 + i\epsilon_3) - 3R^4 \bar{d}_3 = 0,
\end{aligned} \tag{A.17}$$

Coefficients of z^{-j} term, equation (A.18):

$$\begin{aligned}
& \frac{MR\kappa_1}{2\mu_1}(c_1 b_3 + c_2 b_4 + \frac{a_2}{2}) - \frac{2MR^7}{\mu_1}[c_8 \bar{b}_4 + c_7 \bar{b}_3 + c_6 \bar{b}_2 + c_5 \bar{b}_1 + \\
& c_3(2A + B)] - \frac{MR^5}{2\mu_1}[c_6 b_4 + c_5 b_3 + c_4 b_2 + c_3 b_1 + c_1(2A + \bar{B}) - 2c_6 \bar{b}_4 - \\
& 2c_5 \bar{b}_3 - 2c_4 \bar{b}_2 - 2c_3 \bar{b}_1 - 2c_1(2A + B)] + \frac{2MR^7}{\mu_2} \bar{d}_4 + \frac{MR^5}{2\mu_2} \bar{e}_2 + \\
& \frac{NR^7 \kappa_1}{2\mu_1}[c_8 \bar{b}_4 + c_7 \bar{b}_3 + c_6 \bar{b}_2 + c_5 \bar{b}_1 + c_3(2A + B)] + \frac{NR}{\mu_1}(c_1 b_3 + \\
& c_2 b_4 + \frac{a_2}{2}) - \frac{NR^7 \kappa_2}{2\mu_2} \bar{d}_4 - \frac{N(2a_4 - \frac{\bar{a}_4}{2})}{2\mu_1 R} - 4R^6 \bar{d}_4 = 0.
\end{aligned} \tag{A.18}$$

As one of the e_0 and d_0 can be chosen arbitrarily without changing the displacement field (Muskhelishvili, 1963), we arbitrarily choose $e_0=0$. For the case of $m=n$, as

$$M = \frac{m-n}{2}, \quad N = \frac{m+n}{2}, \quad \text{hence, we have } M=0, \quad N=m=n. \quad \text{First, we substitute}$$

interface parameter N by the dimensionless N' , where $N = \frac{\mu_2}{R} N'$, and second, make

the following replacements:

$$a'_1 \sim \frac{R^2 a_1}{2}, \quad a'_2 \sim \frac{R a_2}{2}, \quad a'_3 \sim a_3, \quad a'_4 \sim \frac{a_4}{R};$$

$$b'_1 \sim R^2 b_1, \quad b'_2 \sim R b_2, \quad b'_3 \sim b_3, \quad b'_4 \sim \frac{b_4}{R};$$

$$d'_0 \sim R^3 d_0, \quad d'_1 \sim R^4 d_1, \quad d'_2 \sim R^5 d_2, \quad d'_3 \sim R^6 d_3, \quad d'_4 \sim R^7 d_4;$$

$$e'_1 \sim R^4 e_1, \quad e'_2 \sim R^5 e_2, \quad e'_3 \sim R^6 e_3, \quad e'_4 \sim R^7 e_4.$$

Simplifying the above 17 equations, we get the final equations as follow:

$$\begin{aligned} & \frac{a'_3}{2} + (5c_6 R^0 - 2c_4 R^4) b'_1 + (5c_7 R^7 - 2R^5 c_5) b'_2 + (5c_8 R^8 - 2c_0 R^0) b'_3 + \\ & (c_1 R - 2c_7 R^7) b'_4 - e'_3 + (20R^4 c_4 - 8R^2 c_2) R^4 A = 0, \end{aligned} \quad (\text{A.19})$$

$$\begin{aligned} & a'_2 + (4c_5 R^5 - c_3 R^3) b'_1 + (4c_6 R^0 - c_4 R^4) b'_2 + (4c_7 R^7 - c_5 R^5 + c_1 R) b'_3 + \\ & (4c_8 R^8 - c_0 R^0 + c_2 R^2) b'_4 - 4d'_4 - e'_2 + (16c_3 R^3 A - 4c_1 R) R^4 A = 0, \end{aligned} \quad (\text{A.20})$$

$$a'_1 + 3c_4 R^4 b'_1 + c_1 R b'_2 + (3c_6 R^6 + c_2 R^2) b'_3 + (3c_7 R^7 + c_3 R^3) b'_4 - 3d'_3 - e'_1 + (12c_2 R^2 A + 2) R^4 A = 0, \quad (\text{A.21})$$

$$c_2 R^2 b'_1 + (c_3 R^3 + c_1 R) b'_2 + (c_4 R^4 + c_2 R^2) b'_3 + (c_5 R^5 + c_3 R^3) b'_4 - d'_1 - R^4 A = 0, \quad (\text{A.22})$$

$$a'_2 + R^3 c_3 b'_1 + R^4 c_4 b'_2 + (R^5 c_5 + 3R c_1) b'_3 + (R^6 c_6 + 3R^2 c_2) b'_4 - d'_2 + 4R c_1 R^4 A = 0, \quad (\text{A.23})$$

$$a'_1 - a'_3 - R^4 c_4 b'_1 + (R c_1 - R^5 c_5) b'_2 + (R^2 c_2 - R^6 c_6) b'_3 + (R^3 c_3 - R^7 c_7 - 4R c_1) b'_4 + d'_3 - 4R^2 c_2 R^4 A = 0, \quad (\text{A.24})$$

$$2a'_2 - \frac{3a'_4}{2} - R^5 c_5 b'_1 - R^6 c_6 b'_2 + (2R c_1 - R^7 c_7) b'_3 + (2R^2 c_2 - R^3 c_3) b'_4 + d'_4 - 4R^3 c_3 R^4 A = 0, \quad (\text{A.25})$$

$$a'_4 + (12R^7 c_7 - 6R^5 c_5) b'_1 + (12R^8 c_8 - 6R^6 c_6) b'_2 - 6R^7 c_7 b'_3 - 6R^8 c_8 b'_4 - 2e'_4 + (48c_5 R^5 - 24c_3 R^3) R^4 A = 0, \quad (\text{A.26})$$

$$\begin{aligned} & \frac{\kappa_1}{4} a'_3 + \left(-\frac{5}{2} R^6 c_6 + R^4 c_4\right) b'_1 + \left(-\frac{5}{2} R^7 c_7 + R^5 c_5\right) b'_2 + \left(-\frac{5}{2} R^8 c_8 + R^6 c_6\right) b'_3 + \\ & \left(\frac{\kappa_1}{2} R c_1 + R^7 c_7\right) b'_4 + \left(\frac{\mu_1}{\mu_2} \frac{1}{2} + \frac{3}{N'}\right) e'_3 - 10R^4 c_4 R^4 A = 0, \end{aligned} \quad (\text{A.27})$$

$$\begin{aligned}
& \frac{\kappa_1}{2}a'_2 + \left(\frac{1}{2}R^3c_3 - 2R^5c_5\right)b'_1 + \left(\frac{1}{2}R^4c_4 - 2R^6c_6\right)b'_2 + \left(\frac{R\kappa_1}{2}c_1 - 2R^7c_7\right. \\
& \left. + \frac{1}{2}R^5c_5\right)b'_3 + \left(\frac{R^2\kappa_1}{2}c_2 - 2R^8c_8 + \frac{1}{2}R^6c_6\right)b'_4 + \left(2\frac{\mu_1}{\mu_2} + \frac{8}{N'}\right)d'_4 + \left(\frac{\mu_1}{\mu_2}\frac{1}{2} + \right. \\
& \left. \frac{2}{N'}\right)e'_2 + (2Rc_1A - 8R^3c_3)R^4A = 0,
\end{aligned} \tag{A.28}$$

$$\begin{aligned}
& \frac{\kappa_1}{2}a'_1 - \frac{3}{2}R^4c_4b'_1 + \left(\frac{R\kappa_1}{2}c_1 - \frac{3}{2}R^5c_5\right)b'_2 + \left(\frac{R^2\kappa_1}{2}c_2 - \frac{3}{2}R^6c_6\right)b'_3 + \\
& \left(\frac{R^3\kappa_1}{2}c_3 - \frac{3}{2}R^7c_7\right)b'_4 + \left(\frac{3}{2}\frac{\mu_1}{\mu_2} + \frac{3}{N'}\right)d'_3 + \left(\frac{\mu_1}{\mu_2}\frac{1}{2} + \frac{1}{N'}\right)e'_1 - \\
& (1 + 6R^2c_2)R^4A = 0,
\end{aligned} \tag{A.29}$$

$$\begin{aligned}
& \left(\frac{R\kappa_1}{2}c_1 - R^3c_3 - \frac{1}{2}Rc_1\right)b'_1 + \left(\frac{R^2\kappa_1}{2}c_2 - R^4c_4 - \frac{1}{2}R^2c_2\right)b'_2 + \left(\frac{R^3\kappa_1}{2}c_3 - \right. \\
& \left. R^5c_5 - \frac{1}{2}R^3c_3\right)b'_3 + \left(\frac{R^4\kappa_1}{2}c_4 - R^6c_6 - \frac{1}{2}R^4c_4\right)b'_4 - \frac{\mu_1}{\mu_2}\frac{\kappa_2}{2}d'_0 + \frac{\mu_1}{\mu_2}d'_2 - \\
& - 2Rc_1R^4A = 0,
\end{aligned} \tag{A.30}$$

$$\begin{aligned}
& \left(\frac{R^2\kappa_1}{2}c_2 - \frac{1}{2}R^2c_2\right)b'_1 + \left(\frac{R^3\kappa_1}{2}c_3 - \frac{R^3c_3}{2} - Rc_1\right)b'_2 + \left(\frac{R^4\kappa_1}{2}c_4 - \frac{R^4c_4}{2} - \right. \\
& \left. R^2c_2\right)b'_3 + \left(\frac{R^5\kappa_1}{2}c_5 - \frac{R^5c_5}{2} - R^3c_3\right)b'_4 + \left(\frac{\mu_1}{2\mu_2} - \frac{\mu_1}{\mu_2}\frac{\kappa_2}{2} - \frac{2}{N'}\right)d'_2 - \\
& \left(\frac{\kappa_1}{2} + \frac{1}{2}\right)R^4A = 0,
\end{aligned} \tag{A.31}$$

$$\begin{aligned}
& -\frac{1}{2}a'_2 + \frac{R^3\kappa_1}{2}c_3b'_1 + \frac{R^4\kappa_1}{2}c_4b'_2 + \left(\frac{R^5\kappa_1}{2}c_5 - \frac{3}{2}Rc_1\right)b'_3 + \\
& \left(\frac{R^6\kappa_1}{2}c_6 - \frac{3}{2}R^2c_2\right)b'_4 - \left(\frac{\mu_1}{\mu_2}\frac{\kappa_2}{2} - \frac{2}{N'}\right)d'_2 + 2\kappa_1Rc_1R^4A = 0,
\end{aligned} \tag{A.32}$$

$$\begin{aligned}
& \frac{1}{2}a'_1 - \frac{1}{2}a'_3 + \frac{R^4\kappa_1}{2}c_4b'_1 + \left(\frac{R^5\kappa_1}{2}c_5 + \frac{1}{2}Rc_1\right)b'_2 + \left(\frac{R^6\kappa_1}{2}c_6 + \right. \\
& \left. \frac{1}{2}R^2c_2\right)b'_3 + \left(\frac{R^7\kappa_1}{2}c_7 + \frac{1}{2}R^3c_3 - 2Rc_1\right)b'_4 - \left(\frac{\mu_1}{\mu_2}\frac{\kappa_2}{2} - \frac{3}{N'}\right)d'_3 + \\
& 2\kappa_1R^2c_2R^4A = 0,
\end{aligned} \tag{A.33}$$

$$\begin{aligned}
& a'_2 - \frac{3}{4}a'_4 + \frac{R^5\kappa_1}{2}c_5b'_1 + \frac{R^6\kappa_1}{2}c_6b'_2 + \left(\frac{R^7\kappa_1}{2}c_7 + Rc_1\right)b'_3 + \\
& \left(\frac{R^8\kappa_1}{2}c_8 + R^2c_2\right)b'_4 - \left(\frac{\mu_1}{\mu_2}\frac{\kappa_2}{2} + \frac{4}{N'}\right)d'_4 + 2\kappa_1R^3c_3R^4A = 0,
\end{aligned} \tag{A.34}$$

$$\begin{aligned}
& \frac{\kappa_1}{4}a'_4 + \left(\frac{3}{2}R^5c_5 - 3R^7c_7\right)b'_1 + \left(\frac{3}{2}R^6c_6 - 3R^8c_8\right)b'_2 + \frac{3}{2}R^7c_7b'_3 + \\
& \frac{3}{2}R^8c_8b'_4 + \left(\frac{\mu_1}{\mu_2}\frac{1}{2} + \frac{4}{N'}\right)e'_4 + (6R^3c_3 - 12R^5c_5)R^4A = 0.
\end{aligned} \tag{A.35}$$

For the case of $m=3n$, similarly, we can obtain the final 17 equations in Section 3.2.3. as:

$$\begin{aligned}
& \frac{a'_3}{2} + (5c_6R^6 - 2c_4R^4)b'_1 + (5c_7R^7 - 2R^5c_5)b'_2 + (5c_8R^8 - \\
& 2c_6R^6)b'_3 + (c_1R - 2c_7R^7)b'_4 - e'_3 + (20R^4c_4 - 8R^2c_2)R^4A = 0,
\end{aligned} \tag{A.36}$$

$$\begin{aligned}
& a'_2 + (4c_5R^5 - c_3R^3)b'_1 + (4c_6R^6 - c_4R^4)b'_2 + (4c_7R^7 - \\
& c_5R^5 + c_1R)b'_3 + (4c_8R^8 - c_6R^6 + c_2R^2)b'_4 - 4d'_4 - e'_2 + \\
& (16c_3R^3A - 4c_1R)R^4A = 0,
\end{aligned} \tag{A.37}$$

$$\begin{aligned}
& a'_1 + 3c_4R^4b'_1 + c_1Rb'_2 + (3c_6R^6 + c_2R^2)b'_3 + (3c_7R^7 + c_3R^3)b'_4 - \\
& 3d'_3 - e'_1 + (12c_2R^2A + 2)R^4A = 0,
\end{aligned} \tag{A.38}$$

$$c_2 R^2 b'_1 + (c_3 R^3 + c_1 R) b'_2 + (c_4 R^4 + c_2 R^2) b'_3 + (c_5 R^5 + c_3 R^3) b'_4 - d'_1 - R^4 A = 0, \quad (\text{A.39})$$

$$a'_2 + R^3 c_3 b'_1 + R^4 c_4 b'_2 + (R^5 c_5 + 3R c_1) b'_3 + (R^6 c_6 + 3R^2 c_2) b'_4 - d'_2 + 4R c_1 R^4 A = 0, \quad (\text{A.40})$$

$$a'_1 - a'_3 - R^4 c_4 b'_1 + (R c_1 - R^5 c_5) b'_2 + (R^2 c_2 - R^6 c_6) b'_3 + (R^3 c_3 - R^7 c_7 - 4R c_1) b'_4 + d'_3 - 4R^2 c_2 R^4 A = 0, \quad (\text{A.41})$$

$$2a'_2 - \frac{3a'_4}{2} - R^5 c_5 b'_1 - R^6 c_6 b'_2 + (2R c_1 - R^7 c_7) b'_3 + (2R^2 c_2 - R^8 c_8) b'_4 + d'_4 - 4R^3 c_3 R^4 A = 0, \quad (\text{A.42})$$

$$a'_4 + (12R^7 c_7 - 6R^5 c_5) b'_1 + (12R^8 c_8 - 6R^6 c_6) b'_2 - 6R^7 c_7 b'_3 - 6R^8 c_8 b'_4 - 2e'_4 + (48c_5 R^5 - 24c_3 R^3) R^4 A = 0, \quad (\text{A.43})$$

$$\begin{aligned} & \frac{(3/2 + \kappa_1)}{4} a'_3 + \left(\frac{\kappa_1}{4} R^6 c_6 - \frac{5}{2} R^5 c_5 + R^4 c_4 \right) b'_1 + \left(\frac{\kappa_1}{4} R^7 c_7 - \frac{5}{2} R^6 c_6 + R^5 c_5 \right) b'_2 + \left(\frac{\kappa_1}{4} c_8 R^8 - \frac{5}{2} R^8 c_8 + R^6 c_6 \right) b'_3 + \\ & \left(\frac{3}{4} R c_1 + \frac{\kappa_1}{2} R c_1 + R^7 c_7 \right) b'_4 + \left(\frac{1}{2} \frac{\mu_1}{\mu_2} + \frac{3}{N'} \right) e'_3 + [(\kappa_1 - 10) R^4 c_4 + 4R^2 c_2] R^4 A = 0, \end{aligned} \quad (\text{A.44})$$

$$\begin{aligned}
& \frac{(1+\kappa_1)}{2}a'_2 - \frac{3}{4}a'_4 + \left(\frac{\kappa_1}{4}R^5c_5 + \frac{1}{2}R^3c_3 - 2R^3c_5\right)b'_1 + \\
& \left(\frac{\kappa_1}{4}R^6c_6 + \frac{1}{2}R^4c_4 - 2R^6c_6\right)b'_2 + \left(\frac{\kappa_1}{4}R^7c_7 + \frac{1}{2}Rc_1 + \right. \\
& \left. \frac{\kappa_1}{2}Rc_1 - 2R^7c_7 + \frac{1}{2}R^5c_5\right)b'_3 + \left(\frac{\kappa_1}{4}R^8c_8 + \frac{1}{2}R^2c_2 + \right. \\
& \left. \frac{\kappa_1}{2}R^2c_2 - 2R^8c_8 + \frac{1}{2}R^6c_6\right)b'_4 + \left(2\frac{\mu_1}{\mu_2} - \frac{\kappa_2\mu_1}{4\mu_2} + \frac{8}{N'}\right)d'_4 + \\
& \left(\frac{1}{2}\frac{\mu_1}{\mu_2} + \frac{2}{N'}\right)e'_2 + (2Rc_1 + \kappa_1R^3c_3 - 8R^3c_3)R^4A = 0,
\end{aligned} \tag{A.45}$$

$$\begin{aligned}
& \frac{(1/2+\kappa_1)}{2}a'_1 - \frac{1}{4}a'_3 + \left(\frac{\kappa_1}{4} - \frac{3}{2}\right)R^4c_4b'_1 + \left(\frac{\kappa_1}{4}R^5c_5 + \frac{1}{4}Rc_1 + \right. \\
& \left. \frac{\kappa_1}{2}Rc_1 - \frac{3}{2}R^5c_5\right)b'_2 + \left(\frac{\kappa_1}{4}R^6c_6 + \frac{1}{4}R^2c_2 + \frac{\kappa_1}{2}R^2c_2 - \frac{3}{2}R^6c_6\right)b'_3 \\
& + \left(\frac{\kappa_1}{4}R^7c_7 + \frac{1}{4}R^3c_3 - Rc_1 + \frac{\kappa_1}{2}R^3c_3 - \frac{3}{2}R^7c_7\right)b'_4 + \left(\frac{3}{2}\frac{\mu_1}{\mu_2} - \right. \\
& \left. \frac{\kappa_2}{4}\frac{\mu_1}{\mu_2} + \frac{3}{N'}\right)d'_3 + \left(\frac{1}{2}\frac{\mu_1}{\mu_2} + \frac{1}{N'}\right)e'_1 + (\kappa_1R^2c_2 - 1 - 6R^2c_2)R^4A = 0,
\end{aligned} \tag{A.46}$$

$$\begin{aligned}
& -\frac{1}{4}a'_2 + \left(\frac{\kappa_1}{4}R^3c_3 + \frac{\kappa_1}{2}Rc_1 - R^3c_3 - \frac{1}{2}Rc_1\right)b'_1 + \left(\frac{\kappa_1}{4}R^4c_4 + \right. \\
& \left. \frac{\kappa_1}{2}R^2c_2 - R^4c_4 - \frac{1}{2}R^2c_2\right)b'_2 + \left(\frac{\kappa_1}{4}R^5c_5 - \frac{3}{4}Rc_1 + \frac{\kappa_1}{2}R^3c_3 - \right. \\
& \left. R^5c_5 - \frac{1}{2}R^3c_3\right)b'_3 + \left(\frac{\kappa_1}{4}R^6c_6 - \frac{3}{4}R^2c_2 + \frac{\kappa_1}{2}R^4c_4 - R^6c_6 - \right. \\
& \left. \frac{1}{2}R^4c_4\right)b'_4 - \frac{\kappa_2}{2}\frac{\mu_1}{\mu_2}d'_0 + \left(1 - \frac{\kappa_2}{4}\right)\frac{\mu_1}{\mu_2}d'_2 + (\kappa_1Rc_1 - 4Rc_1)R^4A = 0,
\end{aligned} \tag{A.47}$$

$$\begin{aligned}
& \left(\frac{\kappa_1}{4} R^2 c_2 - \frac{1}{4} R^2 c_2 + \frac{\kappa_1}{2} R^2 c_2 - \frac{1}{2} R^2 c_2 \right) b'_1 + \left(\frac{\kappa_1}{4} R^3 c_3 - \right. \\
& \left. \frac{1}{4} R^3 c_3 - \frac{1}{2} R c_1 + \frac{\kappa_1}{2} R^3 c_3 - \frac{R^3 c_3}{2} - R c_1 \right) b'_2 + \left(\frac{\kappa_1}{4} R^4 c_4 - \right. \\
& \left. \frac{1}{4} R^4 c_4 - \frac{1}{2} R^2 c_2 + \frac{\kappa_1}{2} R^4 c_4 - \frac{R^4 c_4}{2} - R^2 c_2 \right) b'_3 + \left(\frac{\kappa_1}{4} R^5 c_5 - \right. \\
& \left. \frac{1}{4} R^5 c_5 - \frac{1}{2} R^3 c_3 + \frac{\kappa_1}{2} R^5 c_5 - \frac{R^5 c_5}{2} - R^3 c_3 \right) b'_4 + \left(\frac{3\mu_1}{4\mu_2} - \right. \\
& \left. \kappa_2 \frac{3\mu_1}{4\mu_2} - \frac{2}{N'} \right) d'_1 + \left(-\frac{3\kappa_1}{4} + \frac{3}{4} \right) R^4 A = 0,
\end{aligned} \tag{A.48}$$

$$\begin{aligned}
& -\frac{1}{2} a'_2 + \left(\frac{\kappa_1}{4} R c_1 - \frac{R^3}{2} c_3 - \frac{1}{4} R c_1 + \frac{\kappa_1}{2} R^3 c_3 \right) b'_1 + \left(\frac{\kappa_1}{4} R^2 c_2 - \right. \\
& \left. \frac{R^4}{2} c_4 - \frac{1}{4} R^2 c_2 + \frac{\kappa_1}{2} R^4 c_4 \right) b'_2 + \left(\frac{\kappa_1}{4} R^3 c_3 - \frac{R^5}{2} c_5 - \frac{1}{4} R^3 c_3 + \right. \\
& \left. \frac{\kappa_1}{2} R^5 c_5 - \frac{3}{2} R c_1 \right) b'_3 + \left(\frac{\kappa_1}{4} R^4 c_4 - \frac{R^6}{2} c_6 - \frac{1}{4} R^4 c_4 + \frac{\kappa_1}{2} R^6 c_6 - \right. \\
& \left. \frac{3}{2} R^2 c_2 \right) b'_4 - \frac{\kappa_2}{4} \frac{\mu_1}{\mu_2} d'_0 + \left(\frac{1}{2} \frac{\mu_1}{\mu_2} - \frac{\kappa_2}{2} \frac{\mu_1}{\mu_2} - \frac{2}{N'} \right) d'_2 - \\
& 2(1 - \kappa_1) R c_1 R^4 A = 0,
\end{aligned} \tag{A.49}$$

$$\begin{aligned}
& \frac{(1 + \kappa_1/2)}{2} a'_1 - \frac{1}{2} a'_3 + \left(\frac{\kappa_1}{2} - \frac{3}{4} \right) R^4 c_4 b'_1 + \left(\frac{\kappa_1}{4} R c_1 + \frac{\kappa_1}{2} R^5 c_5 + \right. \\
& \left. \frac{1}{2} R c_1 \right) b'_2 + \left(\frac{\kappa_1}{4} R^2 c_2 - \frac{3}{4} R^6 c_6 + \frac{\kappa_1}{2} R^6 c_6 + \frac{1}{2} R^2 c_2 \right) b'_3 + \left(\frac{\kappa_1}{4} R^3 c_3 - \right. \\
& \left. \frac{3}{4} R^7 c_7 + \frac{\kappa_1}{2} R^7 c_7 + \frac{1}{2} R^3 c_3 - 2 R c_1 \right) b'_4 + \left(\frac{3}{4} \frac{\mu_1}{\mu_2} - \frac{\kappa_2}{2} \frac{\mu_1}{\mu_2} - \frac{3}{N'} \right) d'_3 + \\
& \frac{1}{4} \frac{\mu_1}{\mu_2} e'_1 - \left(3 R^2 c_2 - 2 R^2 \kappa_1 c_2 + \frac{1}{2} \right) R^4 A = 0,
\end{aligned} \tag{A.50}$$

$$\begin{aligned}
& (1 + \kappa_1 / 4)a'_2 - \frac{3}{4}a'_4 + (\frac{1}{4}R^3c_3 - R^5c_5 + \frac{\kappa_1}{2}R^5c_5)b'_1 + \\
& (\frac{1}{4}R^4c_4 - R^6c_6 + \frac{\kappa_1}{2}R^6c_6)b'_2 + (\frac{\kappa_1}{4}Rc_1 + \frac{1}{4}R^5c_5 - \\
& R^7c_7 + \frac{\kappa_1}{2}R^7c_7 + Rc_1)b'_3 + (\frac{\kappa_1}{4}R^2c_2 + \frac{1}{4}R^6c_6 - \\
& R^8c_8 + \frac{\kappa_1}{2}R^8c_8 + R^2c_2)b'_4 + (\frac{\mu_1}{\mu_2} - \frac{\kappa_2}{2} \frac{\mu_1}{\mu_2} - \frac{4}{N'})d'_4 + \\
& \frac{1}{4} \frac{\mu_1}{\mu_2} e'_2 + (Rc_1 - 4R^3c_3 + 2\kappa_1 R^3c_3)R^4A = 0,
\end{aligned} \tag{A.51}$$

$$\begin{aligned}
& (\frac{1}{2} + \frac{\kappa_1}{4})a'_4 + (\frac{\kappa_1}{4}R^7c_7 - 3R^7c_7 + \frac{3}{2}R^5c_5)b'_1 + (\frac{\kappa_1}{4}R^8c_8 - \\
& 3R^8c_8 + \frac{3}{2}R^6c_6)b'_2 + \frac{3}{2}R^7c_7b'_3 + \frac{3}{2}R^8c_8b'_4 + (\frac{1}{2} \frac{\mu_1}{\mu_2} + \frac{4}{N'})e'_4 + \\
& (\kappa_1 R^5c_5 - 12R^5c_5 + 6R^3c_3)R^4A = 0.
\end{aligned} \tag{A.52}$$

For the case of *sliding interface* ($m = \infty$, $n=0$), similarly, we can obtain the final 17 equations in Section 3.2.4. as:

$$\begin{aligned}
& \frac{a'_3}{2} + (5c_6R^0 - 2c_4R^4)b'_1 + (5c_7R^7 - 2R^5c_5)b'_2 + (5c_8R^8 - 2c_6R^6)b'_3 + \\
& (c_1R - 2c_7R^7)b'_4 - e'_3 + (20R^4c_4 - 8R^2c_2)R^4A = 0,
\end{aligned} \tag{A.53}$$

$$\begin{aligned}
& a'_2 + (4c_5R^5 - c_3R^3)b'_1 + (4c_6R^6 - c_4R^4)b'_2 + (4c_7R^7 - c_5R^5 + c_1R)b'_3 + \\
& (4c_8R^8 - c_6R^6 + c_2R^2)b'_4 - 4d'_4 - e'_2 + (16c_3R^3A - 4c_1R)R^4A = 0,
\end{aligned} \tag{A.54}$$

$$\begin{aligned}
& a'_1 + 3c_4R^4b'_1 + 3c_1Rb'_2 + (3c_4R^4 + c_2R^2)b'_3 + (3c_7R^7 + c_3R^3)b'_4 - 3d'_3 - e'_1 + \\
& (12c_2R^2A + 2)R^4A = 0,
\end{aligned} \tag{A.55}$$

$$c_2 R^2 b'_1 + (c_3 R^3 + c_1 R) b'_2 + (c_4 R^4 + c_2 R^2) b'_3 + (c_5 R^5 + c_3 R^3) b'_4 - d'_1 - R^4 A = 0, \quad (\text{A.56})$$

$$a'_2 + R^3 c_3 b'_1 + R^4 c_4 b'_2 + (R^5 c_5 + 3R c_1) b'_3 + (R^6 c_6 + 3R^2 c_2) b'_4 - d'_2 + 4R c_1 R^4 A = 0, \quad (\text{A.57})$$

$$a'_1 - a'_3 - R^4 c_4 b'_1 + (R c_1 - R^5 c_5) b'_2 + (R^2 c_2 - R^6 c_6) b'_3 + (R^3 c_3 - R^7 c_7 - 4R c_1) b'_4 + d'_3 - 4R^2 c_2 R^4 A = 0, \quad (\text{A.58})$$

$$2a'_2 - \frac{3a'_4}{2} - R^5 c_5 b'_1 - R^6 c_6 b'_2 + (2R c_1 - R^7 c_7) b'_3 + (2R^2 c_2 - R^8 c_8) b'_4 + d'_4 - 4R^3 c_3 R^4 A = 0, \quad (\text{A.59})$$

$$a'_4 + (12R^7 c_7 - 6R^5 c_5) b'_1 + (12R^8 c_8 - 6R^6 c_6) b'_2 - 6R^7 c_7 b'_3 - 6R^8 c_8 b'_4 - 2e'_4 + (48c_5 R^5 - 24c_3 R^3) R^4 A = 0, \quad (\text{A.60})$$

$$\begin{aligned} & \frac{(3/2 + \kappa_1)}{4} a'_3 + \left(\frac{\kappa_1}{4} R^6 c_6 - \frac{5}{2} R^6 c_6 + R^4 c_4 \right) b'_1 + \left(\frac{\kappa_1}{4} R^7 c_7 - \frac{5}{2} R^7 c_7 + \right. \\ & R^5 c_5 \left. \right) b'_2 + \left(\frac{\kappa_1}{4} c_8 R^8 - \frac{5}{2} R^8 c_8 + R^6 c_6 \right) b'_3 + \left(\frac{3}{4} R c_1 + \frac{\kappa_1}{2} R c_1 + R^7 c_7 \right) b'_4 + \\ & \left(\frac{1}{2} \frac{\mu_1}{\mu_2} + \frac{3}{N'} \right) e'_3 + [(\kappa_1 - 10) R^4 c_4 + 4R^2 c_2] R^4 A = 0, \end{aligned} \quad (\text{A.61})$$

$$\begin{aligned}
& \frac{(1+\kappa_1)}{2}a'_2 - \frac{3}{4}a'_4 + \left(\frac{\kappa_1}{4}R^5c_5 + \frac{1}{2}R^3c_3 - 2R^5c_5\right)b'_1 + \left(\frac{\kappa_1}{4}R^6c_6 + \right. \\
& \left. \frac{1}{2}R^4c_4 - 2R^6c_6\right)b'_2 + \left(\frac{\kappa_1}{4}R^7c_7 + \frac{1}{2}Rc_1 + \frac{\kappa_1}{2}Rc_1 - 2R^7c_7 + \right. \\
& \left. \frac{1}{2}R^5c_5\right)b'_3 + \left(\frac{\kappa_1}{4}R^8c_8 + \frac{1}{2}R^2c_2 + \frac{\kappa_1}{2}R^2c_2 - 2R^8c_8 + \frac{1}{2}R^6c_6\right)b'_4 + \\
& \left(2\frac{\mu_1}{\mu_2} - \frac{\kappa_2\mu_1}{4\mu_2} + \frac{8}{N'}\right)d'_4 + \left(\frac{1}{2}\frac{\mu_1}{\mu_2} + \frac{2}{N'}\right)e'_2 + (2Rc_1 + \kappa_1R^3c_3 - \\
& 8R^3c_3)R^4A = 0,
\end{aligned} \tag{A.62}$$

$$\begin{aligned}
& \frac{(1/2+\kappa_1)}{2}a'_1 - \frac{1}{4}a'_3 + \left(\frac{\kappa_1}{4} - \frac{3}{2}\right)R^4c_4b'_1 + \left(\frac{\kappa_1}{4}R^5c_5 + \frac{1}{4}Rc_1 + \frac{\kappa_1}{2}Rc_1 - \right. \\
& \left. \frac{3}{2}R^5c_5\right)b'_2 + \left(\frac{\kappa_1}{4}R^6c_6 + \frac{1}{4}R^2c_2 + \frac{\kappa_1}{2}R^2c_2 - \frac{3}{2}R^6c_6\right)b'_3 + \left(\frac{\kappa_1}{4}R^7c_7 + \right. \\
& \left. \frac{1}{4}R^3c_3 - Rc_1 + \frac{\kappa_1}{2}R^3c_3 - \frac{3}{2}R^7c_7\right)b'_4 + \left(\frac{3}{2}\frac{\mu_1}{\mu_2} - \frac{\kappa_2}{4}\frac{\mu_1}{\mu_2} + \frac{3}{N'}\right)d'_3 + \\
& \left(\frac{1}{2}\frac{\mu_1}{\mu_2} + \frac{1}{N'}\right)e'_1 + (\kappa_1R^2c_2 - 1 - 6R^2c_2)R^4A = 0,
\end{aligned} \tag{A.63}$$

$$\begin{aligned}
& -\frac{1}{4}a'_2 + \left(\frac{\kappa_1}{4}R^3c_3 + \frac{\kappa_1}{2}Rc_1 - R^3c_3 - \frac{1}{2}Rc_1\right)b'_1 + \left(\frac{\kappa_1}{4}R^4c_4 + \frac{\kappa_1}{2}R^2c_2 - \right. \\
& \left. R^4c_4 - \frac{1}{2}R^2c_2\right)b'_2 + \left(\frac{\kappa_1}{4}R^5c_5 - \frac{3}{4}Rc_1 + \frac{\kappa_1}{2}R^3c_3 - R^5c_5 - \frac{1}{2}R^3c_3\right)b'_3 + \\
& \left(\frac{\kappa_1}{4}R^6c_6 - \frac{3}{4}R^2c_2 + \frac{\kappa_1}{2}R^4c_4 - R^6c_6 - \frac{1}{2}R^4c_4\right)b'_4 - \frac{\kappa_2}{2}\frac{\mu_1}{\mu_2}d'_0 + \\
& \left(1 - \frac{\kappa_2}{4}\right)\frac{\mu_1}{\mu_2}d'_2 + (\kappa_1Rc_1 - 4Rc_1)R^4A = 0,
\end{aligned} \tag{A.64}$$

$$\begin{aligned}
& \left(\frac{\kappa_1}{4}R^2c_2 - \frac{1}{4}R^2c_2 + \frac{\kappa_1}{2}R^2c_2 - \frac{1}{2}R^2c_2\right)b'_1 + \left(\frac{\kappa_1}{4}R^3c_3 - \frac{1}{4}R^3c_3 - \right. \\
& \left. \frac{1}{2}Rc_1 + \frac{\kappa_1}{2}R^3c_3 - \frac{R^3c_3}{2} - Rc_1\right)b'_2 + \left(\frac{\kappa_1}{4}R^4c_4 - \frac{1}{4}R^4c_4 - \frac{1}{2}R^2c_2 + \right. \\
& \left. \frac{\kappa_1}{2}R^4c_4 - \frac{R^4c_4}{2} - R^2c_2\right)b'_3 + \left(\frac{\kappa_1}{4}R^5c_5 - \frac{1}{4}R^5c_5 - \frac{1}{2}R^3c_3 + \frac{\kappa_1}{2}R^5c_5 - \right. \\
& \left. \frac{R^5c_5}{2} - R^3c_3\right)b'_4 + \left(\frac{3\mu_1}{4\mu_2} - \kappa_2 \frac{3\mu_1}{4\mu_2} - \frac{2}{N'}\right)d'_1 + \left(-\frac{3\kappa_1}{4} + \frac{3}{4}\right)R^4A = 0,
\end{aligned} \tag{A.65}$$

$$\begin{aligned}
& -\frac{1}{2}a'_2 + \left(\frac{\kappa_1}{4}Rc_1 - \frac{R^3}{2}c_3 - \frac{1}{4}Rc_1 + \frac{\kappa_1}{2}R^3c_3\right)b'_1 + \left(\frac{\kappa_1}{4}R^2c_2 - \frac{R^4}{2}c_4 - \right. \\
& \left. \frac{1}{4}R^2c_2 + \frac{\kappa_1}{2}R^4c_4\right)b'_2 + \left(\frac{\kappa_1}{4}R^3c_3 - \frac{R^5}{2}c_5 - \frac{1}{4}R^3c_3 + \frac{\kappa_1}{2}R^5c_5 - \right. \\
& \left. \frac{3}{2}Rc_1\right)b'_3 + \left(\frac{\kappa_1}{4}R^4c_4 - \frac{R^6}{2}c_6 - \frac{1}{4}R^4c_4 + \frac{\kappa_1}{2}R^6c_6 - \frac{3}{2}R^2c_2\right)b'_4 - \\
& \frac{\kappa_2}{4} \frac{\mu_1}{\mu_2} d'_0 + \left(\frac{1}{2} \frac{\mu_1}{\mu_2} - \frac{\kappa_2}{2} \frac{\mu_1}{\mu_2} - \frac{2}{N'}\right)d'_2 - 2(1 - \kappa_1)Rc_1R^4A = 0,
\end{aligned} \tag{A.66}$$

$$\begin{aligned}
& \frac{(1 + \kappa_1/2)}{2}a'_1 - \frac{1}{2}a'_3 + \left(\frac{\kappa_1}{2} - \frac{3}{4}\right)R^4c_4b'_1 + \left(\frac{\kappa_1}{4}Rc_1 + \frac{\kappa_1}{2}R^5c_5 + \right. \\
& \left. \frac{1}{2}Rc_1\right)b'_2 + \left(\frac{\kappa_1}{4}R^2c_2 - \frac{3}{4}R^6c_6 + \frac{\kappa_1}{2}R^6c_6 + \frac{1}{2}R^2c_2\right)b'_3 + \left(\frac{\kappa_1}{4}R^3c_3 - \right. \\
& \left. \frac{3}{4}R^7c_7 + \frac{\kappa_1}{2}R^7c_7 + \frac{1}{2}R^3c_3 - 2Rc_1\right)b'_4 + \left(\frac{3}{4} \frac{\mu_1}{\mu_2} - \frac{\kappa_2}{2} \frac{\mu_1}{\mu_2} - \frac{3}{N'}\right)d'_3 + \\
& \frac{1}{4} \frac{\mu_1}{\mu_2} e'_1 - \left(3R^2c_2 - 2R^2\kappa_1c_2 + \frac{1}{2}\right)R^4A = 0,
\end{aligned} \tag{A.67}$$

$$\begin{aligned}
& (1 + \kappa_1/4)a'_2 - \frac{3}{4}a'_4 + \left(\frac{1}{4}R^3c_3 - R^5c_5 + \frac{\kappa_1}{2}R^5c_5\right)b'_1 + \left(\frac{1}{4}R^4c_4 - \right. \\
& \left. R^6c_6 + \frac{\kappa_1}{2}R^6c_6\right)b'_2 + \left(\frac{\kappa_1}{4}Rc_1 + \frac{1}{4}R^5c_5 - R^7c_7 + \frac{\kappa_1}{2}R^7c_7 + \right. \\
& \left. Rc_1\right)b'_3 + \left(\frac{\kappa_1}{4}R^2c_2 + \frac{1}{4}R^6c_6 - R^8c_8 + \frac{\kappa_1}{2}R^8c_8 + R^2c_2\right)b'_4 + \\
& \left(\frac{\mu_1}{\mu_2} - \frac{\kappa_2}{2} \frac{\mu_1}{\mu_2} - \frac{4}{N'}\right)d'_4 + \frac{1}{4} \frac{\mu_1}{\mu_2} e'_2 + (Rc_1 - 4R^3c_3 + 2\kappa_1R^3c_3)R^4A = 0,
\end{aligned} \tag{A.68}$$

$$\begin{aligned}
& \left(\frac{1}{2} + \frac{\kappa_1}{4}\right)a'_{,4} + \left(\frac{\kappa_1}{4}R^7c_7 - 3R^7c_7 + \frac{3}{2}R^5c_5\right)b'_{,1} + \left(\frac{\kappa_1}{4}R^8c_8 - \right. \\
& \left. 3R^8c_8 + \frac{3}{2}R^8c_6\right)b'_{,2} + \frac{3}{2}R^7c_7b'_{,3} + \frac{3}{2}R^8c_8b'_{,4} + \left(\frac{1}{2}\frac{\mu_1}{\mu_2} + \frac{4}{N'}\right)e'_{,4} + \\
& (\kappa_1R^5c_5 - 12R^5c_5 + 6R^3c_3)R^4A = 0.
\end{aligned} \tag{A.69}$$

APPENDIX 2

For the case of the sliding interface ($m = \infty$, $n=0$) under pure shear loading, the relevant equations are derived as follows:

$$\begin{aligned} \frac{a_3}{2R^3} + \left(\frac{4c_4}{R^2} - 5c_6\right)b_1 + \left(\frac{4c_5}{R^2} - 5c_7\right)b_2 + \left(\frac{4c_6}{R^2} - 5c_8\right)b_3 + \left(\frac{c_1}{R^3} + \right. \\ \left. \frac{4c_7}{R^2}\right)b_4 + \frac{e_3}{R^2} + \left(5c_4B - \frac{4c_2B}{R^2}\right) = 0, \end{aligned} \quad (\text{B.1})$$

$$\begin{aligned} \frac{a_2}{2R^6} + \left(\frac{3c_3}{R^2} - 4c_5\right)b_1 + \left(\frac{3c_4}{R^2} - 4c_6\right)b_2 + \left(\frac{3c_5}{R^2} - 4c_7 + \frac{c_1}{R^6}\right)b_3 + \left(\frac{3c_6}{R^2} - \right. \\ \left. 4c_8 + \frac{c_2}{R^6}\right)b_4 + 4d_4 + \frac{e_2}{R^2} + \left(4c_3B - \frac{3c_1B}{R^2}\right) = 0, \end{aligned} \quad (\text{B.2})$$

$$\begin{aligned} \frac{a_1}{2R^4} + \left(3c_4 - \frac{2c_2}{R^2}\right)b_1 + \left(3c_5 - \frac{2c_3}{R^2} - \frac{c_1}{R^4}\right)b_2 + \left(3c_6 - \frac{2c_4}{R^2} - \frac{c_2}{R^4}\right)b_3 + \\ \left(3c_7 - \frac{2c_5}{R^2} - \frac{c_3}{R^4}\right)b_4 - 3d_3 - \frac{e_1}{R^2} - 3c_2B = 0, \end{aligned} \quad (\text{B.3})$$

$$a_1 = 0, \quad (\text{B.4})$$

$$\begin{aligned} \frac{3a_2}{2R^2} - R^2c_3b_1 - R^2c_4b_2 - \left(R^2c_5 - \frac{c_1}{R^2}\right)b_3 - \left(R^2c_6 - \frac{c_2}{R^2}\right)b_4 + R^2d_2 + \\ R^2c_1B = 0, \end{aligned} \quad (\text{B.5})$$

$$\begin{aligned} & \frac{a_1}{2} - \frac{2a_3}{R^2} - R^4 c_4 b_1 + (c_1 - R^4 c_5) b_2 + (c_2 - R^4 c_6) b_3 + (c_3 - R^4 c_7 - \\ & \frac{2c_1}{R^2}) b_4 + R^4 d_3 + R^4 c_2 B = 0, \end{aligned} \quad (\text{B.6})$$

$$\begin{aligned} & a_2 - \frac{5a_4}{2R^2} + R^6 c_5 b_1 + R^6 c_6 b_2 + (2c_1 + R^6 c_7) b_3 + (2c_2 + R^6 c_8) b_4 - \\ & R^6 d_4 - R^6 c_3 A = 0, \end{aligned} \quad (\text{B.7})$$

$$\begin{aligned} & \frac{a_4}{R^{10}} + (\frac{10c_5}{R^2} - 12c_7) b_1 + (\frac{10c_6}{R^2} - 12c_8) b_2 + \frac{10c_7}{R^2} b_3 + \frac{10c_8}{R^2} b_4 - \\ & \frac{2e_4}{R^2} + (12c_3 B - \frac{10c_3}{R^2} B) = 0, \end{aligned} \quad (\text{B.8})$$

$$\begin{aligned} & -\frac{N'(3+\kappa_1)}{4R^8} a_3 + (\frac{\kappa_1}{2} c_6 - \frac{5}{2} c_6 + \frac{2}{R^2} c_4) N' b_1 + (\frac{\kappa_1}{2} c_7 - \frac{5}{2} c_7 + \\ & \frac{2}{R^2} c_5) N' b_2 + (\frac{\kappa_1}{2} c_8 - \frac{5}{2} c_8 + \frac{2}{R^2} c_6) N' b_3 + (\frac{2}{R^2} c_7 - \frac{3}{4R^8} c_1 - \frac{\kappa_1}{2R^8} c_1 \\ &) N' b_4 + (\frac{\mu_1}{\mu_2} \frac{N'}{2R^2} + \frac{3}{R^2}) e_3 - (\frac{\kappa_1 c_4}{2} - \frac{5c_4}{2} + \frac{2c_2}{R^2}) N' B = 0, \end{aligned} \quad (\text{B.9})$$

$$\begin{aligned} & -\frac{N'(2+\kappa_1)}{2R^6} a_2 + \frac{5N'}{4R^8} a_4 + (\frac{\kappa_1}{2} c_5 + \frac{3}{2R^2} c_3 - 2c_5) N' b_1 + (\frac{\kappa_1}{2} c_6 + \\ & \frac{3}{2R^2} c_4 - 2c_6) N' b_2 + (\frac{\kappa_1}{2} c_7 + \frac{3}{2R^2} c_5 - \frac{1}{R^6} c_1 - \frac{\kappa_1}{2R^6} c_1 - 2c_7) N' b_3 + \\ & (\frac{\kappa_1}{2} c_8 + \frac{3}{2R^2} c_6 - \frac{1}{R^6} c_2 - \frac{\kappa_1}{2R^6} c_2 - 2c_8) N' b_4 + (2\frac{\mu_1}{\mu_2} N' - \frac{\kappa_2 \mu_1}{2\mu_2} N' + \\ & 8) d_4 + (\frac{\mu_1}{\mu_2} \frac{N'}{2R^2} + \frac{2}{R^2}) e_2 - (\frac{3}{2R^2} c_1 + \frac{\kappa_1 c_3}{2} - 2c_3) N' B = 0, \end{aligned} \quad (\text{B.10})$$

$$\begin{aligned}
& \frac{N'(\kappa_1 - 1)}{4R^4}a_1 + \frac{N'}{R^6}a_3 + \left(\frac{\kappa_1}{2}c_4 - \frac{3}{2}c_4 + \frac{1}{R^2}c_2\right)N'b_1 + \left(\frac{\kappa_1}{2}c_5 - \right. \\
& \left. \frac{3}{2}c_5 + \frac{1}{R^2}c_3 - \frac{1}{2R^4}c_1 - \frac{\kappa_1}{2R^4}c_1\right)N'b_2 + \left(\frac{\kappa_1}{2}c_6 - \frac{3}{2}c_6 + \frac{1}{R^2}c_4 - \right. \\
& \left. \frac{1}{2R^4}c_2 - \frac{\kappa_1}{2R^4}c_2\right)N'b_3 + \left(\frac{\kappa_1}{2}c_7 - \frac{3}{2}c_7 + \frac{1}{R^2}c_5 - \frac{1}{2R^4}c_3 - \right. \\
& \left. \frac{\kappa_1}{2R^4}c_3 + \frac{1}{R^6}c_1\right)N'b_4 + \left(\frac{3}{2}\frac{\mu_1}{\mu_2}N' - \frac{\kappa_2}{2}\frac{\mu_1}{\mu_2}N' + 3\right)d_3 + \left(\frac{\mu_1}{\mu_2}\frac{N'}{2R^2} + \right. \\
& \left. \frac{1}{R^2}\right)e_1 + \left(\frac{\kappa_1 c_2}{2} + \frac{3}{2}c_2\right)N'B = 0,
\end{aligned} \tag{B.11}$$

$$\begin{aligned}
& \frac{3N'}{4R^4}a_2 + \left(\frac{\kappa_1}{2}c_3 - \frac{\kappa_1}{2R^2}c_1 - c_3 + \frac{1}{2R^2}c_1\right)N'b_1 + \left(\frac{\kappa_1}{2}c_4 - \frac{\kappa_1}{2R^2}c_2 - \right. \\
& \left. c_4 + \frac{1}{2R^2}c_2\right)N'b_2 + \left(\frac{\kappa_1}{2}c_5 - \frac{\kappa_1}{2R^2}c_3 - c_5 + \frac{1}{2R^2}c_3 + \frac{1}{2R^4}c_1\right)N'b_3 + \\
& \left(\frac{\kappa_1}{2}c_6 - \frac{\kappa_1}{2R^2}c_4 - c_6 + \frac{1}{2R^2}c_4 + \frac{1}{2R^4}c_2\right)N'b_4 + \frac{\mu_1}{\mu_2}\frac{\kappa_2 N'}{2R^2}d_0 + \left(\frac{\mu_1}{\mu_2} - \right. \\
& \left. \frac{\mu_1}{\mu_2}\frac{\kappa_2}{2}\right)N'd_2 - \left(\frac{\kappa_1}{2}c_1 - c_1\right)N'B = 0,
\end{aligned} \tag{B.12}$$

$$\begin{aligned}
& \frac{N'}{2R^2}a_1 + \left(\frac{\kappa_1}{2}c_2 + \frac{1}{2}c_2 - \frac{\kappa_1}{2}c_2 - \frac{1}{2}c_2\right)N'b_1 + \left(\frac{\kappa_1}{2}c_3 + \frac{1}{2}c_3 - \frac{\kappa_1}{2}c_3 - \right. \\
& \left. \frac{c_3}{2}\right)N'b_2 + \left(\frac{\kappa_1}{2}c_4 + \frac{1}{2}c_4 - \frac{\kappa_1}{2}c_4 - \frac{c_4}{2}\right)N'b_3 + \left(\frac{\kappa_1}{2}c_5 + \frac{1}{2}c_5 - \frac{\kappa_1}{2}c_5 - \right. \\
& \left. \frac{c_5}{2}\right)N'b_4 - \frac{\mu_1}{\mu_2}\kappa_2 N'd_1 + \left(\frac{\kappa_1}{4} + \frac{1}{4} - \frac{\kappa_1}{4} - \frac{1}{4}\right)N'B = 0,
\end{aligned} \tag{B.13}$$

$$\begin{aligned}
& -\frac{3N'}{4R^2}a_2 + \left(\frac{\kappa_1}{2}c_1 + R^2c_3 - \frac{1}{2}c_1 - \frac{R^2\kappa_1}{2}c_3\right)N'b_1 + \left(\frac{\kappa_1}{2}c_2 + R^2c_4 - \right. \\
& \left. \frac{1}{2}c_2 - \frac{R^2\kappa_1}{2}c_4\right)N'b_2 + \left(\frac{\kappa_1}{2}c_3 + R^2c_5 - \frac{1}{2}c_3 - \frac{R^2\kappa_1}{2}c_5 - \frac{1}{2R^2}c_1\right)N'b_3 + \\
& \left(\frac{\kappa_1}{2}c_4 + R^2c_6 - \frac{1}{2}c_4 - \frac{R^2\kappa_1}{2}c_6 - \frac{1}{2R^2}c_2\right)N'b_4 - \frac{\mu_1}{\mu_2}\frac{\kappa_2}{2}N'd_0 + \\
& \left(\frac{\mu_1}{\mu_2}R^2N' - \frac{\mu_1}{\mu_2}\frac{R^2\kappa_2}{2}N' + 2R^2\right)d_2 - \left(1 - \frac{\kappa_1}{2}\right)R^2c_1N'B = 0,
\end{aligned} \tag{B.14}$$

$$\begin{aligned}
& \frac{(1+\kappa_1)N'}{4}a_1 - \frac{N'}{R^2}a_3 + \left(\frac{3R^4}{2}c_4 - R^2c_2 - \frac{\kappa_1}{2}R^4c_4\right)N'b_1 + \left(\frac{\kappa_1}{2}c_1 + \right. \\
& \left. \frac{3R^4}{2}c_5 - R^2c_3 - \frac{\kappa_1}{2}R^4c_5 + \frac{1}{2}c_1\right)N'b_2 + \left(\frac{\kappa_1}{2}c_2 + \frac{3R^4}{2}c_6 - R^2c_4 - \right. \\
& \left. \frac{\kappa_1}{2}R^4c_6 + \frac{1}{2}c_2\right)N'b_3 + \left(\frac{\kappa_1}{2}c_3 + \frac{3R^4}{2}c_7 - R^2c_5 - \frac{\kappa_1}{2}R^4c_7 + \frac{1}{2}c_3 - \right. \\
& \left. \frac{1}{R^2}c_1\right)N'b_4 - \left(\frac{\mu_1}{\mu_2}\frac{3R^4}{2}N' - \frac{\mu_1}{\mu_2}\frac{R^4\kappa_2}{2}N' - 3R^4\right)d_3 - \frac{\mu_1}{\mu_2}\frac{R^2}{2}N'e_1 - \\
& \left(\frac{3}{2}R^4c_2 - \frac{\kappa_1}{2}R^4c_2\right)N'B = 0,
\end{aligned} \tag{B.15}$$

$$\begin{aligned}
& \frac{(1+\kappa_1/2)N'}{2}a_2 - \frac{5N'}{4R^2}a_4 + \left(2R^0c_5 - \frac{3R^4}{2}c_3 - \frac{R^0\kappa_1}{2}c_5\right)N'b_1 + \\
& \left(2R^0c_6 - \frac{3R^4}{2}c_4 - \frac{R^0\kappa_1}{2}c_6\right)N'b_2 + \left(\frac{\kappa_1}{2}c_1 + 2R^0c_7 - \frac{3R^4}{2}c_5 - \right. \\
& \left. \frac{R^0\kappa_1}{2}c_7 + c_1\right)N'b_3 + \left(\frac{\kappa_1}{2}c_2 + 2R^0c_8 - \frac{3R^4}{2}c_6 - \frac{R^0\kappa_1}{2}c_8 + \right. \\
& \left. c_2\right)N'b_4 + \left(\frac{\mu_1}{\mu_2}\frac{R^0\kappa_2}{2}N' - 2\frac{\mu_1}{\mu_2}R^0N' + 4R^0\right)d_4 - \frac{\mu_1}{\mu_2}\frac{R^4e_2}{2}N' - \\
& \left(R^0c_3 - \frac{3}{2}R^4c_1 - \frac{\kappa_1}{2}R^0c_3\right)N'B = 0,
\end{aligned} \tag{B.16}$$

$$\begin{aligned}
& -\frac{(2+\kappa_1/2)N'}{2R^{10}}a_4 + \left(\frac{\kappa_1}{2}c_7 - 3c_7 + \frac{5}{2R^2}c_5\right)N'b_1 + \left(\frac{\kappa_1}{2}c_8 - 3c_8 + \right. \\
& \left. \frac{5}{2R^2}c_6\right)N'b_2 + \frac{5}{2R^2}c_7N'b_3 + \frac{5}{2R^2}c_8N'b_4 + \left(\frac{\mu_1}{\mu_2}\frac{1}{2R^2}N' + \frac{4}{R^2}\right)e_4 - \\
& \left(\frac{\kappa_1}{2}c_5 - 3c_5 + \frac{5}{2R^2}c_3\right)N'B = 0.
\end{aligned} \tag{B.17}$$

If we make the following replacements:

$$a'_1 \sim \frac{R^2 a_1}{2}, \quad a'_2 \sim \frac{R a_2}{2}, \quad a'_3 \sim a_3, \quad a'_4 \sim \frac{a_4}{R};$$

$$b'_1 \sim R^2 b_1, \quad b'_2 \sim R b_2, \quad b'_3 \sim b_3, \quad b'_4 \sim \frac{b_4}{R};$$

$$d'_0 \sim R^3 d_0, \quad d'_1 \sim R^4 d_1, \quad d'_2 \sim R^5 d_2, \quad d'_3 \sim R^6 d_3, \quad d'_4 \sim R^7 d_4;$$

$$e'_1 \sim R^4 e_1, \quad e'_2 \sim R^5 e_2, \quad e'_3 \sim R^6 e_3, \quad e'_4 \sim R^7 e_4.$$

Then, the final 17 equations are given by:

$$\begin{aligned} \frac{a'_3}{2} + (4c_4 R^4 - 5c_6 R^6) b'_1 + (4R^5 c_5 - 5c_7 R^7) b'_2 + (4c_6 R^6 - 5c_8 R^8) b'_3 + \\ (c_1 R + 4c_7 R^7) b'_4 + e'_3 = (4R^2 c_2 - 5R^4 c_4) R^4 B, \end{aligned} \quad (\text{B.18})$$

$$\begin{aligned} a'_2 + (3c_3 R^3 - 4c_5 R^5) b'_1 + (3c_4 R^4 - 4c_6 R^6) b'_2 + (3c_5 R^5 - 4c_7 R^7 + \\ c_1 R) b'_3 + (3c_6 R^6 - 4c_8 R^8 + c_2 R^2) b'_4 + 4d'_4 + e'_2 = (3c_1 R - 4c_3 R^3 A) R^4 B, \end{aligned} \quad (\text{B.19})$$

$$\begin{aligned} a'_1 + (3c_4 R^4 - 2c_2 R^2) b'_1 + (3c_5 R^5 - 2c_3 R^3 - c_1 R) b'_2 + (3c_6 R^6 - 2c_4 R^4 - \\ c_2 R^2) b'_3 + (3c_7 R^7 - 2c_5 R^5 - c_3 R^3) b'_4 - 3d'_3 - e'_1 = 3c_2 R^2 R^4 B, \end{aligned} \quad (\text{B.20})$$

$$a'_1 = 0, \quad (\text{B.21})$$

$$\begin{aligned} 3a'_2 - R^3 c_3 b'_1 - R^4 c_4 b'_2 + (R c_1 - R^5 c_5) b'_3 + (R^2 c_2 - R^6 c_6) b'_4 + d'_2 \\ = -R c_1 R^4 B, \end{aligned} \quad (\text{B.22})$$

$$a'_1 - 2a'_3 - R^4 c_4 b'_1 + (Rc_1 - R^5 c_5) b'_2 + (R^2 c_2 - R^6 c_6) b'_3 + (R^3 c_3 - R^7 c_7 - 2Rc_1) b'_4 + d'_3 = -R^2 c_2 R^4 B, \quad (\text{B.23})$$

$$2a'_2 - \frac{5a'_4}{2} + R^5 c_5 b'_1 + R^6 c_6 b'_2 + (2Rc_1 + R^7 c_7) b'_3 + (2R^2 c_2 + R^8 c_8) b'_4 - d'_4 = R^3 c_3 R^4 B, \quad (\text{B.24})$$

$$a'_4 + (10R^5 c_5 - 12R^7 c_7) b'_1 + (10R^6 c_6 - 12R^8 c_8) b'_2 + 10R^7 c_7 b'_3 + 10R^8 c_8 b'_4 - 2e'_4 = (10c_3 R^3 - 12c_5 R^5) R^4 B, \quad (\text{B.25})$$

$$\begin{aligned} & -\frac{(3+\kappa_1)}{4} a'_3 + \left(\frac{\kappa_1}{2} R^6 c_6 - \frac{5}{2} R^6 c_6 + 2R^4 c_4\right) b'_1 + \left(\frac{\kappa_1}{2} R^7 c_7 - \frac{5}{2} R^7 c_7 + 2R^5 c_5\right) b'_2 \\ & + \left(\frac{\kappa_1}{2} c_8 R^8 - \frac{5}{2} R^8 c_8 + 2R^6 c_6\right) b'_3 + \left(2R^7 c_7 - \frac{3}{4} Rc_1 - \frac{\kappa_1}{2} Rc_1\right) b'_4 + \\ & \left(\frac{1}{2} \frac{\mu_1}{\mu_2} + \frac{3}{N'}\right) e'_3 = \left[\frac{(\kappa_1 - 5)}{2} R^4 c_4 + 2R^2 c_2\right] R^4 B, \end{aligned} \quad (\text{B.26})$$

$$\begin{aligned} & -\frac{(2+\kappa_1)}{2} a'_2 + \frac{5}{4} a'_4 + \left(\frac{\kappa_1}{2} R^5 c_5 + \frac{3}{2} R^3 c_3 - 2R^5 c_5\right) b'_1 + \left(\frac{\kappa_1}{2} R^6 c_6 + \frac{3}{2} R^4 c_4 - 2R^6 c_6\right) b'_2 \\ & + \left(\frac{\kappa_1}{2} R^7 c_7 + \frac{3}{2} R^5 c_5 - 2R^7 c_7 - Rc_1 - \frac{\kappa_1}{2} Rc_1\right) b'_3 + \left(\frac{\kappa_1}{2} R^8 c_8 + \frac{3}{2} R^6 c_6 - 2R^8 c_8 - R^2 c_2 - \frac{\kappa_1}{2} R^2 c_2\right) b'_4 \\ & + \left(2\frac{\mu_1}{\mu_2} - \frac{\kappa_2 \mu_1}{4\mu_2} + \frac{8}{N'}\right) d'_4 + \left(\frac{1}{2} \frac{\mu_1}{\mu_2} + \frac{2}{N'}\right) e'_2 = \left(\frac{\kappa_1}{2} R^3 c_3 - 2R^3 c_3 + \frac{3}{2} Rc_1\right) R^4 B, \end{aligned} \quad (\text{B.27})$$

$$\begin{aligned}
& \frac{(\kappa_1 - 1)}{2} a'_1 + a'_3 + \left(\frac{\kappa_1}{2} R^4 c_4 - \frac{3}{2} R^4 c_4 + R^2 c_2 \right) b'_1 + \left(\frac{\kappa_1}{2} R^5 c_5 - \right. \\
& \left. \frac{3}{2} R^5 c_5 + R^3 c_3 - \frac{1}{2} R c_1 - \frac{\kappa_1}{2} R c_1 \right) b'_2 + \left(\frac{\kappa_1}{2} R^6 c_6 - \frac{3}{2} R^6 c_6 + R^4 c_4 - \right. \\
& \left. \frac{1}{2} R^2 c_2 - \frac{\kappa_1}{2} R^2 c_2 \right) b'_3 + \left(\frac{\kappa_1}{2} R^7 c_7 - \frac{3}{2} R^7 c_7 + R^5 c_5 - \frac{1}{2} R^3 c_3 - \right. \\
& \left. \frac{\kappa_1}{2} R^3 c_3 + R c_1 \right) b'_4 + \left(\frac{3}{2} \frac{\mu_1}{\mu_2} - \frac{\kappa_2}{4} \frac{\mu_1}{\mu_2} + \frac{3}{N'} \right) d'_3 + \left(\frac{1}{2} \frac{\mu_1}{\mu_2} + \frac{1}{N'} \right) e'_1 = \\
& - \left(\frac{\kappa_1}{2} R^2 c_2 + \frac{3}{2} R^2 c_2 \right) R^4 B,
\end{aligned} \tag{B.28}$$

$$\begin{aligned}
& \frac{3}{2} a'_2 + \left(\frac{\kappa_1}{2} R^3 c_3 - \frac{\kappa_1}{2} R c_1 - R^3 c_3 + \frac{1}{2} R c_1 \right) b'_1 + \left(\frac{\kappa_1}{2} R^4 c_4 - \frac{\kappa_1}{2} R^2 c_2 - \right. \\
& \left. R^4 c_4 + \frac{1}{2} R^2 c_2 \right) b'_2 + \left(\frac{\kappa_1}{2} R^5 c_5 - \frac{\kappa_1}{2} R^3 c_3 - R^5 c_5 + \frac{1}{2} R^3 c_3 + \frac{1}{2} R c_1 \right) b'_3 + \\
& \left(\frac{\kappa_1}{2} R^6 c_6 - \frac{\kappa_1}{2} R^4 c_4 - R^6 c_6 + \frac{1}{2} R^4 c_4 + \frac{1}{2} R^2 c_2 \right) b'_4 + \frac{\kappa_2}{2} \frac{\mu_1}{\mu_2} d'_0 + \\
& \left(1 - \frac{\kappa_2}{4} \right) \frac{\mu_1}{\mu_2} d'_2 = \left(\frac{\kappa_1}{2} R c_1 - R c_1 \right) R^4 B,
\end{aligned} \tag{B.29}$$

$$a'_1 - \frac{\mu_1}{\mu_2} \kappa_2 d'_1 = 0, \tag{B.30}$$

$$\begin{aligned}
& - \frac{3}{2} a'_2 + \left(\frac{\kappa_1}{2} R c_1 + R^3 c_3 - \frac{1}{2} R c_1 - \frac{\kappa_1}{2} R^3 c_3 \right) b'_1 + \left(\frac{\kappa_1}{2} R^2 c_2 + R^4 c_4 - \right. \\
& \left. \frac{1}{2} R^2 c_2 - \frac{\kappa_1}{2} R^4 c_4 \right) b'_2 + \left(\frac{\kappa_1}{2} R^3 c_3 + R^5 c_5 - \frac{1}{2} R^3 c_3 - \frac{\kappa_1}{2} R^5 c_5 - \right. \\
& \left. \frac{1}{2} R c_1 \right) b'_3 + \left(\frac{\kappa_1}{2} R^4 c_4 + R^6 c_6 - \frac{1}{2} R^4 c_4 - \frac{\kappa_1}{2} R^6 c_6 - \frac{1}{2} R^2 c_2 \right) b'_4 - \\
& \frac{\kappa_2}{2} \frac{\mu_1}{\mu_2} d'_0 - \left(\frac{\mu_1}{\mu_2} - \frac{\kappa_2}{2} \frac{\mu_1}{\mu_2} - \frac{2}{N'} \right) d'_2 = (1 - \kappa_1 / 2) R c_1 R^4 B,
\end{aligned} \tag{B.31}$$

$$\begin{aligned}
& \frac{(1+\kappa_1)}{2}a'_1 - a'_3 + \left(\frac{3}{2}R^4c_4 - R^2c_2 - \frac{\kappa_1}{2}R^4c_4\right)b'_1 + \left(\frac{\kappa_1}{2}Rc_1 + \right. \\
& \left. \frac{3}{2}R^5c_5 - R^3c_3 - \frac{\kappa_1}{2}R^5c_5 + \frac{1}{2}Rc_1\right)b'_2 + \left(\frac{\kappa_1}{2}R^2c_2 + \frac{3}{2}R^6c_6 - \right. \\
& \left. R^4c_4 - \frac{\kappa_1}{2}R^6c_6 + \frac{1}{2}R^2c_2\right)b'_3 + \left(\frac{\kappa_1}{2}R^3c_3 + \frac{3}{2}R^7c_7 - R^5c_5 - \right. \\
& \left. \frac{\kappa_1}{2}R^7c_7 + \frac{1}{2}R^3c_3 - Rc_1\right)b'_4 - \left(\frac{3}{2}\frac{\mu_1}{\mu_2} - \frac{\kappa_2}{2}\frac{\mu_1}{\mu_2} - \frac{3}{N'}\right)d'_3 - \frac{1}{2}\frac{\mu_1}{\mu_2}e'_1 \\
& = \left(\frac{3}{2}R^2c_2 - \frac{\kappa_1}{2}R^2c_2\right)R^4B,
\end{aligned} \tag{B.32}$$

$$\begin{aligned}
& (1+\kappa_1/2)a'_2 - \frac{5}{4}a'_4 + \left(2R^5c_5 - \frac{3}{2}R^3c_3 - \frac{\kappa_1}{2}R^5c_5\right)b'_1 + \left(2R^6c_6 - \right. \\
& \left. \frac{3}{2}R^4c_4 - \frac{\kappa_1}{2}R^6c_6\right)b'_2 + \left(\frac{\kappa_1}{2}Rc_1 + 2R^7c_7 - \frac{3}{2}R^5c_5 - \frac{\kappa_1}{2}R^7c_7 + \right. \\
& \left. Rc_1\right)b'_3 + \left(\frac{\kappa_1}{2}R^2c_2 + 2R^8c_8 - \frac{3}{2}R^6c_6 - \frac{\kappa_1}{2}R^8c_8 + R^2c_2\right)b'_4 - \\
& \left(2\frac{\mu_1}{\mu_2} - \frac{\kappa_2}{2}\frac{\mu_1}{\mu_2} - \frac{4}{N'}\right)d'_4 - \frac{1}{2}\frac{\mu_1}{\mu_2}e'_2 = \left(R^3c_3 - \frac{3}{2}Rc_1 - \frac{\kappa_1}{2}R^3c_3\right)R^4B,
\end{aligned} \tag{B.33}$$

$$\begin{aligned}
& -\left(1+\frac{\kappa_1}{4}\right)a'_4 + \left(\frac{\kappa_1}{2}R^7c_7 - 3R^7c_7 + \frac{5}{2}R^5c_5\right)b'_1 + \left(\frac{\kappa_1}{2}R^8c_8 - \right. \\
& \left. 3R^8c_8 + \frac{5}{2}R^6c_6\right)b'_2 + \frac{5}{2}R^7c_7b'_3 + \frac{5}{2}R^8c_8b'_4 + \left(\frac{1}{2}\frac{\mu_1}{\mu_2} + \frac{4}{N'}\right)e'_4 = \\
& \left(\frac{\kappa_1}{2}R^5c_5 - 3R^5c_5 + \frac{5}{2}R^3c_3\right)R^4B.
\end{aligned} \tag{B.34}$$

For the case of elastic interphase layer ($m=3n$) under pure shear loading, the final equations are given by:

$$\frac{a'_3}{2} + (4c_4R^4 - 5c_6R^6)b'_1 + (4R^5c_5 - 5c_7R^7)b'_2 + (4c_6R^6 - 5c_8R^8)b'_3 + (c_1R + 4c_7R^7)b'_4 + e'_3 = (4R^2c_2 - 5R^4c_4)R^4B, \quad (\text{B.35})$$

$$a'_2 + (3c_3R^3 - 4c_5R^5)b'_1 + (3c_4R^4 - 4c_6R^6)b'_2 + (3c_5R^5 - 4c_7R^7 + c_1R)b'_3 + (3c_6R^6 - 4c_8R^8 + c_2R^2)b'_4 + 4d'_4 + e'_2 = (3c_1R - 4c_3R^3A)R^4B, \quad (\text{B.36})$$

$$a'_1 + (3c_4R^4 - 2c_2R^2)b'_1 + (3c_5R^5 - 2c_3R^3 - c_1R)b'_2 + (3c_6R^6 - 2c_4R^4 - c_2R^2)b'_3 + (3c_7R^7 - 2c_5R^5 - c_3R^3)b'_4 - 3d'_3 - e'_1 = 3c_2R^2R^4B, \quad (\text{B.37})$$

$$a'_1 = 0, \quad (\text{B.38})$$

$$3a'_2 - R^3c_3b'_1 - R^4c_4b'_2 + (Rc_1 - R^5c_5)b'_3 + (R^2c_2 - R^6c_6)b'_4 + d'_2 = -Rc_1R^4B, \quad (\text{B.39})$$

$$a'_1 - 2a'_3 - R^4c_4b'_1 + (Rc_1 - R^5c_5)b'_2 + (R^2c_2 - R^6c_6)b'_3 + (R^3c_3 - R^7c_7 - 2Rc_1)b'_4 + d'_3 = -R^2c_2R^4B, \quad (\text{B.40})$$

$$2a'_2 - \frac{5a'_4}{2} + R^5c_5b'_1 + R^6c_6b'_2 + (2Rc_1 + R^7c_7)b'_3 + (2R^2c_2 + R^8c_8)b'_4 - d'_4 = R^3c_3R^4B, \quad (\text{B.41})$$

$$a'_4 + (10R^5c_5 - 12R^7c_7)b'_1 + (10R^6c_6 - 12R^8c_8)b'_2 + 10R^7c_7b'_3 + 10R^8c_8b'_4 - 2e'_4 = (10c_3R^3 - 12c_5R^5)R^4B, \quad (\text{B.42})$$

$$\begin{aligned}
& -\frac{(3/2+\kappa_1)}{4}a'_3 + (\frac{\kappa_1}{4}R^6c_6 - \frac{5}{2}R^6c_6 + 2R^4c_4)b'_1 + (\frac{\kappa_1}{4}R^7c_7 - \frac{5}{2}R^7c_7 + \\
& 2R^5c_5)b'_2 + (\frac{\kappa_1}{4}c_8R^8 - \frac{5}{2}R^8c_8 + 2R^6c_6)b'_3 + (2R^7c_7 - \frac{3}{4}Rc_1 - \frac{\kappa_1}{2}Rc_1)b'_4 + \\
& (\frac{1}{2}\frac{\mu_1}{\mu_2} + \frac{3}{N'})e'_3 = [\frac{(\kappa_1-10)}{4}R^4c_4 + 2R^2c_2]R^4B,
\end{aligned} \tag{B.43}$$

$$\begin{aligned}
& -\frac{(1+\kappa_1)}{2}a'_2 + \frac{5}{8}a'_4 + (\frac{\kappa_1}{4}R^5c_5 + \frac{3}{2}R^3c_3 - 2R^5c_5)b'_1 + (\frac{\kappa_1}{4}R^6c_6 + \frac{3}{2}R^4c_4 - \\
& 2R^6c_6)b'_2 + (\frac{\kappa_1}{4}R^7c_7 + \frac{3}{2}R^5c_5 - 2R^7c_7 - \frac{1}{2}Rc_1 - \frac{\kappa_1}{2}Rc_1)b'_3 + (\frac{\kappa_1}{4}R^8c_8 + \\
& \frac{3}{2}R^6c_6 - 2R^8c_8 - \frac{1}{2}R^2c_2 - \frac{\kappa_1}{2}R^2c_2)b'_4 + (2\frac{\mu_1}{\mu_2} - \frac{\kappa_2\mu_1}{4\mu_2} + \frac{8}{N'})d'_4 + \\
& (\frac{1}{2}\frac{\mu_1}{\mu_2} + \frac{2}{N'})e'_2 = (\frac{\kappa_1}{4}R^3c_3 - 2R^3c_3 + \frac{3}{2}Rc_1)R^4B,
\end{aligned} \tag{B.44}$$

$$\begin{aligned}
& \frac{(\kappa_1-1/2)}{2}a'_1 + \frac{3}{2}a'_3 + (\frac{\kappa_1}{4}R^4c_4 - \frac{3}{2}R^4c_4 + R^2c_2)b'_1 + (\frac{\kappa_1}{4}R^5c_5 - \\
& \frac{3}{2}R^5c_5 + R^3c_3 - \frac{1}{4}Rc_1 - \frac{\kappa_1}{2}Rc_1)b'_2 + (\frac{\kappa_1}{4}R^6c_6 - \frac{3}{2}R^6c_6 + R^4c_4 - \\
& \frac{1}{4}R^2c_2 - \frac{\kappa_1}{2}R^2c_2)b'_3 + (\frac{\kappa_1}{4}R^7c_7 - \frac{3}{2}R^7c_7 + R^5c_5 - \frac{1}{4}R^3c_3 - \\
& \frac{\kappa_1}{2}R^3c_3 + \frac{Rc_1}{2})b'_4 + (\frac{3}{2}\frac{\mu_1}{\mu_2} - \frac{\kappa_2}{4}\frac{\mu_1}{\mu_2} + \frac{3}{N'})d'_3 + (\frac{1}{2}\frac{\mu_1}{\mu_2} + \frac{1}{N'})e'_1 = \\
& -(\frac{\kappa_1}{4}R^2c_2 + \frac{3}{2}R^2c_2)R^4B,
\end{aligned} \tag{B.45}$$

$$\begin{aligned}
& \frac{3}{4}a'_2 + \left(\frac{\kappa_1}{4}R^3c_3 - \frac{\kappa_1}{2}Rc_1 - R^3c_3 + \frac{1}{2}Rc_1\right)b'_1 + \left(\frac{\kappa_1}{4}R^4c_4 - \frac{\kappa_1}{2}R^2c_2 - \right. \\
& R^4c_4 + \frac{1}{2}R^2c_2\right)b'_2 + \left(\frac{\kappa_1}{4}R^5c_5 - \frac{\kappa_1}{2}R^3c_3 - R^5c_5 + \frac{1}{2}R^3c_3 + \frac{1}{4}Rc_1\right)b'_3 + \\
& \left(\frac{\kappa_1}{4}R^6c_6 - \frac{\kappa_1}{2}R^4c_4 - R^6c_6 + \frac{1}{2}R^4c_4 + \frac{1}{4}R^2c_2\right)b'_4 + \frac{\kappa_2}{2}\frac{\mu_1}{\mu_2}d'_0 + \\
& \left(1 - \frac{\kappa_2}{4}\right)\frac{\mu_1}{\mu_2}d'_2 = \left(\frac{\kappa_1}{4}Rc_1 - 4Rc_1\right)R^4B,
\end{aligned} \tag{B.46}$$

$$\begin{aligned}
& \frac{a'_1}{2} + \left(\frac{\kappa_1}{4}R^2c_2 + \frac{1}{4}R^2c_2 - \frac{\kappa_1}{2}R^2c_2 - \frac{1}{2}R^2c_2\right)b'_1 + \left(\frac{\kappa_1}{4}R^3c_3 + \frac{1}{4}R^3c_3 - \right. \\
& \left.\frac{\kappa_1}{2}R^3c_3 - \frac{R^3c_3}{2}\right)b'_2 + \left(\frac{\kappa_1}{4}R^4c_4 - \frac{1}{4}R^4c_4 - \frac{\kappa_1}{2}R^4c_4 - \frac{R^4c_4}{2}\right)b'_3 + \\
& \left(\frac{\kappa_1}{4}R^5c_5 - \frac{1}{4}R^5c_5 - \frac{\kappa_1}{2}R^5c_5 - \frac{R^5c_5}{2}\right)b'_4 + \left(\frac{\mu_1}{4\mu_2} - \kappa_2\frac{3\mu_1}{4\mu_2}\right)d'_1 = \\
& \left(\frac{\kappa_1}{8} + \frac{1}{8}\right)R^4B,
\end{aligned} \tag{B.47}$$

$$\begin{aligned}
& -\frac{3}{2}a'_2 + \left(\frac{\kappa_1}{4}Rc_1 + \frac{R^3}{2}c_3 - \frac{1}{2}Rc_1 - \frac{\kappa_1}{2}R^3c_3\right)b'_1 + \left(\frac{\kappa_1}{4}R^2c_2 + \frac{R^4}{2}c_4 - \right. \\
& \left.\frac{1}{2}R^2c_2 - \frac{\kappa_1}{2}R^4c_4\right)b'_2 + \left(\frac{\kappa_1}{4}R^3c_3 + \frac{R^5}{2}c_5 - \frac{1}{2}R^3c_3 - \frac{\kappa_1}{2}R^5c_5 - \right. \\
& \left.\frac{1}{2}Rc_1\right)b'_3 + \left(\frac{\kappa_1}{4}R^4c_4 + \frac{R^6}{2}c_6 - \frac{1}{2}R^4c_4 - \frac{\kappa_1}{2}R^6c_6 - \frac{1}{2}R^2c_2\right)b'_4 - \\
& \frac{\kappa_2}{4}\frac{\mu_1}{\mu_2}d'_0 - \left(\frac{1}{2}\frac{\mu_1}{\mu_2} - \frac{\kappa_2}{2}\frac{\mu_1}{\mu_2} - \frac{2}{N'}\right)d'_2 = \frac{(1-\kappa_1)}{2}Rc_1R^4B,
\end{aligned} \tag{B.48}$$

$$\begin{aligned}
& \frac{(1+\kappa_1/2)}{2}a'_1 - a'_3 + \left(\frac{3}{4}R^4c_4 - \frac{1}{2}R^2c_2 - \frac{\kappa_1}{2}R^4c_4\right)b'_1 + \left(\frac{\kappa_1}{4}Rc_1 + \right. \\
& \left. \frac{3}{4}R^5c_5 - \frac{1}{2}R^3c_3 - \frac{\kappa_1}{2}R^5c_5 + \frac{1}{2}Rc_1\right)b'_2 + \left(\frac{\kappa_1}{4}R^2c_2 + \frac{3}{4}R^6c_6 - \right. \\
& \left. \frac{1}{2}R^4c_4 - \frac{\kappa_1}{2}R^6c_6 + \frac{1}{2}R^2c_2\right)b'_3 + \left(\frac{\kappa_1}{4}R^3c_3 + \frac{3}{4}R^7c_7 - \frac{1}{2}R^5c_5 - \right. \\
& \left. \frac{\kappa_1}{2}R^7c_7 + \frac{1}{2}R^3c_3 - Rc_1\right)b'_4 - \left(\frac{3}{4}\frac{\mu_1}{\mu_2} - \frac{\kappa_2}{2}\frac{\mu_1}{\mu_2} - \frac{3}{N'}\right)d'_3 - \frac{1}{4}\frac{\mu_1}{\mu_2}e'_1 \\
& = \left(\frac{3}{4}R^2c_2 - \frac{\kappa_1}{2}R^2c_2\right)R^4B,
\end{aligned} \tag{B.49}$$

$$\begin{aligned}
& (1+\kappa_1/4)a'_2 - \frac{5}{4}a'_4 + \left(R^5c_5 - \frac{3}{4}R^3c_3 - \frac{\kappa_1}{2}R^5c_5\right)b'_1 + \left(R^6c_6 - \right. \\
& \left. \frac{3}{4}R^4c_4 - \frac{\kappa_1}{2}R^6c_6\right)b'_2 + \left(\frac{\kappa_1}{4}Rc_1 + R^7c_7 - \frac{3}{4}R^5c_5 - \frac{\kappa_1}{2}R^7c_7 + \right. \\
& \left. Rc_1\right)b'_3 + \left(\frac{\kappa_1}{4}R^2c_2 + R^8c_8 - \frac{3}{4}R^6c_6 - \frac{\kappa_1}{2}R^8c_8 + R^2c_2\right)b'_4 - \\
& \left(\frac{\mu_1}{\mu_2} - \frac{\kappa_2}{2}\frac{\mu_1}{\mu_2} - \frac{4}{N'}\right)d'_4 - \frac{1}{4}\frac{\mu_1}{\mu_2}e'_2 = \left(R^3c_3 - \frac{3}{4}Rc_1 - \frac{\kappa_1}{2}R^3c_3\right)R^4B,
\end{aligned} \tag{B.50}$$

$$\begin{aligned}
& -\left(\frac{1}{2} + \frac{\kappa_1}{4}\right)a'_4 + \left(\frac{\kappa_1}{4}R^7c_7 - 3R^7c_7 + \frac{5}{2}R^5c_5\right)b'_1 + \left(\frac{\kappa_1}{4}R^8c_8 - \right. \\
& \left. 3R^8c_8 + \frac{5}{2}R^6c_6\right)b'_2 + \frac{5}{2}R^7c_7b'_3 + \frac{5}{2}R^8c_8b'_4 + \left(\frac{1}{2}\frac{\mu_1}{\mu_2} + \frac{4}{N'}\right)e'_4 = \\
& \left(\frac{\kappa_1}{4}R^5c_5 - 3R^5c_5 + \frac{5}{2}R^3c_3\right)R^4B.
\end{aligned} \tag{B.51}$$